


This is to certify that the

dissertation entitled

3-D VOLUME RECONSTRUCTION OF THE DEVELOPMENT OF THE EYE-TENTACLE COMPLEX IN PULMONATE GASTROPODS: NEW APPROACHES TO AN EVOLUTIONARY QUESTION

presented by

Timothy Lancaster Murphy

has been accepted towards fulfillment
of the requirements for

Ph.D. degree in Zoology

James W. Atkinson
Major professor

Date 17 December 1999

# 3-D VOLUME RECONSTRUCTION OF THE DEVELOPMENT OF THE EYE-TENTACLE COMPLEX IN PULMONATE GASTROPODS: NEW APPROACHES TO AN EVOLUTIONARY QUESTION

By

Timothy Lancaster Murphy

A DISSERTATION

Submitted to
Michigan State University
in partial fulfillment of the requirements
for the degree of

DOCTOR OF PHILOSOPHY

Department of Zoology

1999

# ABSTRACT

## 3-D VOLUME RECONSTRUCTION OF THE DEVELOPMENT OF THE EYE-TENTACLE COMPLEX IN PULMONATE GASTROPODS: NEW APPROACHES TO AN EVOLUTIONARY QUESTION

By

Timothy Lancaster Murphy

The development of the eye-tentacle complex in a basommatophoran snail, *Helisoma anceps*, and a stylommatophoran snail, *Anguispira alternata*, was examined to determine whether the differences in adult pattern can be attributed to early differences in developmental position and/or possible tissue interactions. In order to carry out the analysis it was necessary to develop a method that allows for the precise comparison of position in all three dimensions of the developing cerebral ganglia, eyes, and tentacles. The approach used in this study was to combine a laser scanning microscope's (Zeiss) ability to create high resolution digital images, with the power of a Silicon Graphics, Inc. workstation running the "volume rendering" software program VoxelView/E (VitalImages, Inc.). The software program creates three-dimensional "virtual" embryos that can be manipulated in ways impossible to perform with the "real" embryos.

The results of this study found that the point of invagination of the eye vesicles was in the same dorso-lateral position of the cephalic plates for both species. However, in *Anguispira alternata*, the cerebral ganglia were not found in close proximity to the cephalic plates in the precise location of the eye vesicles either before or during invagination, while in *Helisoma anceps*, the cerebral ganglia were found in contact with the cephalic plates from the very beginning of eye-vesicle invagination. The eye vesicle were found to maintain connection even after the eye vesicles had separated from the overlying ectoderm. These results are discussed in terms of the ability of the cerebral ganglia in some adult basommatophoran snails to induce the formation of supernumerary eyes and tentacles, thus suggesting that induction may play an important role in the formation of eyes and tentacles during embryogenesis.

The value of the method developed in carrying out this analysis, laser scanning microscopy coupled with 3-D reconstruction by volume rendering, is demonstrated in addressing these questions in snail development/evolution and its tremendous potential for other such analyses is explored.

In memory of my brother Daniel:
May we never stop believing in ourselves and may we always remember to dream good dreams.

## ACKNOWLEDGMENTS

I take this opportunity to thank all the people who directly or indirectly helped to make this dissertation project become a reality. With gratitude, I thank my mentor, Dr. James W. Atkinson, for his support, guidance and overall patience without which I would not have been able to complete this work. I thank him for allowing me to share in his awe of wonder for the natural world around us. But most importantly, I thank him for believing in me. I also thank my committee members for all their time and support: Drs. Martin Balaban, John I. Johnson, Donald O. Straney, and Joanne H. Whallon. I am grateful to Dr. Shirley A. Owens and fellow graduate student Geoffrey Williams, for their support, friendship, and most importantly humor. I thank fellow lab slugs, Alyssa L. Shearer and Miranda A. Karson for showing just how interesting snails can be even after they hatch. I especially thank Drs. Diana and Nestor Bello-DeOcampo for their support, encouragement, and friendship. I am also grateful to my parents, Donald H. and Jane B. Murphy, and my brother Dr. James B. Murphy for their unconditional support and encouragement. Special thanks go to Dr. Joanne Whallon and my father for their critical review of this manuscript.

Finally and most importantly, I extend my warmest appreciation to Kelly J. Stevens for his great humor, love, and always being there when I needed him most.

TABLE OF CONTENTS

LIST OF TABLES

LIST OF FIGURES

**ANG** ***Anguispira alternata***
**ASE** ***Anguispira alternata embryo***
**ANSI/IEEE 488-1978 (American National Standards Institute: Determines hardware-related standards**
**CCD Charge-couple devise (used for digital cameras)**
**CD-ROM Compact Disk Read Only Memory (optical disk)**
**DOS Disk operating system**
**FAA Formaldehyde-alcohol-acetic acid . A common fixative.**
**FTP File transfer protocol**
**GPIB AT (General Purpose Interface Bus for an AT class PC clone)**
**HAS** ***Helisoma anceps***
**IBM PC** Refers to a family of personal computers produced by IBM. The term can also refer to computers that conform to set of loosely controlled standards. These are also called *IBM clones*, *IBM compatibles*, or simply compatibles. These terms are actually misnomers because many of the PCs produced by IBM do not conform to industry standards. For example, IBM attempted to change the expansion bus to MCA in its PS/2 line of PCs, but the industry did not follow suit. (http://webopedia.internet.com/TERM/I/IBM_PC.html)
**IEEE 488 (Standard for GPIB established by Institute of Electrical and Electronics Engineers)**
**LSM Laser scanning microscopy**
**MB megabyte**
**N.A. Numerical aperture**
**nm nano-meter**
**PC Clone (IBM Clone; IBM Compatibles)** Other companies adjusted to IBM's dominance by building IBM clones, computers that were internally almost the same as the IBM PC, but that cost less. Because IBM clones used the same microprocessors as IBM PCs, they were capable of running the same software. (http://webopedia.internet.com/TERM/p/personal_computer.html)
**PC** Short for *personal computer* or *IBM PC*. The first personal computer produced by IBM was called the *PC,* and increasingly the term PC came to mean IBM or IBM-compatible personal computers, to the exclusion of other types of personal computers, such as Macintoshes.
In recent years, the term *PC* has become more and more difficult to pin down. In general, though, it applies to any personal computer based on an Intel microprocessor, or on an Intel-compatible microprocessor. For nearly every other component, including the operating system, there are several options, all of which fall under the rubric of PC. [http://webopedia.internet.com/TERM/P/PC.html]
**PERSONAL COMPUTER** A small, relatively inexpensive computer designed for an individual user. In price, personal computers range anywhere from a few hundred dollars to over five thousand dollars. All are based on the microprocessor technology that enables manufacturers to put an entire CPU on one chip. Businesses use personal computers for word processing, accounting, desktop publishing, and for running spreadsheet and database management applications.
Other companies adjusted to IBM's dominance by building IBM clones, computers that were internally almost the same as the IBM PC, but that cost less. Because IBM clones

used the same microprocessors as IBM PCs, they were capable of running the same software. (http://webopedia.internet.com/TERM/p/personal_computer.html)

**RAM Random access memory**

**SGI Silicon Graphics, Inc.**

**SP Standard play (VHS recording speed)**

**SVHS Super VHS**

**TAR Tape Archive (Unix system)**

**TCP/IP Transmission control protocol/Internet protocol**

**μ(m) micro-meter (microns)**

**UNIX** Pronounced *yoo-niks,* a popular *multi-user, multitasking* operating system developed at Bell Labs in the early 1970s. Created by just a handful of programmers, UNIX was designed to be a small, flexible system used exclusively by programmers. Although it has matured considerably over the years, UNIX still betrays its origins by its cryptic command names and its general lack of user-friendliness. This is changing, however, with graphical user interfaces such as MOTIF.

UNIX was one of the first operating systems to be written in a high-level programming language, namely C. This meant that it could installed on virtually any computer for which a C compiler existed. This natural portability combined with its low price made it a popular choice among universities. (It was inexpensive because antitrust regulations prohibited Bell Labs from marketing it as a full-scale product.)

Bell Labs distributed the operating system in its source language form, so anyone who obtained a copy could modify and customize it for his own purposes. By the end of the 1970s, dozens of different versions of UNIX were running at various sites.

After its breakup in 1982, AT&T began to market UNIX in earnest. It also began the long and difficult process of defining a standard version of UNIX. To date, there are two main dialects of UNIX; one produced by AT&T known as *System V* and one developed at Berkeley University and known as *BSD4.x,* x being a number from 1 to 3.

Due to its portability, flexibility, and power, UNIX has become the leading operating system for workstations. Historically, it has been less popular in the personal computer market, but the emergence of a new version called *Linux* is revitalizing UNIX across all platforms. (http://webopedia.internet.com/TERM/U/UNIX.html)

**WORKSTATION** 1) A type of computer used for engineering applications (CAD/CAM), desktop publishing, software development, and other types of applications that require a moderate amount of computing power and relatively high quality graphics capabilities.

Workstations generally come with a large, high-resolution graphics screen, at least 64 MB (megabytes) of RAM, built-in network support, and a graphical user interface. Most workstations also have a mass storage device such as a disk drive, but a special type of workstation, called a diskless workstation, comes without a disk drive. The most common operating systems for workstations are UNIX and Windows NT.

In terms of computing power, workstations lie between personal computers and minicomputers, although the line is fuzzy on both ends. High-end personal computers are equivalent to low-end workstations. And high-end workstations are equivalent to minicomputers.

Like personal computers, most workstations are single-user computers. However, workstations are typically linked together to form a local-area network, although they can also be used as stand-alone systems.

The leading manufacturers of workstations are Sun Microsystems, Hewlett-Packard Company, Silicon Graphics Incorporated, and Compaq.
(2) In networking, *workstation* refers to any computer connected to a local-area network. It could be a workstation or a personal computer.
[http://webopedia.internet.com/TERM/w/workstation.html]

# INTRODUCTION

Evolutionary changes in morphology often occur when a group of organisms invades a new habitat. Since changes in morphology are derived from changes in developmental processes and patterns of gene expression, evolution can be defined as changes in developmental patterns over time.

Within the gastropod group Pulmonata (air-breathing snails and slugs), one of the major differences between the "Basommatophora," a primarily aquatic group of snails, and the "Stylommatophora," a primarily terrestrial group of snails and slugs, is in the structure and pattern of their eye-tentacle complex. The names of these two groups are based upon the position of the eyes relative to the tentacles. The water-dwelling basommatophoran snails have their eyes situated *at the base* of a single pair of cephalic tentacles. The land-dwelling stylommatophoran snails and slugs have two sets of cephalic tentacles, a pair of smaller "anterior" tentacles situated just above the "labial palps" or upper lips, and a larger pair of "posterior" or "optic" tentacles located further back on top of the "head." Their eyes are *at the top* of this larger, posterior set of cephalic tentacles (Figure 1).

The evolution of the stylommatophoran eye-tentacle complex represents a major restructuring of the main sensory system of these animals. Included in this evolutionary modification was not only a

reorganization of parts, such as eyes moved to the top of the posterior tentacles, but the creation of novel features such as 1) the sensory pad at the tip of the tentacles, 2) the largest and most complex tentacular ganglia of any gastropods (Haszprunar, 1988), 3) and the ability to fully retract the tentacles by invagination.

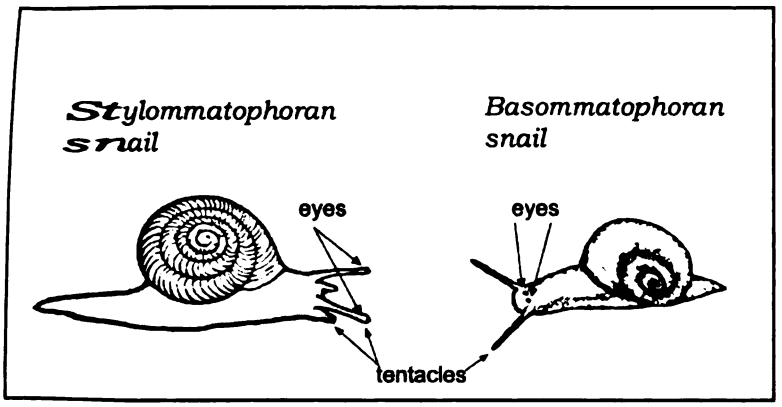


**Figure 1** Eye-tentacle complex Comparison
(snails redrawn after Solem, 1974)

It is not known what, if any, the adaptive significance of these two very different patterns of the main sensory structures, which are so highly correlated with life in different environments, may be. Although there is disagreement as to the ancestry of these two groups (see below), there is little doubt that the pattern of tentacles and eyes found in the Stylommatophora was an evolutionary novelty within the Gastropoda. How this restructuring of such important organ systems occurred evolutionarily is not known. Since all evolutionary changes in morphology are based on changes in the underlying developmental pattern, to fully understand the evolution of these structures requires knowledge as to where and how the developmental pattern was altered.

While there have been descriptive studies of the general development of several species of each group, there have not been any clear comparative studies of how the different patterns of the eye-tentacle complex are established during development. Do the changes occur early in development, with major reorganization and/or novel developmental patterns? Alternatively, do the patterns of development differ only later, with minor adjustments to existing developmental pathways?

Snails are asymmetric animals, and during development, their organs and tissues go through many different patterns of arrangement. To understand how one pattern develops into another, it is necessary to be able to study the structure of the embryo at different stages in all three dimensions. Because of the small size of pulmonate embryos, traditional approaches to the study of their development have involved collecting embryos at different stages of development, fixing them, embedding them in some sort of supportive medium, sectioning, and staining the sections for observation under a microscope. While this yields very good two-dimensional images of these very small embryos, the technique is limited in determining the three-dimensional information needed to understand and compare precise changes in developmental patterns. A novel approach is needed that not only utilizes the spatial information available in the two-dimensional

sections, but extends that information allowing better determination of spatial relationships in all three dimensions.

In this study the approach used to study snail development was to combine a laser scanning microscope's ability to create high resolution digital images, with the power of sophisticated computer "volume rendering" three-dimensional reconstruction software running on a graphics workstation. While both of these technologies have been used separately, as well as together, their combined complementary capability had not been brought to bear on these types of questions of development. This approach creates a "virtual embryo" on the computer that can be studied and manipulated in ways impossible to perform on "real" embryos. Changes in pattern in all three dimensions can be examined quantitatively as well as qualitatively with great precision, accuracy, and repeatability.

The importance of accurately mapping the position of developing structures and tissues is underscored when the role of tissue interactions during embryogenesis is understood. Classic studies in vertebrate embryology revealed the phenomenon of "induction" in which the fate of one tissue is determined by substances produced by adjacent tissues (See Wolpert, 1998). Of special importance to the investigation at hand is the well-studied phenomenon in which the developing nervous system of the vertebrate embryo induces overlying ectoderm to differentiate into the lens and cornea of the eye. Recent transplantation

studies involving adult basommatophoran snails indicate that the nervous system of gastropods may have inductive properties also. Cerebral ganglia transplanted into an adult host induced the formation of supernumerary eyes and tentacles (Moffett and Austin, 1981). Because of their extremely small size, comparable transplantation studies have not been attempted on the embryos of pulmonate snails.

Nevertheless, the inducing ability of cerebral ganglia in adult snails suggests that such induction may play an important role in the formation of eyes and tentacles in the developing embryo. To determine whether this is the case it is essential that the precise spatial relationships among these tissues (developing ganglia, eyes, and tentacles) be followed through development. Creation of a technique for mapping these positions in three dimensions is of critical importance.

If the cerebral ganglia are responsible for inducing the formation of the eyes and tentacles, one would expect to find a close positional relationship between the cerebral ganglia and overlying ectoderm, in the precise area where these structures will form. The differences in the adult pattern of the eye-tentacle complex may be reflected in differences in positional relationships in the embryo. Thus, it may be possible to explain the difference in eye location between these two groups of snails as based on a change in the position of the cerebral ganglia relative to the overlying ectoderm during development.

This study set out:

1) to develop a method that allows for the precise comparison of position in all three dimensions of the developing cerebral ganglia and eyes, relative to the overlying ectoderm, between aquatic basommatophoran and terrestrial stylommatophoran gastropods;

2) to determine the precise location within the cephalic plates of eye-vesicle formation, and if the cerebral ganglia move into a position to be able to interact with the overlying ectoderm in the exact area required for their induction; and

3) to determine if there is a difference in the position of the cerebral ganglia relative to the overlying ectoderm that may account for the changes in the position of the eyes relative to the tentacles between these two groups.

*Chapter 1*

# A SNAIL'S VIEW

*How to separate dice from design - that is a major question*

*facing evolutionary biology today.*

*- Tyler Volk (1990)*

The phylum Mollusca CUVIER 1797 is made up of eight "classes" with Class Gastropoda CUVIER 1797 comprising nearly 80% of the phylum (Solem, 1974). The class Gastropoda, which contains the snails and slugs, is further divided into the subclasses Prosobranchia, Opisthobranchia, and Pulmonata. The subclass Prosobranchia is the oldest, and is believed to have given rise to the other two subclasses (Schmekel, 1985; Solem, 1974, 1985; Hasprunar, 1988). Prosobranchs are predominately marine, with some freshwater and terrestrial members. Opisthobranchs are all marine. Pulmonates are mainly terrestrial and freshwater.

Historically, gastropods have been divided into two groups based on whether or not the pleural-visceral connectives of their nervous system are crossed ("streptoneury"), forming a figure eight of the visceral loop, or not crossed, or only slightly crossed peripheral nerves ("euthyneury") (Bullock and Horridge, 1965)[1] (Figure 2). It is from an

euthyneurous group of the Prosobranchia that the Opisthobranchia and the Pulmonata are believed to have arisen (Hyman, 1967; Fretter and Graham, 1962; Thompson, 1976). Although their relationship to each other is still under debate, the Gastropoda are believed to form a monophyletic group (Haszprunar, 1988).

## Evolutionary Modification of the Eye-Tentacle Complex: Adaptation to Terrestrial Habitats?

As the ancestors of modern gastropods moved from marine to freshwater and terrestrial habitats many physiological as well as structural modifications occurred, e.g., changes involving water-balance, reproduction, shell formation, etc. (See Fretter and Graham, 1962; Graham, 1985; Andrews, 1965; Andrews and Little, 1972; Creek, 1951; Solem, 1974, 1985). Along with obvious adaptive alterations in structure and physiology, modification of the major sensory system, the eye-tentacle complex, has changed in the structure, function, number of cephalic tentacles, and the position of the eyes relative to them, of those animals that most successfully invaded land -- the stylommatophoran pulmonates.

Aquatic snails have a single pair of cephalic tentacles, with their eyes located at the base of the tentacles. The eyes are fused to the base (as in the pulmonate basommatophoran snails, *Lymnaea* and *Helisoma*), or located on short eyestalks located at the base (as in the prosobranch *Pomacea*). The largest and most diverse group of terrestrial

gastropods is the Order Stylommatophora. All these animals (snails and slugs), in contrast, have two pairs of cephalic tentacles, with their eyes located at the tip of the larger posterior set of tentacles. (Figure 1) Each of the four tentacles has a large, complex, peripheral ganglion innervating a chemo-sensory pad at the tip.

With the exception of the Limnaeids, in which the tentacles are immobile spade-like structures, basommatophoran snails have long slender solid tentacles that can only be shortened a small amount and have very limited range of mobility. They move almost freely in the water currents. On the other hand, stylommatophoran snails have tentacles that can be retracted by invagination completely back into the body and are highly mobile. The larger posterior "optic" tentacles can also be lengthened and may be deployed in a variety of patterns and directions.

The success of the Stylommatophora (over 30,000 species in terrestrial habitats throughout the world -- which incidentally out-numbers all terrestrial vertebrates {Barker, 1999; Solem, 1974, 1984}) -- and the universality among them of the same basic eye-tentacle-cerebral ganglion pattern is strongly suggestive that the evolution of the pattern has played an important role in their success.

## DEVELOPMENT OF THE EYE-TENTACLE COMPLEX IN PULMONATE GASTROPODS

The general development of gastropod molluscs has been worked out for several species. Numerous cell lineage studies since the late

nineteenth century have established the general pattern of gastropod development (Blochmann, 1882: *Neritina*; Heymons, 1893: *Umbrella*; Kofoid, 1895: *Limax*; Meisenheimer, 1896; *Limax*; Conklin, 1897: *Crepidula*, 1907: *Fulgur*; Holmes, 1900: *Planorbis*; Robert, 1902: *Trochus*; Casteel, 1904: *Fiona*; Carazzi, 1905: *Aplysia*; Wierzeiski, 1905: *Physa*; Delsman, 1912: *Littorina*). (For a more detailed review of their findings, see Raven, 1966.) Organization of the gastropod embryo is based upon a fixed relationship to the pattern of the blastomeres (Raven, 1966; Verdonk and Biggelaar, 1983).

Cleavage in all molluscs, except the cephalopods which have meroblastic discoidal cleavage (Raven, 1966), is a modified form of the radial type of holoblastic cleavage termed "spiral cleavage" by Wilson in 1892. The system of nomenclature used to label and thus follow the cell lineage was developed by Conklin (1897) and modified slightly by Wierzejski (1905). The first cleavage divides the egg into two cells AB and CD. Second cleavage divides these cells further in to the four "quadrants" of the egg, "A," "B," "C," and "D". Third cleavage separates an animal "micromere" from the vegetative "macromere" of each quadrant, thus forming the "first quartette" of micromeres, designated "1a-1d" and the macromeres now designated "1A-1D" (Raven, 1966; Verdonk, 1965).

Gastropods have what is termed "alternating spiral cleavage" with the direction of cleavage alternating between "dexiotropic" ("move to the

right" or in a clockwise direction), and "laeotropic" ("move to the left" or in an anti-clockwise direction). When *third* cleavage[2] is laeotropic instead of dexiotropic, the cleavage pattern of the embryo becomes "a mirror image" of the original pattern, and thus the morphology of the adult animals become reversed (Raven, 1966; Verdonk and van den Biggelaar, 1983). Crampton (1894) discovered the correlation between the pattern of cleavage and direction of coiling of the shell (Verdonk and van den Biggelaar, 1983). Some species of basommatophoran snails, such as the *Biomphalaria, Planorbis, Physa,* and *Helisoma,* have sinistral (or left-handed) coiling shells, all have the reversed cleavage type and thus reversed body plans also (Verdonk and van den Biggelaar, 1983). (See Figure 3)

The ectoderm is formed from the first three quartettes of micromeres. The ectoderm is divided into two regions by a band of ciliated cells called the "prototroch". The ectoderm anterior to this prototroch is called "pretrochal ectoderm" and the ectoderm posterior to the prototroch is called "posttrochal ectoderm" (Raven, 1966).

It is the pretrochal ectoderm, derived from the first quartette of micromeres (1a-1d), that gives rise to the head region. Within this head region, two rounded areas develop from micromeres 1a and 1c, called the "cephalic plates". It is from these specific regions of pretrochal ectoderm that the cerebral ganglia, cephalic eyes, tentacles, and any tentacular ganglia are derived[3] (Crofts, 1937; Moritz, 1939; Raven,

1966; Demian and Yousif, 1975; Verdonk and van den Biggelaar, 1983; Jacob, 1984; Page, 1992).

In pulmonates, the cerebral ganglia are derived from the ectoderm of the cephalic plates by cellular proliferation and delamination, and invagination. (Henchman, 1890: *Limax maximus*; Verdonk, 1965: *Limnaea stagnalis*; Camey and Verdonk, 1970: *Biomphalaria glabrata*; Morrill, 1982: *Lymnaea palustris*; Reviews: Raven, 1966; Moor, 1983.) A pair of invaginations[4] occurs with the innermost end forming a thickening of the ectodermal wall with cells apparently migrating to the cerebral ganglia, and developing into the "procerebrum" in the Stylommatophora, or the "lateral lobes" in the Basommatophora (Henchman, 1890; Raven, 1966; Moor, 1983).

The formation of the eyes in pulmonates occurs by invagination in the lateral or dorsal lateral region of the cephalic plate forming a small, single-layered vesicle (Henchman, 1890; Raven, 1966; Eakin and Brandenburger, 1967; Moor, 1983). The eye vesicle then pinches off from the overlying ectoderm forming a closed ball of cells. In the prosobranch freshwater snail *Marisa cornuarietis* (Demian and Yousif, 1975), the eyes form in the lateral region of the cephalic plates and then migrate to a small protuberance that has formed in the lateral side of each tentacle. The ectoderm above the eye thins out and becomes the cornea. In the pulmonate stylommatophoran snail *Helix aspersa* (Eakin and Brandenburger, 1967) the eye-vesicle is said to form in the tentacle

anlage, and then gets "carried up" with the developing tentacle. The cephalic eyes are innervated by the cerebral ganglia in all gastropods.

At the time the eye-vesicles begin to form, the anlagen of the tentacles start to sprout from the cephalic plates. The single pair of cephalic tentacles of basommatophorans are solid and filled with mesoderm cells, while the two pairs of cephalic tentacles of stylommatophorans are hollow (Henchman, 1890; Raven, 1966; Moor, 1983). The tentacles of stylommatophorans have a large, complex tentacular ganglion located just below the tip of each tentacle.

While this general pattern of pulmonate eye-tentacle complex development has been well established, these studies are not precise enough to make direct comparisons of developmental pattern of the eye-tentacle complex between species. For example, these studies only refer to where the eye-vesicles actually form in the cephalic plates as being "dorsal" or "dorsal lateral" to the developing tentacles (Raven, 1966; Eakin and Brandenburger, 1967; Moor, 1983). These descriptions, while generally useful for gross comparisons, are not precise enough to rule out or support the possibility for a change in the location of the eye-vesicle formation that may account for the difference in the location of the eyes in the adults. The lack of precision of these descriptions is due in part to the techniques used is these studies, i.e., sectioned and whole mounted embryos, which can make it difficult to determine the precise position of very small structures in all three dimensions.

Figure 2 Patterns of Gastropod Nervous Systems

Structure and patterns of the nervous system from the three sub-classes of gastropod molluscs. The visceral loop of the Prosobranchia is crossed (streptoneury), while the Opisthobranchia and Pulmonata are not crossed (euthyneury).

The ganglia believed to be homologous are shown in the same color: Cerebral ganglia are in white; visceral loop ganglia are in green; and pedal ganglia are in red.

(Based on Bullock, T. H., and Horridge, G. A. (1965). *Structure and Function in the Nervous Systems of Invertebrates.* Vol. **2**. W. H. Freeman and Company, San Francisco.)

## Prosobranchia

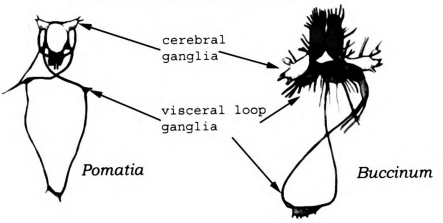


## Opisthobranchia

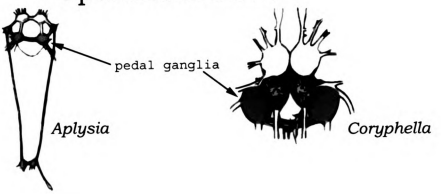


## Pulmonata


**Basommatophora** Stylommatophora

Figure 3 Dextral vs. sinistral spiral cleavage patterns

Comparison of cleavage pattern of dextral (a-e) verses sinistral (f-j) gastropods. Dextral snails have a dexiotropic third cleavage with a clockwise shifting of the resulting micromeres. Sinistral snails have a laeotropic third cleavage with a counter-clockwise shifting of the resulting micromeres.

Macromeres are labeled with uppercase letters and micromeres are labeled with lowercase letters.

(Based on Verdonk and van den Biggelaar, 1983)

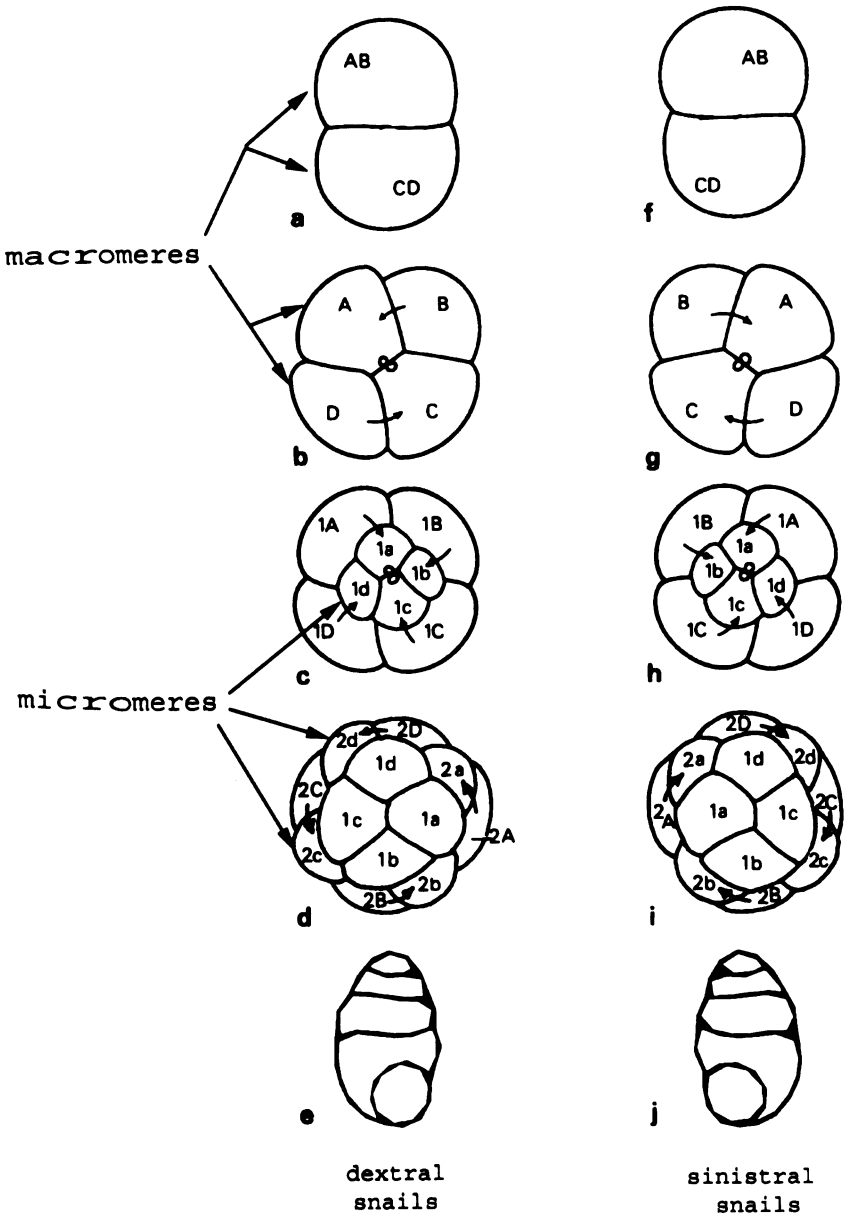
macromeres
micromeres
AB
CD
a
A
B
D
C
b
1A
1B
1a
1b
1d
1c
1D
1C
c
2d
2D
1d
2a
2C
1c
1a
2A
2c
1b
2b
2B
d
e
f
g
h
i
j
dextral
snails
sinistral
snails

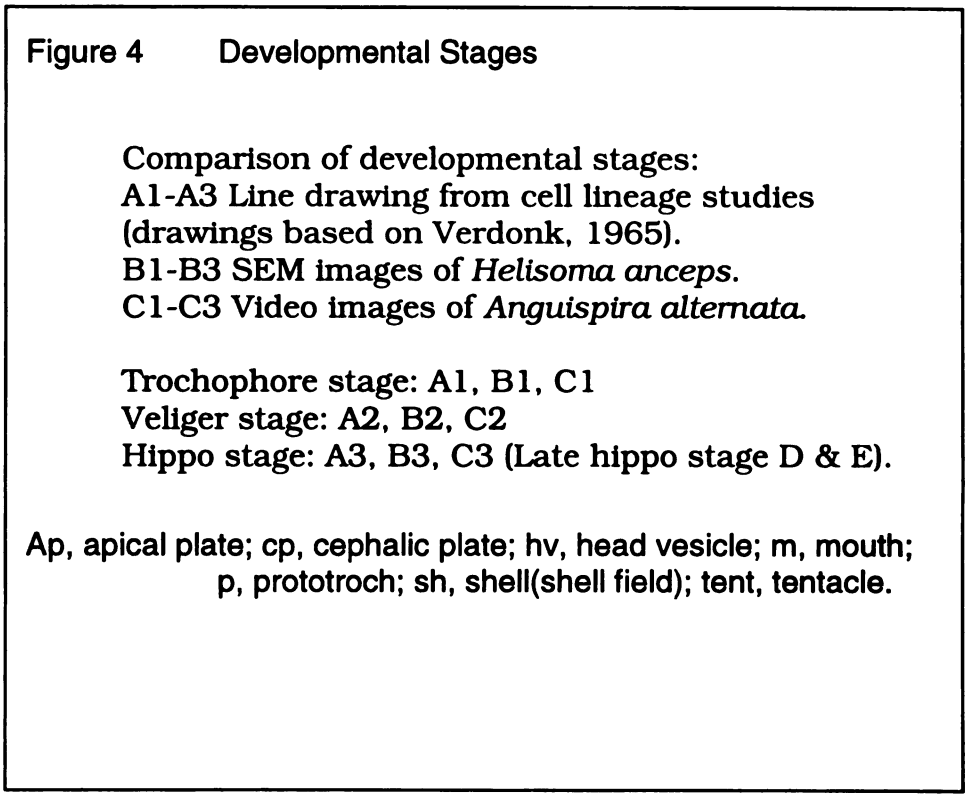

Figure 4 Developmental Stages

Comparison of developmental stages:
A1-A3 Line drawing from cell lineage studies (drawings based on Verdonk, 1965).
B1-B3 SEM images of *Helisoma anceps*.
C1-C3 Video images of *Anguispira alternata*.

Trochophore stage: A1, B1, C1
Veliger stage: A2, B2, C2
Hippo stage: A3, B3, C3 (Late hippo stage D & E).

Ap, apical plate; cp, cephalic plate; hv, head vesicle; m, mouth; p, prototroch; sh, shell(shell field); tent, tentacle.

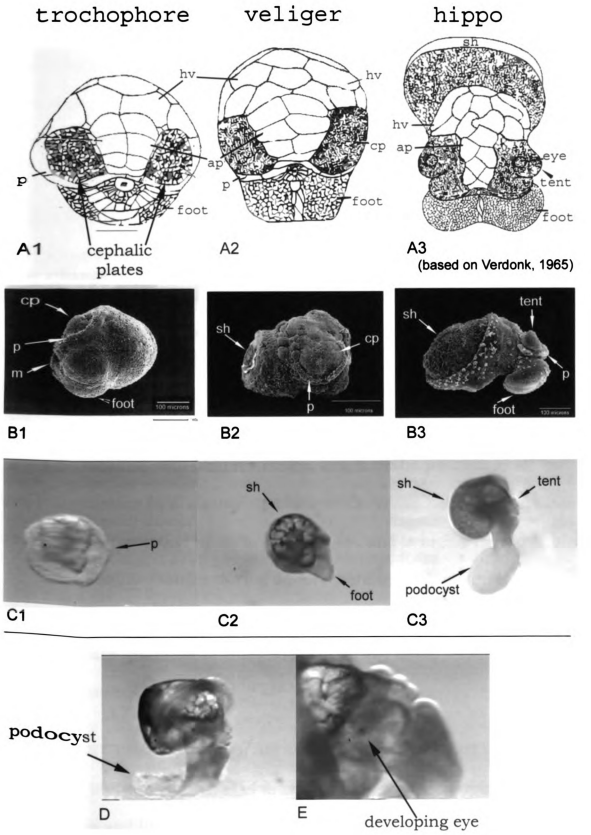
trochophore
veliger
hippo
hv
hv
sh
hv
ap
cp
eye
p
ap
p
tent
foot
foot
foot
A1
cephalic plates
A2
A3
(based on Verdonk, 1965)
cp
sh
cp
tent
p
p
m
sh
p
foot
foot
B1
B2
B3
p
sh
sh
tent
foot
podocyst
C1
C2
C3
podocyst
developing eye
D
E

If the

achie

durin

temp

techr

three

objec

com

cha

glas

*Chapter 2*

# RESEARCH APPROACH

*``The first object of the painter is to make a flat plane appear as a body in relief and projecting from that plane."*

*- Leonardo da Vinci*

If the change in position of the eyes in stylommatophoran snails is achieved by a change in timing and/or position of the cerebral ganglia during development, one must be able to determine the precise spatial-temporal changes that occur at the tissue level during development. The technical challenges are:

to visualize, with high resolution, cell & tissue position in all three dimensions in a manner that decreases researcher bias, increases objective interpretation by other researchers, and is highly reproducible;

to quantify changes during development by making direct comparisons between specimens in a time sequence; and

to make quantitative comparisons of these developmental changes between species.

## TRADITIONAL METHODS/APPROACHES & THEIR LIMITATIONS

The traditional method of drawing tracings of section images onto glass plates and lining up these plates is an old (and inventive)

techni

structu

techni

limited

struct

image

task r

must

some

resea

as op

of a c

exist

(See

biolo

any

the

reco

corr

older

comp

technique used to help visualize the three-dimensional (3D) position of structures, as well as to convey the information to others. This technique, (while useful in helping to visualize structures in 3D), is limited in precision of positional information and its ability to help with structural identification.

Tracing techniques are based on the creation of "wire-frame" images (called polygons on the computer) traced by hand, a laborious task requiring days to months to create even one model. The researcher must already have some idea of the identity and position (and sometimes even shape) of structures to trace. Thus, there is the risk of researcher-bias in drawing the structures as they are "believed" to be, as opposed to how they "really are". The technique requires the creation of a definitive "hard" boundary, whether or not such a boundary really exists, before the specimen can be reconstructed and visualized in 3D. (See Walter (1999) for a discussion on the use of "Fuzzy logic" in biology.) The final images are only of the tracings themselves, without any of the rest of the data including the data used in determining where the boundary was drawn. This limits the use of the resulting reconstructions as a "feedback" system allowing refinement and correction of the 3D model.

Other techniques based on outlines or boundaries, such as the older clay modeling technique, or more recently, the use of the computer to create "virtual" three-dimensional models, while adding to

the infor

"surface

based or

techniqu

enhance

efficient

determi

possible

changes

USIN

A

investig

traditio

the high

(LSM) w

softwar

C

resultir

of techn

dimens

comput

the information obtained are still subject to the same criticisms. The "surface rendered" computer models, while a big improvement, are still based on wire-frame (polygon) images. None of these methods allows techniques such as digital filtering and histogram manipulation to enhance visualization of unknown structures. Thus, they are less efficient in differentiation and determination of structures, and in determining the precise location of tissue positions needed to determine possible sites of tissue interactions such as "induction" during early changes in developing organ systems.

## USING LASER SCANNING MICROSCOPY & COMPUTER 3D "VOLUME" RECONSTRUCTION

A new approach was developed as part of the present investigation to overcome the limitations and drawbacks of these traditional methods of 3D visualization. This new approach combines the high resolution digitizing capabilities of a laser scanning microscope (LSM) with the power of computer three-dimensional "volume rendering" software (e.g., VoxelView/E by Vital Images Inc., Fairfield Iowa).

Once serially sectioned embryos are digitized by the LSM, the resulting images can be visually enhanced and manipulated by the use of techniques such as digital filtering or deconvolution. The two-dimensional (2D) images of the series are then "stacked" by the computer software to form a "virtual" three-dimensional whole embryo,

whi

con

wh

bo

rer

all

Th

car

vis

an

ba

inf

3D

co

all

du

dis

int

the

str

which is then manipulated as a single "volume" (or object) by the computer.

Unlike "surface rendering" techniques for 3D reconstruction, which use only the "trace files" (or hand-drawn tracing around the borders of structures) separated from the original data, "volume rendering" maintains all the information from the original 2D images, allowing for continual adjustment and manipulations of 3D renderings. There is no need to create definitive "hard" boundaries (the computer can display and manipulate gradations or "soft" boundaries) before visualization, thus lessening the risk of researcher bias. Digital filtering and segmentation routines (to help differentiate objects from their background, needed to get quantitative information) can utilize all the information in the data from all three dimensions.

After the section images of the embryos are digitized and "rebuilt," 3D volume rendering programs can make direct point-to-point comparisons between embryos in a developmental time sequence, allowing for accurate and precise tracking and analyses of changes during development. It is now possible on the computer to "digitally dissect" extremely small embryos, (i.e. to remove the structure(s) of interest from the rest of the embryo, or to remove structures obscuring the structures of interest). Thus creating an accurate 3D visualization of structural detail and spatial-temporal information.

Combining laser scanning microscopy to create high resolution digital images, with computer "volume rendering" techniques to create virtual 3D models of embryos, solves the challenges of creating accurate visualization of 3D structure, and allows precise, quantifiable comparisons within and between species in a manner unmatched by any other method.

*Chapter 3*

# MATERIALS AND METHODS

*"It is not enough to believe what you see. You must also understand what you see."*

*Leonardo da Vinci*

## SELECTION OF SPECIES COMPARED

### Stylommatophoran snails

The stylommatophoran snail used in this study was *Anguispira alternata* SAY 1816. These animals breed and lay eggs readily in the lab. Their eggs have a hard calcium crystalline shell, which allows relatively easy removal of the embryos without damaging them. The time to hatching is 28-34 days at 20-24 °C.

Adult snails were collected from Raynor Park woodlot, Mason, Michigan. They were placed in one gallon, three gallon, or ten-gallon glass bowls or tanks with 1-2 inches of commercial topsoil. Decaying leaves and bark collected with the snails was added to the tanks. De-ionized water was added every few days to maintain a moist environment. Snails were fed carrots and lettuce every two or three days, and any leftover food was removed at this time. White chalk was

added as a source of calcium. The top quarter inch of soil was removed every week and new clean topsoil was added to maintain soil depth.

The soil in breeding tanks was checked each day for new egg batches, which were placed in a covered stender dish lined with a piece of moist paper towel. Each batch was assigned a unique identification number with the date laid, tank number, and batch sequence. One or more eggs in each batch were opened to check stage of development. Each batch contained seven to twenty-five eggs, and it takes up to 34 days to hatch. To collect representative embryos of each day of development, the date the first embryo from a given batch was collected varied from day one to day fifteen. This staggering of collection starting dates allowed collection of embryos at all stages of development. One *A. alternata* embryo was sampled from each batch each day, thus embryos from batches at different stages of development were collected each day. Under a dissecting microscope, the embryos were removed from their eggshells with dissecting forceps by cracking open the shell and pouring the contents out onto a clean glass microscope slide in a glass petri dish. The embryos were washed clean of their capsule fluid using a Pasteur pipette to rinse them with distilled water.

### Basommatophoran snails

The basommatophoran snail used in this study was *Helisoma anceps* MENKE 1830. They reproduce readily in the lab and their egg

masses and capsules are transparent which makes it possible to view developing embryos *in vivo*. The egg masses and outer casing are semi-brittle, allowing removal of the embryos without damaging them. The snails hatched in seven to eleven days at 21-24 °C. Adult snails were collected from a pond in Vevay Township, Ingham County, Michigan. They were placed in a five, ten, or fifteen-gallon aquarium with under-gravel filtration, and accessory above-gravel filters. Aquarium heaters were used to maintain temperatures between 21-24 °C. Food such as lettuce, carrots, and TetraFin Basic Diet Goldfish Food was added every few days, and any left over food was removed. One-quarter of the water was removed and replaced with filtered pond water or de-ionized water every two weeks.

Breeding tanks were checked each day for new egg masses. Egg masses in this species are laid on the glass walls of the aquarium. Each egg mass contained nine to twenty egg capsules. The egg masses were removed by sliding a razor blade under them to separate them from the aquarium walls and placed in a stender dish with de-ionized water. *H. anceps* embryos were collected from one every four – six hours, to one a day per case. Each egg mass was assigned a unique identification number with the date laid, tank, and case sequence number recorded. Under a dissecting microscope, embryos were removed from their egg capsule by gently teasing apart the transparent case and capsule and pouring the contents out onto a clean glass microscope slide in a glass

petri dish. Embryos were washed clean of their capsule fluid using a Pasteur pipette to rinse them with distilled water.

## STAGING OF EMBRYOS

To compare development of the embryos within and between the two species of snails studied, forty to fifty embryos of each species were analyzed. Since *A. alternata* takes twenty-eight to thirty-four days to hatch at 20-24$^0$ Celsius, and *H. anceps* takes seven to eleven days at 21-24$^0$ Celsius, direct comparison based on time was not possible. A rough staging system was created based on the presence and level of development of structures such as the shell field/ shell material, mantle, stomodeum, radular sac/ radula, alimentary tract, heart, kidney, foot/ podocyst (*A. alternata*), pedal ganglia, statocysts, etc. This staging system followed the basic system of Morrill (1982), Cumin (1972), and Raven (1966).

### Video tape recording of live embryos prior to fixation

To compare fixed, sectioned, and 3D reconstructed embryos with the morphology of living embryos so as to determine the stage of development, live snail embryos of both species were recorded for two or three minutes on videotape. This was done after their release from the egg capsule and prior to fixation. In addition, some *H. anceps* embryos were recorded while still in their egg masses and capsules (which, as previously noted, are completely transparent). Videotaping was done

through a Wild M5-41059 dissecting microscope with a phototube attachment (404892) connected to a Javelin Ultrichip CCTV camera (JE-7442). This CCD camera was connected to a video recorder (VHS) and images were captured on T-120 VHS tape media recorded at Standard Speed (SP).

## Microscopy Preparation

### Fixation of embryos

The embryos were picked up with a glass Pasteur pipette (7.0 mm OD) and transferred to 1-DRAM glass vials, containing Formalin-Acetic Acid-Alcohol (FAA) Galigher formulation (Galigher and Kozloff, 1971) for fixation of the embryos. The fixative was washed out with, and the embryos stored in, 70% ethyl alcohol.

### Scanning Electron Microcopy

After fixation, some *H. anceps* embryos were prepared for scanning electron microscopy (SEM). They were dehydrated in a 70%-95%-100% ethyl alcohol series, with several changes of absolute alcohol. Specimens were critical-point dried in $CO_2$, sputter coated with gold, and imaged in a JEOL JSM-6400V Scanning Electron Microscope at 15kV accelerating voltage and a working distance of 39mm. Images were stored as Tagged Image File Format (TIFF) images on a 1-gigabyte optical disk, as well as on 100-megabyte ZIP™ disks.

## Light Microscopy

Embryos for light microscopy were dehydrated in 70%-95%-100% ethyl alcohol series, cleared with methyl benzoate, and infiltrated and embedded in Paraplast (HRI 8889-501006) or Paraplast Plus (56-57$^{0}$C) paraffin. Embryos were mechanically sectioned at a thickness of five or ten microns. Sections were attached to glass slides using Mayer albumen adhesive. Section ribbons were floated on water onto the slides, warmed, and dried on a hot plate set to 37$^{0}$C.

Slides were de-paraffinized in methyl benzoate. Sections were stained following Heidenhain's Iron Hematoxylin Method and counter-stained with Orange G, as outlined in Galigher and Kozloff (1971). Sections were cleared with Hemo-D clearing fluid and cover slips set with canada balsam.

## Digitization of Section Images

The sectioned embryos were imaged and digitized in transmitted (brightfield) (non-confocal) mode on a Zeiss 210 Laser Scanning Confocal Microscope (LSM) (Carl Zeiss, Inc., Thornwood, New York) using a 20X (0.5 N.A.) dry or 25X (0.8 N.A.) immersion objective lenses and the 633 nm line from the Helium-neon laser.

Images were collected starting with the middle section in the series, which acted as a template or fiducial image for alignment of the next two images. The last image aligned was used as the new fiducial

image for the next images. Aligning the images was done by hand using the LSM's "protect image" routine which allows the live image to be overlaid on the protected image.

**Image format conversion and transfer from the LSM to the SGI graphics workstation**

For volume rendering and image processing, the images created on the LSM were transferred to a Silicon Graphics 4-D 30 Personal Iris workstation running *IRIX 4.0.5C* (Silicon Graphics, Inc., Mountain View, CA) in one of two ways:

1) Images were transferred from the LSM directly to the SGI via a GPIB-AT (IEEE 488) (National Instruments Corp., Austin, TX) connection, using the program *VoxelScanZeiss*. This program automatically converts the native LSM picture file format "PIC" (not to be confused with PICT or PIC used by Apple, Inc. brand computers) into the native slice file format of the volume reconstruction program *VoxelView/E*.

2) Alternatively, images were transferred from the LSM to a Dell Dimensions P90 computer (PC clone running DOS 6.22 and Windows for Workgroups 3.11) via a GPIB-AT (IEEE 488) connection using the software program *LSM_NET* (Carl Zeiss, Inc.). Images were transferred in native LSM file format "PIC", and copies stored on 100-megabyte (MB) ZIP™ disks and on CD-ROMs. The software program *LSM_PC* (Carl

Zeiss, Inc.) was then used to convert the images to TIFF 6.0 compliant format (referred to as "TIFF", "TIF", "tiff", or "tif") (one of the formats suitable for use in the software programs *VoxelView/E* 2.1.2 and *VoxelMath* 2.1).

Unedited TIFF 6.0 image file copies were stored on 100MB ZIP™ disks and on CD-ROMs. Images converted to TIFF format were transferred to the Silicon Graphics, Inc., workstation. The SGI workstation and DELL PC clone were connected via direct Ethernet connection, facilitating image and file transfers between the computers using FTP (File Transfer Protocol) client software over a TCP/IP network.

## IMAGE PREPARATION ON THE SGI WORKSTATION

### Rectangular pixels to square pixels: Maintaining correct image aspect ratio

The LSM creates images of 512(x-axis) by 512(y-axis) pixels. The individual pixels on the LSM have a 3:2 x/y aspect ratio, making them rectangular. PC clones and workstations (such as the SGI) work with 1:1 x/y aspect ratio (square) pixels. Thus images created on the LSM and displayed on a PC clone, MAC, or SGI, will appear "squeezed" along the x-axis (see Discussion chapter).

This effect was corrected by "resampling" the number of pixels in the y-axis from the original 512 to 341 pixels returning the images back to their correct proportions. For the images transferred from the LSM

directly to the SGI via the GPIB AT connection, the program *VoxelScanZeiss* performed the resampling from 512 x 512 pixels to 512 x 341 pixels automatically. The images transferred from the LSM to the DELL PC clone then to the SGI were corrected using *VoxelMath 2.1* routine Merge Operations> Resample XY.

### Voxel-padding in VoxelView

The program VoxelView requires the dimensions to be evenly divisible by four. Since the converted images are 512 x 341, the y-axis dimension has three pixels added by *VoxelView/E* (although only when viewing and saving) making the images 512 x 344 in memory. These added pixels were removed when the images were "cropped" to remove the LSM menu bar from the bottom of the images or to remove extra "space" around the specimen or when creating a sub-volume of the specimen. The final y-axis dimension was cropped to a number evenly divisible by four.

### The importance of the order of images

In this study, most of the images were collected from the middle of the embryo back to the beginning and then to the end. This allowed alignment of the subsequent sections to the largest section with the most structures present for registration (see Figure 28). Image files were then renumbered individually or by the freeware program "Rname-IT" (by Steve H.).

The program *VoxelView/E* reconstructs (or builds) the volume from back-to-front by laying down whichever image has the file name "1" (or "0") then stacking the file named "2" on top of it, and so on, stacking the highest numbered (named) file on top (Figure 26 A). If this is not the correct order for the images to be stacked, the resulting embryo will have its left-right axis reversed. This is corrected by renaming the files in reverse order, i.e., if there are fifty images in the set, image number "1" becomes image number "50", and image number "50" becomes image number 1, etc., as shown in Figure 28c. This was done with the program *VoxelMath* 2.1 by "flipping" the images along their z-axis ("Flip-Z").

**Filling in the Z dimension: Interpolations**

The software program *VoxelView/E* calculates the dimension of the 3D voxels from the dimensions of the 2D pixels such that the resulting voxels are iso-dimensional. Since the pixel resolution (i.e., x-axis dimension or distance value of the specimen represented by the pixel along the x-axis) is smaller than the distance between the images or z-interval (in this study z-interval equaled the thickness of the sections), and thus each voxel will only be as "thick" as the pixels are wide, the resulting 3D reconstruction will appear "flattened" in the z-axis. To fill out the space to better represent the true thickness of each section "interpolated" images are calculated to fill in the distance.

The number of interpolations needed was determined by dividing the z-interval or step size (which in the present study since using mechanically sectioned embryos equaled the section thickness) by the "pixel resolution" (Table 1) or full field view covered or represented by each pixel in the x-axis (see Table 2). The size of the pixels was determined by dividing the total x-axis distance of the sample in the image (the screen width or "full field width" of the LSM monitor) by the number of pixels (512) (See Table 1). The full field width of the image was measured using the function "Measure" of the LSM 210. *VoxelMath* 2.1 Merge Operations > Resample Z was used to create interpolations using non-integer resample values.

***Reduction of interpolations: Sub-sectioning the sections***

The 20X and 25X objectives were used to create higher resolution images of just the developing eye-tentacle region of some of the embryos. Since both the 20X and 25X objectives have a depth of focus (depth of field) smaller than the 10-µm thick sections (see Table 1) two images of each section were created: one at the top of the section, and one focused 5 microns into the sample. This allowed for a reduction by half of the number of interpolated images per "real" image required (see Table 2) thus creating more accurate reconstructions (comparing with whole mount, video taped images, or SEM images of embryos of the same stage).

Table 1 Calculation of Pixel Size (resolution) in the X-axis.

| Depth of Focus | | | | Image Resolution | | | |
|---|---|---|---|---|---|---|---|
| Objective Lens | N. A. | $\lambda$ | Dz(nm)= $\lambda$/N.A.$^2$ | LSM Zoom | Screen width μm | # of Screen pixels | Pixel width μm |
| 5x | 0.15 | 633 | 28133.3 | 20 | 2838.8 | 512 | 5.545 |
| 10x | 0.3 | 633 | 7033.3 | 20 | 1419.4 | 512 | 2.772 |
| 20x | 0.5 | 633 | 2532.0 | 20 | 709.7 | 512 | 1.386 |
| 25x | 0.8 | 633 | 989.06 | 20 | 567.8 | 512 | 1.109 |

N. A. = numerical aperture $\lambda$ = wavelength of light Dz = depth of field in focus

Table 2 Calculation of Z-axis Interpolations

| Pixels to Voxel Interpolations | | | | | | |
|---|---|---|---|---|---|---|
| Objective Lens | LSM Zoom | # of screen pixels | Pixel Size (μm) x-axis resolution | z-axis resolution (μm) (z interval) | z-interval ÷ pixel size | = # of interpolations (Z axis) |
| 20x | 20 | 512 | 1.386 | 10 | 10 ÷ 1.386 | =7.215 |
| 20x | 20 | 512 | 1.386 | 5 | 5 ÷ 1.386 | =3.607 |
| 25x | 20 | 512 | 1.109 | 10 | 10 ÷ 1.109 | =9.017 |
| 25x | 20 | 512 | 1.109 | 5 | 5 ÷ 1.109 | =4.508 |

**Precise adjustment of section image-alignment using "Negative" interpolations**

For very precise alignment [of sections], the program *VoxelMath* 2.1 was used to shift or rotate the problem slice the exact number of voxels needed to "best fit" alignment. By using a negative integer for interpolation in the "_dimensions" file of a volume data set, the programs *VoxelMath 2.1* and *VoxelView/E* will display the 3D volume with "empty" space between the sections instead of interpolated images. By viewing the embryo with empty space between the "real" slice images it is easier to determine which sections are out of alignment with the other sections.

Combining the use of negative interpolations with the ability of *VoxelMath 2.1* to view 2D images of the embryo "re-sectioned" in the X-Z or Y-Z axis, and its ability to determine the X,Y, and Z coordinates of all voxels by simply placing the cursor in the section image window on the part of the slice out of alignment and reading the voxel coordinates displayed, it was possible to count the exact number of voxels an image needed to be shifted to adjust its alignment with the rest of the embryo (Figure 29). (It was very helpful to change all the scale values in the "_dimensions" file to the value "1.0" so the coordinate readout equaled the number of voxels in each direction as opposed to the "real world" distance.)

Once the number of voxels a given slice image needed to be shifted was determined, it was possible to use the "x-shift" or "y-shift" math function in the Math Ops panel of *VoxelMath 2.1* to correct its alignment as compared with whole mount embryos, video images, or SEM images of other embryos at the same stage of development.

## IMAGE PROCESSING AND ANALYSIS

### Determination and delimitation of cell and tissue types

#### *3D visualization of 2D tracings: The "Geometry" Function*

In early stages of embryo-genesis many structures have not developed to the point of being readily recognizable (compared to the adult or even older embryos). To help make comparisons of structures at different stages of development, and thus help identify unknown structures in younger stage embryos the function "Geometry" in *VoxelView/E* was used. This feature made it possible to trace known and unknown features in the 2D section images and immediately visualize their position in 3D relative to each other, and to the whole reconstructed embryo. When the whole virtual embryo is rotated, the image of traced structures in 3D rotates in synchrony (Figure 5).

#### *Enhanced visualization*

The LSM creates 8-bit images having 256 shades of gray. While the developing nervous system and eyes are distinguishable by

morphological, positional, and in some cases cellular cues, the grayscale value of each pixel/voxel (referred to as "voxel-value" in both *VoxelView/E* and *VoxelMath 2.1*) overlapped with other structures in the embryo. This overlapping of voxel values limited the programs *VoxelView/E* and *VoxelMath* 2.1's ability to differentiate and delimit by voxel value or voxel position the developing structures of the eye-tentacle complex when three-dimensionally reconstructed.

To help visualize and differentiate the different structures two techniques were employed to enhance their visualization (and thus relative position) within the embryo: 1) "Digital Dissection" , and 2) "Voxel-Value Range Partitioning" (assigning different ranges of voxel values to different structures).

Digital Dissection

To enhance visibility of the developing eye-tentacle complex, the nervous system and eyes were "digitally dissected" from the rest of the embryo (i.e., the images of the cells forming the nervous system were isolated from the rest of the embryo and made into their own separate volume). The dissection of structures digitally is best performed before adding interpolations if there are a large number of images.

Using the image manipulation program, Adobe *Photoshop* (version 3.0 or higher) or in some cases *VoxelMath*, each image was opened, its histogram inverted, and the pixels of the image that represent non-nervous system tissue were "painted over" with (i.e., converted to) the

same pixel color or value as that of the background of the image (i.e., turned black -- grayscale value=0) (Figure 21). The set of images created was then saved as a new independent data set (volume), which consisted of just the developing nervous system while still in correct spatial registration with the rest of the embryo. Adding Z-axis interpolations for this new set of images creates a three-dimensional volume of just the nervous system.

Voxel-Value Range Partitioning

To highlight the separate structures (e.g., the eyes, nervous system, prototroch) following their digital dissection, each was assigned to a different range of non-overlapping voxel values. The cells of the developing eye vesicles were assigned values in the range of 1-63 (0 being the value of the background), the cells of the developing nervous system in the range of 64-127 (Figures 22-25), and the rest of the embryo assigned values of 128-255. The assigning of structures to separate ranges of voxel values was accomplished with the program *VoxelMath* 2.1 in one of two ways:

1) Assigning a different range of voxel values to different volumes; or

2) Assigning a different range of voxel values to structures within the same volume by using "selective application" of mathematical operations using "Grease Pencil."

*Assigning different ranges of voxel values to different volumes*

Each volume had its range of grayscale values (histogram range) shifted accordingly by applying the mathematical operations as listed in Table 3.

Table 3: Sub-dividing Histogram range: Mathematical operations

| Structure/ organ | Histogram range 1-63 | Histogram range 64-127 | Histogram range 128-255 |
|---|---|---|---|
| Eye anlagen | * 63 / 255 | | |
| Nervous system | | * 63 / 255 bias=64[1] | |
| Rest of embryo | | | * 127 / 255 Bias = 128 |

*Assigning different ranges of voxel values to structures within the same volume: Selective application of mathematical operations using "Grease Pencil"*

For younger embryos, which are smaller and thus comprised of fewer images, assigning voxel values to given structures was accomplished by first shifting the whole volume into the range of voxel values 128-255. Then, using the "Grease Pencil" function in *VoxelMath* 2.1 to apply the current Ops List only to those voxels selected, the structures of the eyes, ganglia, prototroch etc., were shifted into their own range of voxel values, as stated above.

To delineate the borders of the cephalic plates the function Grease Pencil was used to convert the voxels representing the cells of the prototroch (which are the ventral, medial to lateral borders) to voxel value 1, and the last columnar cells of the dorsal most edge of the cephalic plates to voxel value 2. Each had a unique color assigned using the look-up table (LUT) features of the Histogram function of *VoxelMath*.

[1] "Bias" function adds the Argument value to each non-zero voxel value. This increases equally all non-zero voxel values, thus shifting the histogram range from 0-63, to 64-127.

**Recombining volumes Visually vs. Structurally**

Which software analysis functions will be applied (i.e., how the 3D reconstruction will be analyzed) determines what, if any, slice image (2D) preprocessing is required. Some functions of the volume reconstruction software, e.g., the ability to re-slice the virtual embryo in any plane ("VoxelSlicer") and analyze the resulting images can only be applied to a single volume in memory. Other functions allow for the formation of images composed of several volumes in memory, i.e., "Multi-channel View." The latter function requires fewer processing steps and so is faster, but limits the types of analysis available. The following functions cannot be used on a Multi-channel rendered volume: VoxelSlicer, VoxelSeed, VoxelTrace, Histogram, any option in Manage Data (Add Data set, Encode Volume, Save Volume, etc.), or the add-on module *VoxelAnimator*.

***Visual merging: Multi-channel viewing***

The individual volumes of the nervous system, eyes, and whole embryo had separate color look-up tables and opacity settings applied. The eye vesicles were assigned a green spectrum. The developing nervous system was assigned a red spectrum, and the volume of the whole embryo was left in gray -scale. The prototroch was colored a solid blue, and the dorsal border of the cephalic plates a solid magenta within the whole embryo volume.

All the volumes were recombined visually as a single volume, with their correct position maintained relative to each other, using the function "Multi-channel View" in the program *VoxelView/E.*

### *Structural merging: Merge Volume (VoxelMath)*

The separate volumes (see section Digital Dissection above) of the eyes, ganglia, and the body of the embryo were recombined into a single volume (one set of images) using *VoxelMath*'s "Merge Volume> option "Montage" with Alternate Mode: Scalar=255. The offsets in each volumes "_dimensions" file was set to "0" creating 100% overlap. This maintains the correct spatial registration of all structures to each other.

## Image rendering

### *Single Images and Animations*

3D images rendered with *VoxelView/E* were either saved using the Animations> Save Picture command, or 3D rotation images were generated by using the Animations> Save Images to Disk command. In the latter function, the computer generates multiple images "rotated" around either the azimuth or elevation in steps of the number of degrees specified (from 1 to 360). The combined set of images can be viewed in quick secession as an "animation" thus aiding the visual 3D effect. In both rendering functions the images are saved as SGI format (.rgb) images.

Image flipping between SGI and PC

Images of the rendered virtual embryos which were saved in the SGI image format RGB (. rgb) were converted to the TIFF image format by the SGI program IMGCOPY before transfer to the PC. Since the SGI workstation reads images from the lower left corner, and PC and MACs read images from the upper left corner, the images transferred to the PC needed to be flipped vertically. This was done with the program Adobe *Photoshop* (3.0 or above), or by other image processing programs.

*Annotations*

The annotations (axis lines, measurement lines, and bounding box) were created using the Measurements> Annotations function in *VoxelView/E*. The color of the lines can be selected, as well as distance measurement values and calibration lines. The measurement values are based on the values in the volume dimension file ("_dimensions") for the axes scale values. The labels of the axis determined by the axes label fields in the volume dimension file ("_dimensions"). The axes units value is also determined by the text in the "units" field of the dimensions file.

[IMAGES IN THIS DISSERTATION ARE PRESENTED IN COLOR]

*Chapter 4*

# RESULTS

*There is a single light of science, and to brighten it anywhere*

*is to brighten it everywhere."*

*-Isaac Asimov*

## PART I: EFFICACY OF 3D VOLUME RENDERING FOR THE STUDY OF SNAIL EMBRYOLOGY

The use of three-dimensional reconstruction, which combines LSM digital imaging and the functions in the volume rendering software program VoxelView/E 2.1.2 provided the following features for this investigation.

### Enhanced visualization and identification of developing structures

#### *Visualization of unidentified structures in 3D*

The "Geometry" function of the software program made it possible to trace known or unknown features in the 2D section images and immediately visualize their position in 3D relative to each other, and to the whole reconstructed embryo. When the whole virtual embryo is rotated, the image of traced structures in 3D rotates in synchrony (Figure 5). The 3D views of unknown structures were then able to be

compared with older more developed embryos in 3D, thus aiding the identification of structures unknown in the younger stage embryos.

*Visualization of internal structures by digital "dissection"*

Embryos the size of the pulmonate snail embryos (80-300μm) studied in this investigation are far to small to dissect in real life. Once the 2D images are "rebuilt" into 3D virtual embryos, it is possible to remove the outer tissues and organs leaving only the system of interest, in this case the developing nervous system (Figure 6 ). This made it possible to determine the actual shape of the developing cerebral ganglia and the trajectories of their "branches" or nerve tracks (Figures 7, 8, 9).

*Visualization of structures with increased contrast by digital "staining"*

Many structures of interest in this investigation were groups of cells not yet developed to the point where they differentially stain. The ability digitally to add or modify color for the purpose of improving contrast enhanced the visualization of the structures, and aided in their identification (Figures 8 & 9). A good example, the cells of the prototroch, are readily identifiable in a given 2D section image (Figure 10) as large clear ciliated cell(s). In 3D reconstructions and SEM images (Figure 11) it clearly delineates the ventral and posterior-lateral border of the cephalic plates (Figures 8 & 10) Adding color to it to differentiates it from the rest of the ectoderm greatly enhancing its

visibility in the reconstructed embryo and thus improving its ability to serve as a marker for the borders of the cephalic plates.

### *Visualization of slices taken in planes independent of the original plane of sectioning by "re-sectioning"*

The virtual embryos were "re-sectioned" in planes perpendicular to those that the "real" embryos were physically cut. The small size of the snail embryos in this investigation makes determining the orientation of the embryos in mounting medium, and thus determining the plane of sectioning, a major obstacle. Re-sectioning embryos makes localization and identification of structures easier. This capability is one of the great advantages of digital imaging. "Matched" sets of slice images in different planes can be viewed simultaneously (Figure 12).

### *Visualization of the whole embryo and any "sub-sets" of it, from all angles simultaneously*

The ability to visualize the 3D shape of structures from multiple angles simultaneously in separate viewing windows greatly aided in their identification (Figure 13 & 14). Multiple views of the same embryo or different embryos (or parts there of) side by side was very useful, especially for side by side comparisons between embryos at different stages of development.

**Ability to determine in all three dimensions the precise spatial-temporal position and development of structures**

The ability to visualize the virtual embryo utilizing the features and functions listed above (e.g., with overlying structures at various degrees of being "dissected" away or rendered transparent and structures of interest visually enhanced by the addition of color) allowed the discovery of : 1) the exact position within the cephalic plates of the invagination of the eye-vesicles (and distinguishing them from other ingression of groups of cells), and in relation to the position of the cerebral ganglia (and their branches) (Figures 8, 9, 10), and 2) the exact position (and shape) of the cerebral ganglia before, during, and after eye-vesicle invagination (Figures 7, 8, 9, 10, 13, 14, 15).

**Ability to make direct quantitative measurements and comparisons**

***Measuring the accurate distance between structures from sectioned embryos***

One of the continuing problems in microscopy is the ability to determine distances among three-dimensional structures. By using the "Trace" function of the volume rendering software it is possible to select any two points (voxels) within the 3D volume and have the computer determine the distance between them in three dimensions (Figure 16). Since structures are more complex than just two points in 3D space, the Trace function allowed multiple distance measurements to be made

and the resulting values analyzed statistically. The results can be formatted for importation into statistical analysis packages or spreadsheet programs.

The distance of the cerebral ganglia from the buccal mass was measured using the "Trace" function. The statistical analysis of the results was automatically calculated (Figure 16). The distance from five different locations from the edge of the buccal mass to five locations of the cerebral ganglion (two from the top side, and three from the bottom) were measured. The mean average distance of all the measurements was 48.7µm. The longest distance measured was 71.7µm (top most edge of cerebral ganglion, thus furthest away), and the shortest distance measured 33.8µm. These distances compare well to the overall size of the embryo.

### *Volumetric measurements of developing organ systems (morphometrics)*

The capability to easily determine volume differences and changes of structures (within and between species) used in morphometric analysis was demonstrated by using the "VoxelSeed" function. In addition to displaying the results of statistical analysis, the program changes the opacity settings of the voxels measured and those that were not and displays the 3D volume showing which structures were measured within the whole volume (or sub-volume) (Figure 17). Results of the statistical analysis of the comparison of developing nervous

system (NS) and eyes in an *H. anceps* embryo are shown in the Table 4. The measurement of the nervous system on the right also included ganglia tissue besides the cerebral ganglion, thus accounting for its much larger volume measurement of 144305.00 $\mu m^3$. The measurement of the left cerebral ganglion only included the left cerebral ganglion tissue and thus had a smaller measured volume of 45047.00 $\mu m^3$. The right and left eye-vesicles where found to have very similar measured volumes

(14154.00 $\mu m^3$, and 14342.00 $\mu m^3$, respectively).

Table 4 VoxelSeed Summary of Statistical Analysis

| **Morphometric Statistics of 4 Selected Volumes** | | | | | |
|---|---|---|---|---|---|
| Minimum | Maximum | Mean | Median | Mode | Std. Dev |
| 14154.00 | 144305.00 | 54462.00 | 14342.00 | 14154.00 | 61629.96 |
| **Voxel - Metrics of Selected Points** | | | | | |
| Total Voxels Rendered = | | 160154 | Total Integral = | | 1.219689E+07 |
| Minimum | Maximum | Mean | Median | Mode | Std. Dev. |
| 2 | 118 | 76.16 | 79 | 64 | 0.10 |
| **Morphometric Summary of 4 Individual Volumes (μm3)** | | | | | |
| Left Cerebral Ganglion | | 45047.00 | | | |
| Left Eye | | 14342.00 | | | |
| Right Eye | | 14154.00 | | | |
| Right NS | | 144305.00 | | | |
| | | | | | |

## PART II: DEVELOPMENT OF THE EYE-TENTACLE COMPLEX IN THE AQUATIC BASOMMATOPHORAN SNAIL *HELISOMA ANCEPS* AND THE TERRESTRIAL SNAIL *ANGUISPIRA ALTERNATA*

### General pattern of pulmonate development

To compare development of the embryos within and between the two species of snails, forty to fifty embryos of each species were analyzed to determine stages of development. The eye-tentacle formation occurs in stages (late) A & B & C (Figure 4 A-C:2&3), which corresponds to "trochophore," "veliger" and "adult-like form" of Morrill (1982), "trochophore," "veliger" and "hippo" stage of Raven (1949) and "E2," "E3" to "E5" of Cumin (1972).

Stage A (trochophore stage):

The embryo develops into a trochophore larva following gastrulation. At this stage the following structures first become visible: the protonephridia (larval kidneys); the "prototroch", a band of ciliated cells which delineates the dorsal and lateral sides of the stomodeum and the ventral and lateral borders of two bilateral regions of numerous small cells -- "cephalic plates"; a line of ciliated cells running longitudinally along the ventral side of the foot anlage is present; and the shell gland is visible as a concave or invaginated region of the posterior ectoderm.

Stage B (veliger stage):

At this stage of development, the foot is visible as an outgrowth below the stomodeum (Figure 4: A2, B2, C2). In *Anguispira alternata* the foot is more developed than in *Helisoma anceps* mainly due to the presence of the "podocyst" (an enlargement of the end of the foot found in Stylommatophora) (Figure 4). The pedal ganglia are separate from the ectoderm of the foot (Figure 18) and the statocysts are visible with obvious lumina. The stomodeum is continuous with the esophagus, and the radular sac is visible as a posterior outgrowth of the floor of the stomodeum (Figure 13). There is shell material of larval shell or "protoconch" visible covering the shell field. The prototroch is more distinct in *H. anceps* (Figure 4) and clearly delineates the ventral borders of the now more distinct cephalic plates. The prototroch is not as continuous in *A. alternata.*

At this stage of development the relatively few cells forming the cerebral ganglia ( ~25-50) have separated from the overlying ectoderm. These cells, along with the cells of the larger (more developed) pedal ganglia, have larger nuclei than the cells of the surrounding mesoderm or ectoderm. Their cytoplasm appears lighter stained than the ectodermal cells or surrounding mesodermal cells, with a single large and dense staining nucleolus (Figures 18 & 19), as has been commonly reported for many other gastropods (Henchman, 1890; Raven, 1966).

In both species studied, under the developing tentacle (dorso-posterior pair in *A. alternata*) of the latero-ventral region of the cephalic plate, a large indentation has formed (Figures 10 & 11, and 18a & 27a). This large indentation appears in more developed embryos as a larger tube-like pocket. From the 2D sections cells appear to be proliferating at the inner-most end of the indentation/tubes along-side the developing cerebral ganglia. From the 3D reconstructions a large branch of the cerebral ganglion can be seen projecting directly towards this indentation (Figures 9 & 11). (See discussion chapter for consideration if these develop into what is described as "cephalic tubes").

Stage C (Hippo stage):

This stage corresponds with Morrill's (1982) "Adult-like form" and Cumin's (1972) "E5" stage. At this stage, the shell covers a third or more of the embryo (Figure 4:A3-C3). The foot, as well as the podocyst of *A. alternata*, is much larger than in the previous stage, and the head vesicle (a swelling of the head ectoderm, dorsal and posterior to the cephalic plates) is more pronounced (Figure 4: C3, D, E). The anterior-most region of the ventral surface of foot of *H. anceps* is ciliated. Radular material, forming the radula, is now visible, and the nephridial organs are more pronounced. The prototroch is no longer an uninterrupted band in *H. anceps*, (Figure 4: B3) and is further reduced in *A. alternata*.

Selection

Thirty to forty embryos of each species were selected from these stages. They were imaged on the LSM and further categorized as to suitability for reconstruction (i.e., overall quality of sectioning, staining properties, etc.), whether in whole or in part. Five to ten of each species were reconstructed using "volume rendering" 3D reconstruction software to determine the precise location of the points of invagination of the eye-vesicles within the cephalic plates and the exact position of the cerebral ganglia at that time. SEM images were also collected of *H. anceps* (Figure 4; Figure 18:b; Figure 11:d-f); these were compared to the 3D reconstructed embryos to help determine the level of development, as well as the timing and positioning of points of invagination of the eye-vesicles (Figures 7, 10, 11, 20).

## Eye-tentacle complex development in the stylommatophoran snail *Anguispira alternata*

In stage B embryos (early veliger) a very small ingression of cells was observed in the dorso-medial region of the cephalic plates (Figure 8). This ingression consisted of 4-5 cells and was seen in two contiguous sections. Thus it extended between only 10-20μm. This structure was not seen in any younger or older stage embryos.

3D reconstruction revealed that this ingression of cells lay just above a group of cells forming a portion of the cerebral ganglion. It also revealed that this dorso-medial ingression was relatively far removed

from the dorso-lateral location of the developing eye in later embryos. (See Chapter 5 for discussion of the possible identity of this ingression of cells.) A small line of cells "branching" off the cerebral ganglia as can be seen directed at (almost in contact with) this small medial ingression of cells (Figure 8). At this stage of development, there is no similar branch or line of cells directed at the dorso-lateral point within the cephalic plates where the invagination of the eye-vesicles will occur.

The earliest signs of the development of the eye-vesicles were found in late stage B (veliger stage) to early stage C embryos. The eye-vesicles were first identifiable as small invaginations of the ectoderm forming a rosette of cells which pinch off from the ectoderm (Figure 10). The eye-vesicles were visible spanning three to five sections, thus about 30-50μm in size. They consisted of approximately fifty to seventy-five cells each. There is a lumen formed which increases in size with age after the vesicle has separated from the overlying ectoderm. Pigmentation first was visible in late stage C embryos. Later still, a lens formed in the middle of the lumen.

The point of invagination of the eye-vesicles was in the dorso-lateral edge of the cephalic plates (Figure 10). The location of where the eye-vesicle formed <u>was not</u> on the tentacle anlage, but posterior to it (as seen in Figures 10 & 11). The cerebral ganglia <u>were not</u> found in contact with or near the developing eyes. In over forty embryos analyzed in both 2D sections as well as in the 3D reconstructions(Figures 8, 9, 11),

spanning the stages of development from A to late C, neither the cerebral ganglia, nor any of their parts (branches) were ever found in contact with or even close to the eye vesicles, or the overlying ectoderm from where they arose.

**Eye-tentacle complex development in the basommatophoran snail *Helisoma anceps*.**

In *H. anceps*, the earliest signs of the development of the eye-vesicles were found in late stage A embryos. The eye-vesicles were first identifiable as small invaginations of the ectoderm forming a rosette of cells which pinch off from the ectoderm (Figure 7 b). The eye-vesicles spanned two contiguous sections, thus about 10-20µm in size, and consisting of approximately ten cells. There is a lumen formed, which is larger in size in older embryos. In stage B embryos the eye-vesicles are larger, composed of approximately twenty to thirty cells, and have separated from the overlying ectoderm. In late stage C embryos the first signs of pigmentation becomes visible. Later still, a lens forms in the middle of the lumen.

The point of invagination of the eye-vesicles was in the dorso-lateral edge of the cephalic plates, slightly dorso-lateral and posterior to the tentacle anlagen (Figure 11:d-f; Figure 15). Comparison of the SEM images (Figure 11:d-f) with the 3D reconstructed embryos and 2D

images of sections (Figure 7) confirms this relatively early time of eye-vesicle invagination compared with *A. alternata*.

At the time of invagination of the eye-vesicles the cerebral ganglia were found were in direct contact (Figure 7). The cerebral ganglia were found to be in contact with the eye-vesicles even after the eye-vesicles had separated from the overlying ectoderm in older embryos (Figures 12,13, 14).

Table 5 Developmental stages

| | A (trochophore) | B (veliger) | C (hippo) |
|---|---|---|---|
| *Anguispira alternata* | development of cerebral ganglia | ingression of unknown cells | Pigmentation of eyes |
| | | eye-vesicle invagination | Radula teeth formed |
| | | tentacle development | |
| | | large indentation/ "cerebral tubes" | |
| *Helisoma anceps* | development of cerebral ganglia | tentacle development | Pigmentation of eyes |
| | eye-vesicle invagination | | Radula teeth formed |
| | | large indentation/ "cerebral tubes" | |

## Comparisons

In both species studied the eye-vesicles developed from invaginations of the ectoderm in the dorso-lateral region of the cephalic plates dorso-lateral to the tentacle anlagen. In *Helisoma anceps* this

invagination occurred early in development (trochophore - stage A) and was laterally asynchronous -- the left side developing somewhat earlier than the right. In *Anguispira alternata* the invagination occurred relatively later in development (late veliger - stage B) and was laterally synchronous -- both sides occurring at the same time.

In *H. anceps* the developing cerebral ganglion tissue was in contact with the presumptive eye-tissue throughout the period of development looked at during the present study. In contrast, the presumptive eye-tissue of *A. alternata* was never in contact with developing cerebral ganglion tissue.

In both species a large indentation of cells in the ventro-lateral region of the cephalic plates (corresponding to the "cerebral tubes") appeared during the veliger stage (stage B).

# PLATES

IMAGES IN THIS DISSERTATION ARE PRESENTED IN COLOR

Figure 5 "Geometry" Function in VoxelView/E

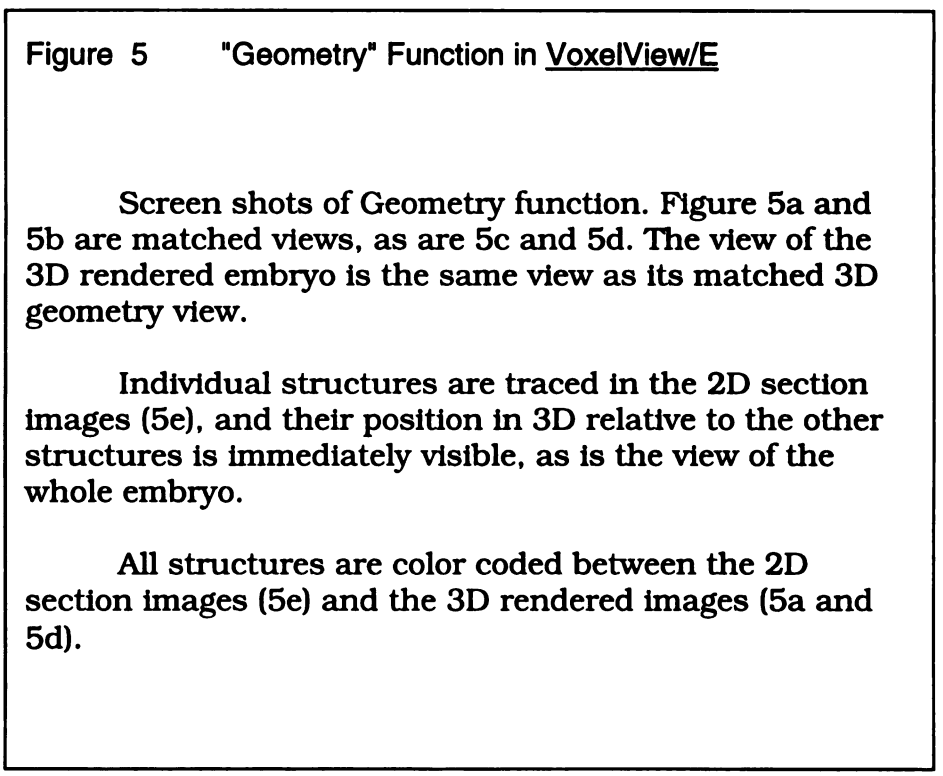

Screen shots of Geometry function. Figure 5a and 5b are matched views, as are 5c and 5d. The view of the 3D rendered embryo is the same view as its matched 3D geometry view.

Individual structures are traced in the 2D section images (5e), and their position in 3D relative to the other structures is immediately visible, as is the view of the whole embryo.

All structures are color coded between the 2D section images (5e) and the 3D rendered images (5a and 5d).

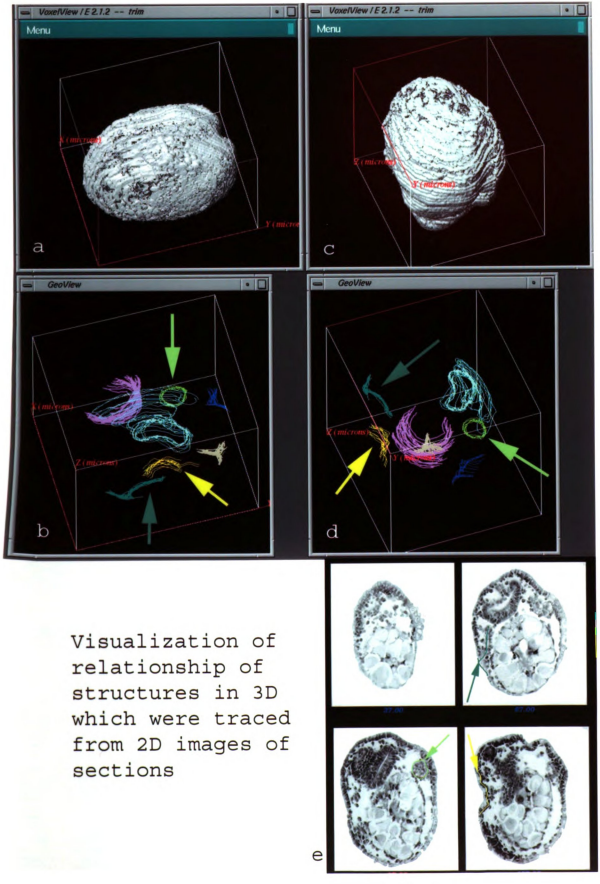


Visualization of relationship of structures in 3D which were traced from 2D images of sections

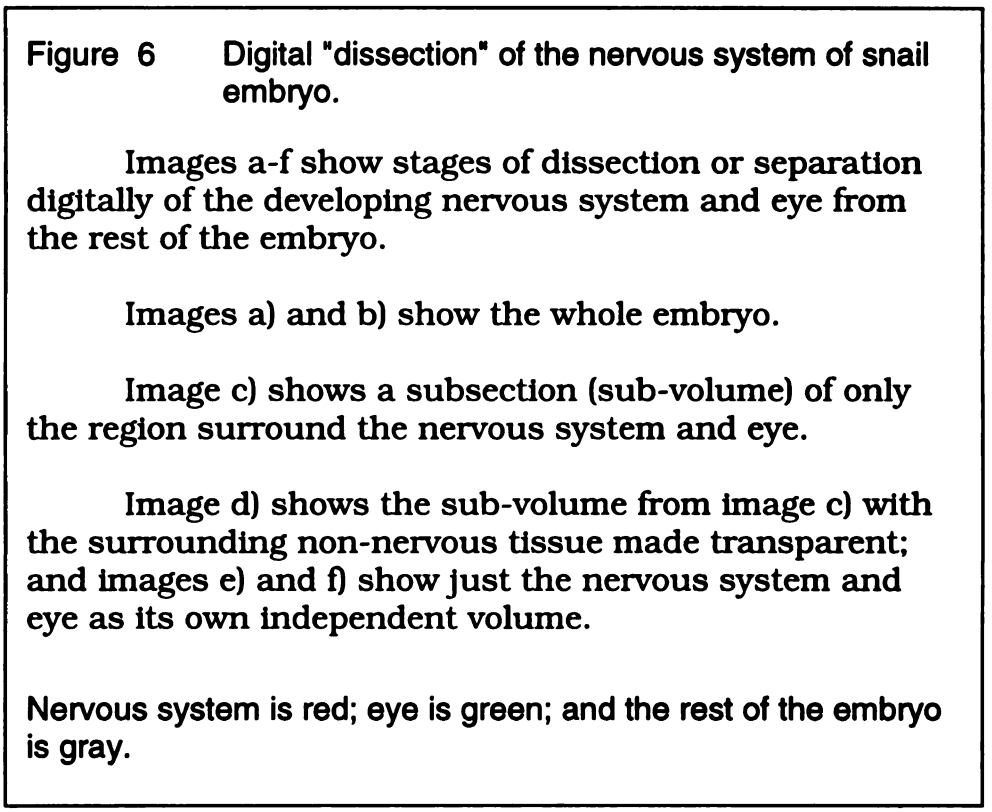

Figure 6 Digital "dissection" of the nervous system of snail embryo.

Images a-f show stages of dissection or separation digitally of the developing nervous system and eye from the rest of the embryo.

Images a) and b) show the whole embryo.

Image c) shows a subsection (sub-volume) of only the region surround the nervous system and eye.

Image d) shows the sub-volume from image c) with the surrounding non-nervous tissue made transparent; and images e) and f) show just the nervous system and eye as its own independent volume.

Nervous system is red; eye is green; and the rest of the embryo is gray.

# Digital "dissection"

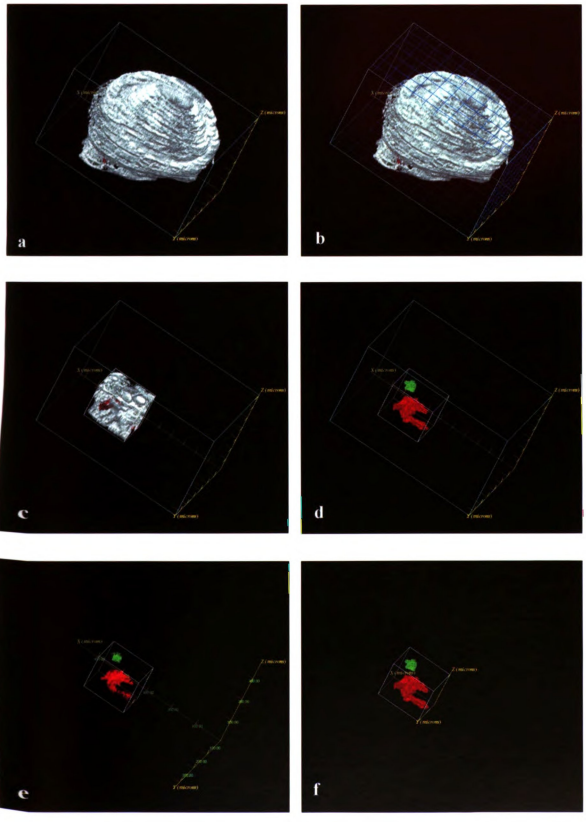

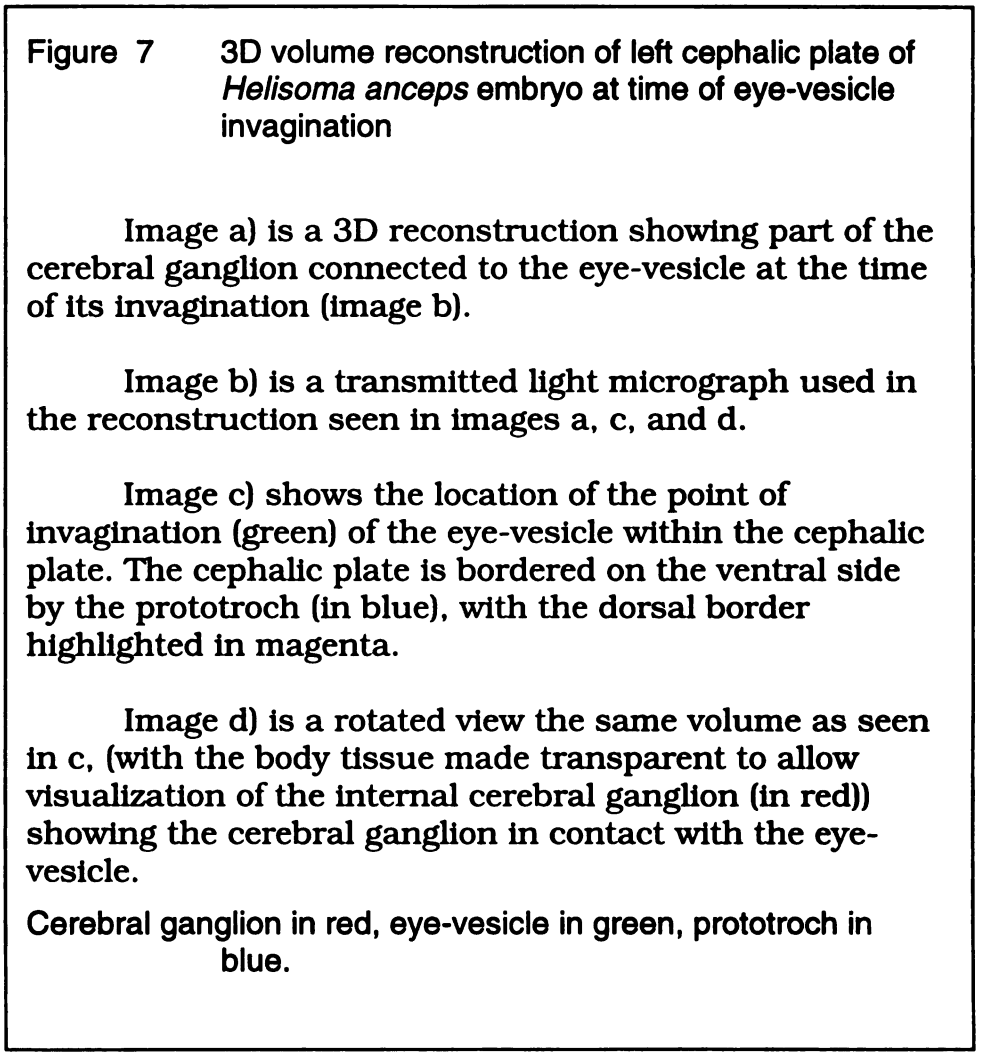

Figure 7 3D volume reconstruction of left cephalic plate of *Helisoma anceps* embryo at time of eye-vesicle invagination

Image a) is a 3D reconstruction showing part of the cerebral ganglion connected to the eye-vesicle at the time of its invagination (image b).

Image b) is a transmitted light micrograph used in the reconstruction seen in images a, c, and d.

Image c) shows the location of the point of invagination (green) of the eye-vesicle within the cephalic plate. The cephalic plate is bordered on the ventral side by the prototroch (in blue), with the dorsal border highlighted in magenta.

Image d) is a rotated view the same volume as seen in c, (with the body tissue made transparent to allow visualization of the internal cerebral ganglion (in red)) showing the cerebral ganglion in contact with the eye-vesicle.

Cerebral ganglion in red, eye-vesicle in green, prototroch in blue.

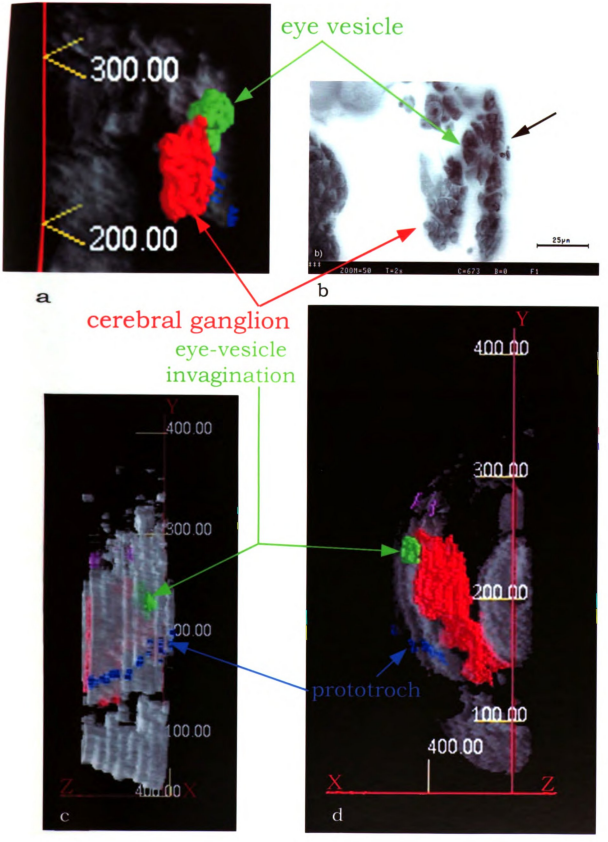
eye vesicle
300.00
200.00
a
b)
25µm
b
cerebral ganglion
eye-vesicle
invagination
Y
400.00
300.00
200.00
100.00
400.00
Z
X
c
Y
400.00
300.00
200.00
prototroch
100.00
400.00
X
Z
d

Figure 8 3D reconstructions the left cephalic plate of a stage B *Anguispira alternata* embryo

The 3D reconstruction this stage B *A. alternata* embryo shows the left cephalic plate with its borders highlighted. There is an ingression of a small group of cells located dorso-medial within the cephalic plate seen in images a, b, and c. Also the location of a large indentation, which in later embryos appears as a larger tube-like structure, can be seen.

In image b) the body tissue was made transparent allowing the visualization of internal structures. The cerebral ganglion has a small branch extending toward the small ingression of cells. Image c shows a side view of the left cephalic plate.

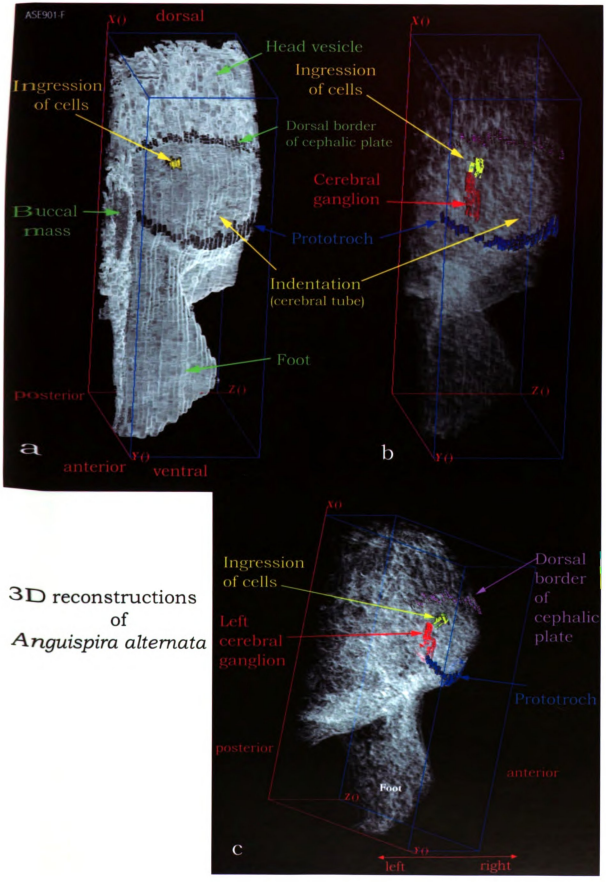


3D reconstructions of *Anguispira alternata*

Figure 9 3D reconstruction of left and right cephalic plates in *Anguispira alternata* at time of eye-vesicle invagination

These images show the position of the cerebral ganglia at the time of eye-vesicle invagination. Image b (bottom) shows the position of the cerebral ganglia relative to the invagination of the eye-vesicles, and to the cephalic plates (bordered by the prototroch).

There are four main branches of the cerebral ganglia visible. The anterior dorsal branches form the cerebral commissure; the anterior ventral branches are the cerebral-pedal connectives. The largest ventral posterior branch extends to the innermost end of the large indentation. The smaller medial posterior branch extends toward the point of invagination of cells seen in Figure 8. As can be seen in Figure 9 a and Figure 9 b, the branches of the cerebral ganglia neither extend nor contact the eye-vesicles.

Structures in red are cerebral ganglia; Green are the eye-vesicles, and blue the prototroch.

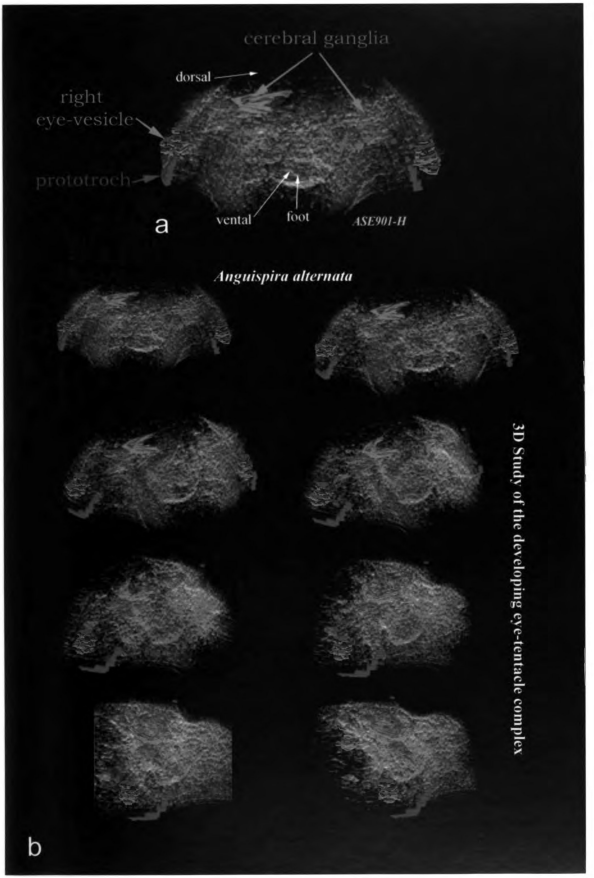
cerebral ganglia
dorsal
right
eye-vesicle
prototroch
a
ventral
foot
ASE901-H
Anguispira alternata
3D Study of the developing eye-tentacle complex
b

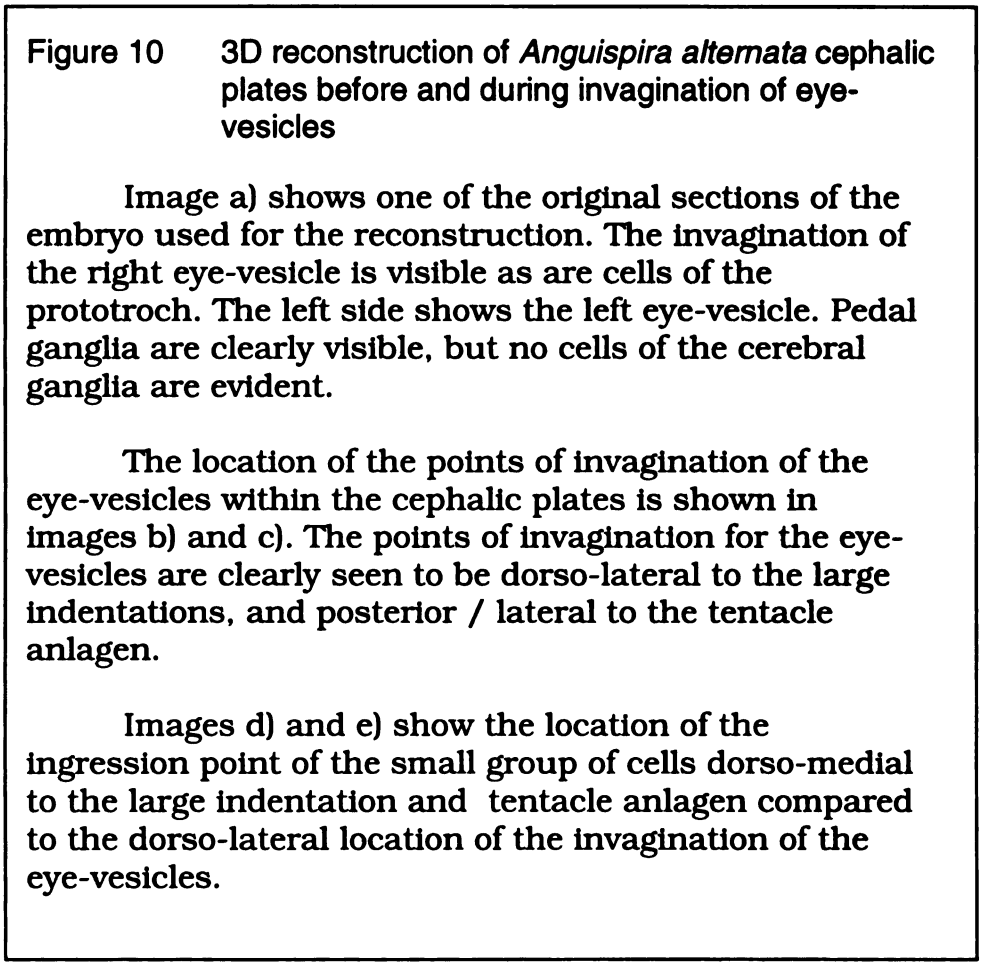

Figure 10 3D reconstruction of *Anguispira alternata* cephalic plates before and during invagination of eye-vesicles

Image a) shows one of the original sections of the embryo used for the reconstruction. The invagination of the right eye-vesicle is visible as are cells of the prototroch. The left side shows the left eye-vesicle. Pedal ganglia are clearly visible, but no cells of the cerebral ganglia are evident.

The location of the points of invagination of the eye-vesicles within the cephalic plates is shown in images b) and c). The points of invagination for the eye-vesicles are clearly seen to be dorso-lateral to the large indentations, and posterior / lateral to the tentacle anlagen.

Images d) and e) show the location of the ingression point of the small group of cells dorso-medial to the large indentation and tentacle anlagen compared to the dorso-lateral location of the invagination of the eye-vesicles.

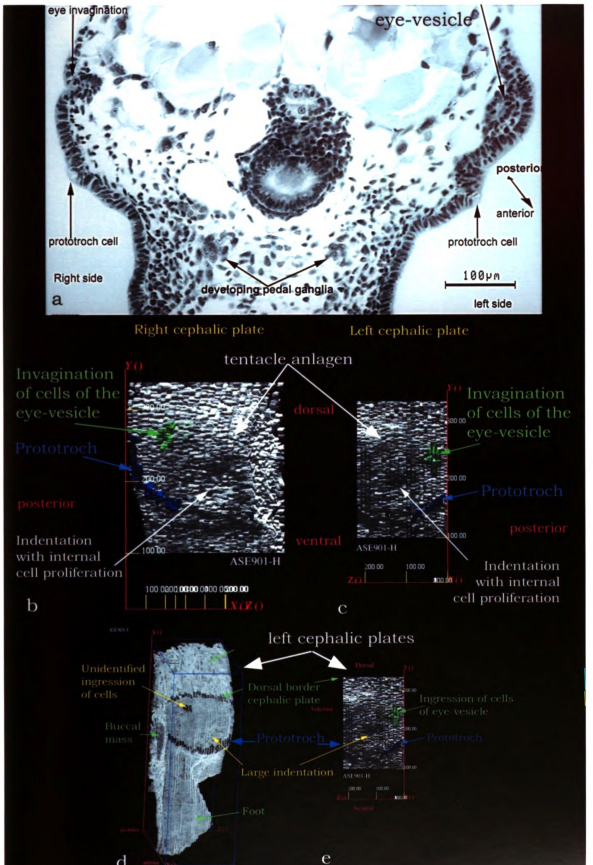
eye invagination
eye-vesicle
posterior
anterior
prototroch cell
prototroch cell
Right side
developing pedal ganglia
100µm
a
left side
Right cephalic plate
Left cephalic plate
tentacle anlagen
Invagination of cells of the eye-vesicle
Prototroch
posterior
Indentation with internal cell proliferation
dorsal
ventral
ASE901-H
Invagination of cells of the eye-vesicle
Prototroch
posterior
Indentation with internal cell proliferation
ASE901-H
b
c
left cephalic plates
Unidentified ingression of cells
Dorsal border cephalic plate
Buccal mass
Prototroch
Large indentation
Foot
Ingression of cells of eye vesicle
Prototroch
d
e

Figure 11 Comparison of 3D volume reconstructed embryo with SEM images

Images a-c are of the right cephalic plate at the time of eye-vesicle invagination of *Anguispira alternata* with different levels of opacity applied to the body tissue revealing the internal cerebral ganglion. Notice the branch of the cerebral ganglion that is directed at the large indentation. No branch is directed at the eye-vesicle.

Images d-f are SEM images of *Helisoma anceps* at the time of eye-vesicle invagination. Comparison of the SEM images *H. anceps* with the 3D reconstructions of *A. alternata* show the location of the point of invagination of the eye-vesicles are the same for both species.

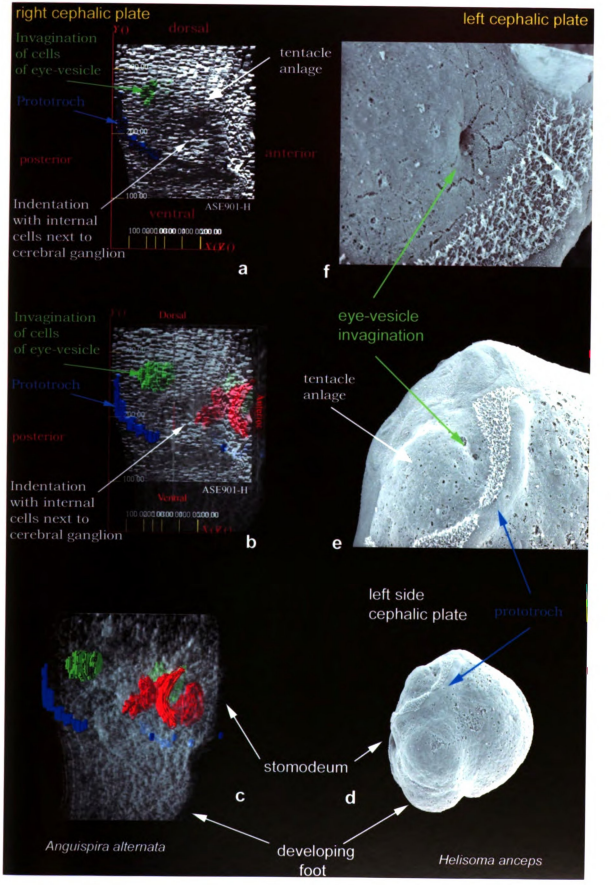
right cephalic plate
left cephalic plate
Invagination of cells of eye-vesicle
dorsal
tentacle anlage
Prototroch
posterior
anterior
Indentation with internal cells next to cerebral ganglion
ventral
ASE901-H
a
f
Invagination of cells of eye-vesicle
Dorsal
eye-vesicle invagination
Prototroch
tentacle anlage
posterior
Indentation with internal cells next to cerebral ganglion
Ventral
ASE901-H
b
e
left side cephalic plate
prototroch
stomodeum
c
d
Anguispira alternata
developing foot
Helisoma anceps

Figure 12 Digital re-sectioning of embryo

These images are of digitally re-sectioning of Helisoma anceps embryo in planes perpendicular to the plane in which the embryo was mechanically sectioned.

The eye-vesicles (in green) and the nervous system (in red) are visible in cross section. While the resolution of the images of re-sectioning is much less than the original section images, they are still useful in determining the positional relationship of structures.

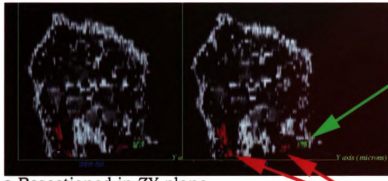


a Resectioned in ZY plane

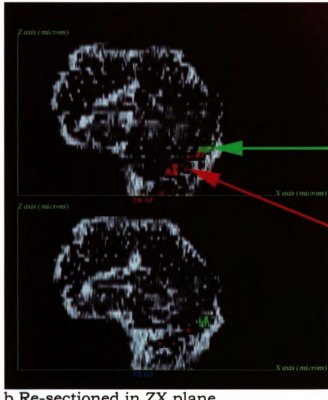


cells of the nervous system

cells of the eye-vesicle

cells of the nervous system

b Re-sectioned in ZX plane

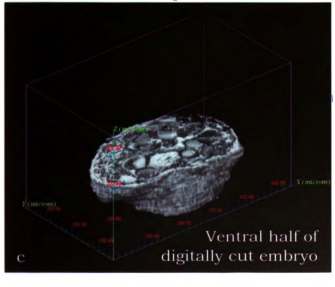


c Ventral half of digitally cut embryo

Figure 13 Original 2D section image and 3D reconstruction showing nervous system of *Helisoma anceps* embryo

Image a) is of one of the 2D images of the original sections. The image had its grayscale inverted. Images b) and c) are 3D reconstructions with different levels of opacity (transparency) applied to all non-nervous tissues.

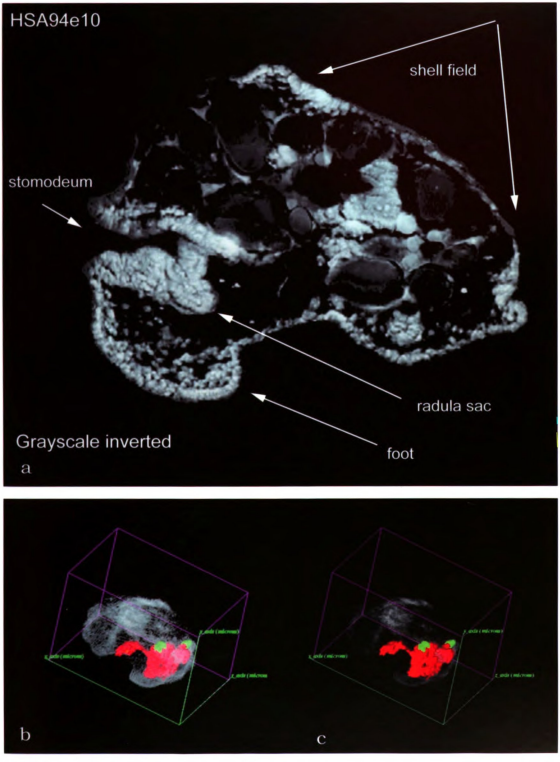


*Helisoma anceps* stage C embryo

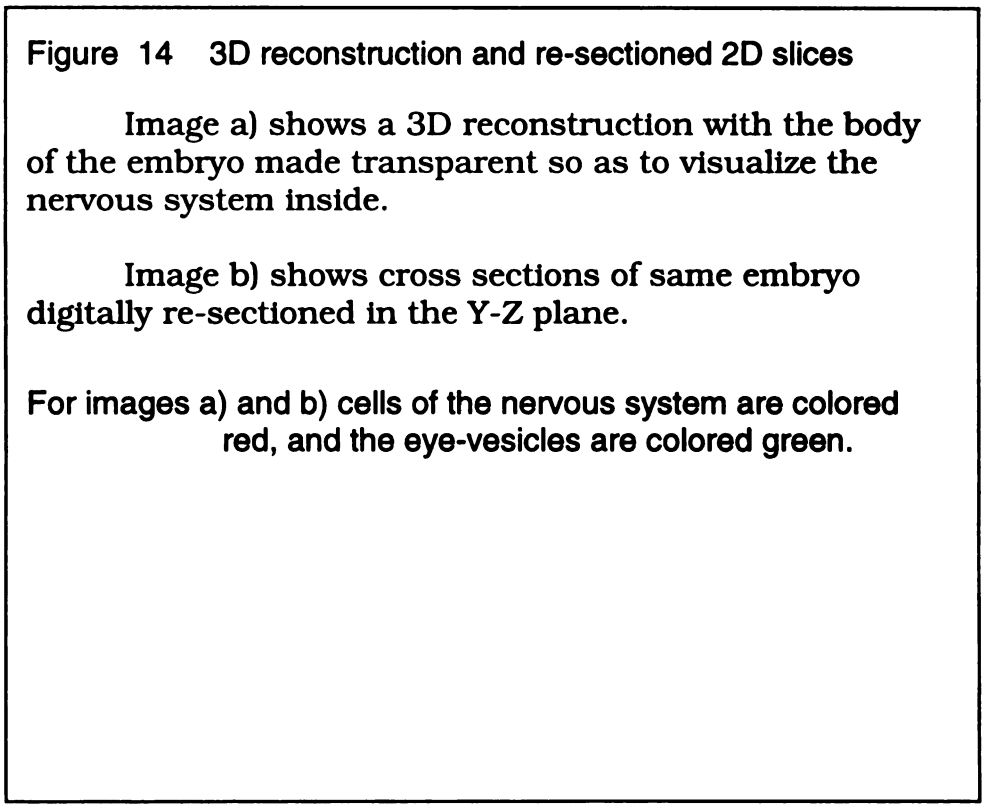

Figure 14 3D reconstruction and re-sectioned 2D slices

Image a) shows a 3D reconstruction with the body of the embryo made transparent so as to visualize the nervous system inside.

Image b) shows cross sections of same embryo digitally re-sectioned in the Y-Z plane.

For images a) and b) cells of the nervous system are colored red, and the eye-vesicles are colored green.

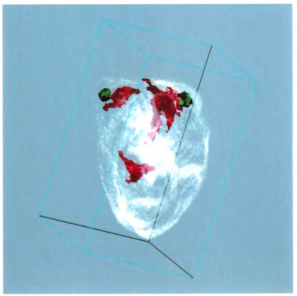

a

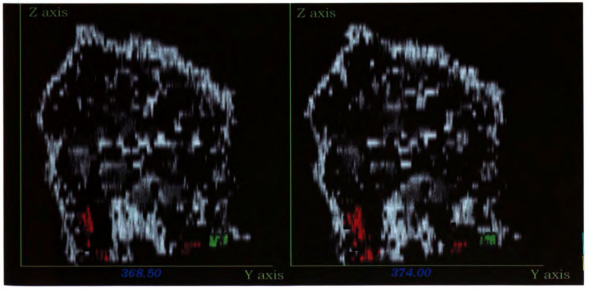


b

3D reconstruction and re-sectioning
of stage C *Helisoma anceps* embryo

Figure 15 More 3D reconstruction images of left cephalic plate at time of eye-vesicle invagination in *Helisoma anceps*

Images a) shows the location of eye-vesicle invagination as dorso-lateral within the cephalic plate. Images b) and c) show the cerebral ganglion in contact with the eye-vesicle.

Nervous system tissue is in red, eye-vesicle in green, and prototroch in blue.

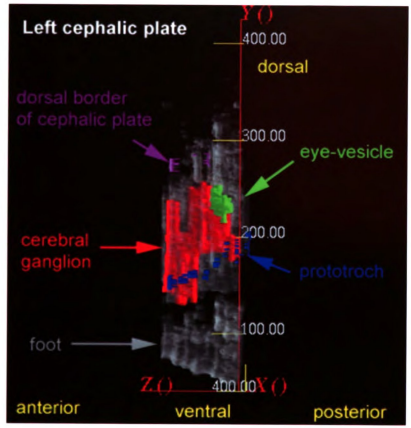
Left cephalic plate
Y()
400.00
dorsal
dorsal border
of cephalic plate
300.00
eye-vesicle
cerebral
ganglion
200.00
prototroch
100.00
foot
Z()
400.00
X()
anterior
ventral
posterior

a

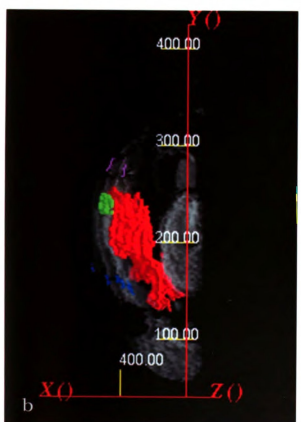
Y()
400.00
300.00
200.00
100.00
400.00
X()
Z()

b

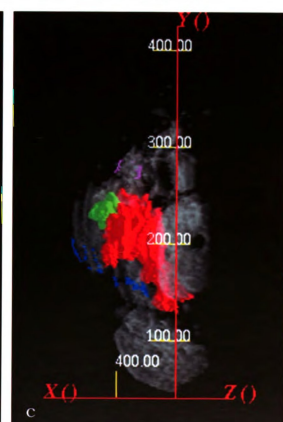
Y()
400.00
300.00
200.00
100.00
400.00
X()
Z()

c

Figure 16 Measuring distances in 3D using the "Trace" function

This is a screen shot of VoxelView/E's "Trace" function. Any two (or more) section images are selected and then a line (or multiple lines) are drawn from a selected point in one section to a selected point in the second section. Only the points of where the lines stared in one section and ended in the other are visible in the sections. The black arrows and arrow heads point to the starting and ending points for some of the distances measured.

In this example, five lines were drawn from the buccal mass (lower image) to the cerebral ganglion (upper image). Statistical analyses (morphometrics of the lines, and distances) are displayed in the blue boxes.

***Measuring distance between objects in 3-Dimensions using VoxelMath's TRACE feature***

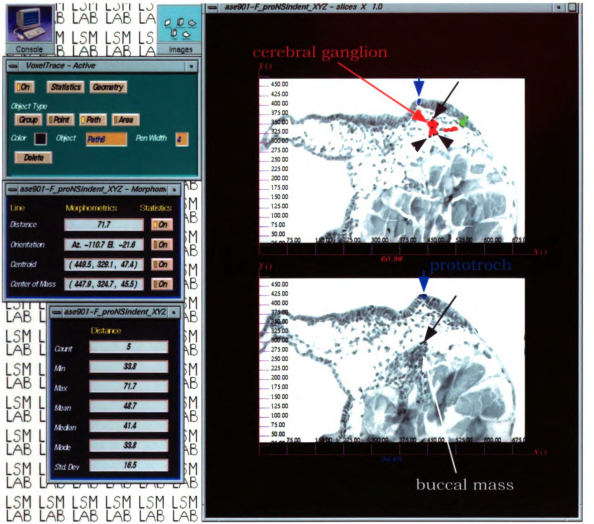

Figure 17 Volume measurements using the "VoxelSeed" function

Image a) shows the eye-vesicles (in green), and the nervous system(in red) after being "seeded" (i.e., the voxels that matched the criteria set in the green window of image b) have their volume measured. The rest of the embryo has its voxel opacity set to 50%, making the structures that were measured more apparent.

Image b) shows the measurements determined by VoxelSeed. The histogram and morphometrics of the voxels counted are displayed in the blue windows.

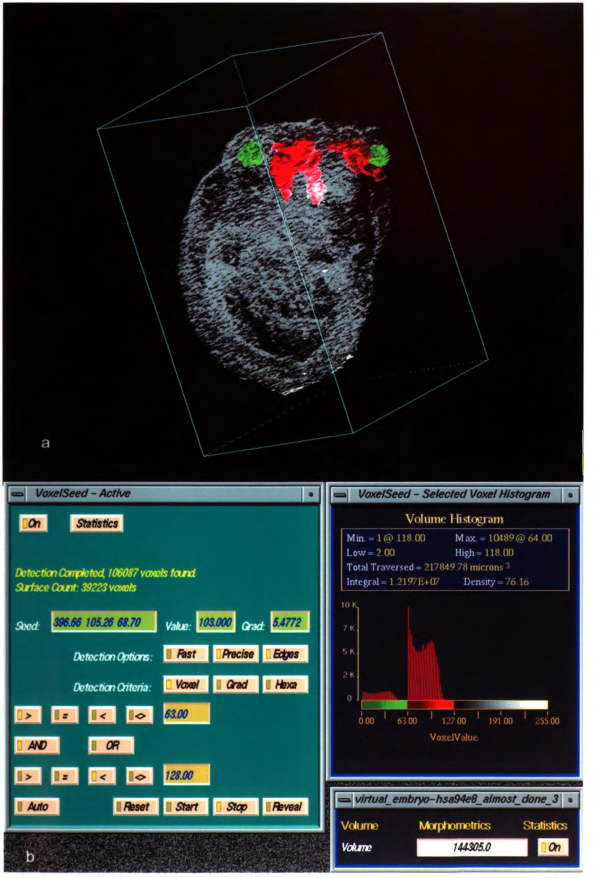
a
VoxelSeed – Active
On
Statistics
Detection Completed, 106087 voxels found
Surface Count: 39223 voxels
Seed:
396.66 105.26 68.70
Value:
103.000
Grad:
5.4772
Detection Options:
Fast
Precise
Edges
Detection Criteria:
Voxel
Grad
Hexa
>
=
<
<>
83.00
AND
OR
>
=
<
<>
128.00
Auto
Reset
Start
Stop
Reveal
b
VoxelSeed – Selected Voxel Histogram
Volume Histogram
Min. = 1 @ 118.00
Max. = 10489 @ 64.00
Low = 2.00
High = 118.00
Total Traversed = 217849.78 microns 3
Integral = 1.219?E+07
Density = 76.16
10 K
7 K
5 K
2 K
0
0.00
63.00
127.00
191.00
255.00
VoxelValue
virtual_embryo-hsa94e8_almost_done_3
Volume
Morphometrics
Statistics
Volume
144305.0
On

Figure 18 SEM image of *H. anceps* and original 2D section of *A. alternata* with labels

Image a) shows an SEM image of a veliger stage (stage B) *H. anceps* with labeled structures.

Image b) is one of the section images used for reconstruction of veliger stage (stage B) *A. alternata*, with structures labeled.

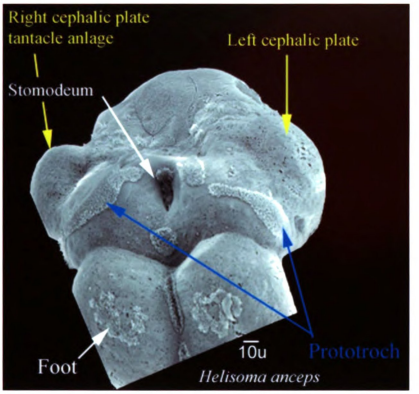
Right cephalic plate
tantacle anlage
Left cephalic plate
Stomodeum
Foot
10u
Prototroch
Helisoma anceps

a

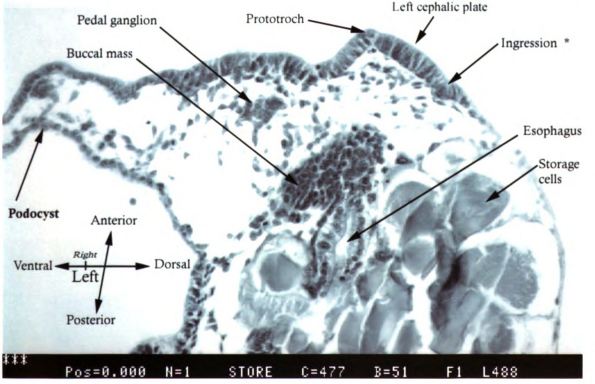
Pedal ganglion
Prototroch
Left cephalic plate
Ingression *
Buccal mass
Esophagus
Storage cells
Podocyst
Anterior
Ventral
Right
Left
Dorsal
Posterior
Pos=0.000 N=1 STORE C=477 B=51 F1 L488

b

Figure 19 Light micrographs of cells of cerebral ganglion

Light micrographs showing visual and structural differences of the cells forming a cerebral ganglion in *Anguispira alternata.*

The cells of the developing cerebral ganglion have a larger nucleus than the surrounding mesoderm or ectoderm cells, nucleus stains lightly with hemotoxylin stains (more transparent), with a single large denser staining nucleolus than the others cells around them.

Image b) is a higher magnification of the same section as seen in image a).

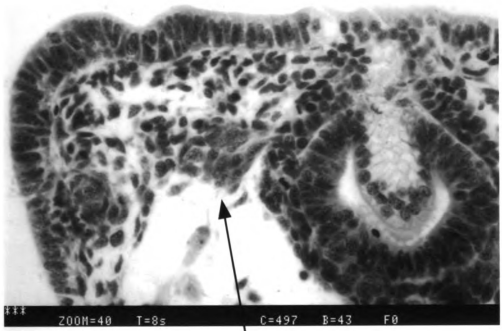


a

cerebral ganglion

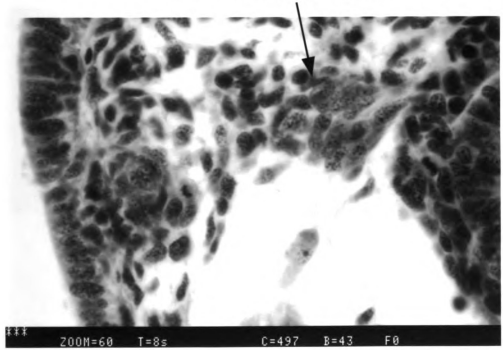


b

*Anguispira alternata*

Figure 20 Conversion of 2D sections to a 3D volume

Images a-e show the change from a single 2D section image (a), to a stack of 2D section images (b), then to a stack of images with interpolated images added(c), to 3D volume rendered reconstructions (d & e).

Image d) shows the position of eye-vesicle invagination (arrow).

Image e) is the same data set with different rendering settings applied. The prototroch is highlighted in blue (arrow).

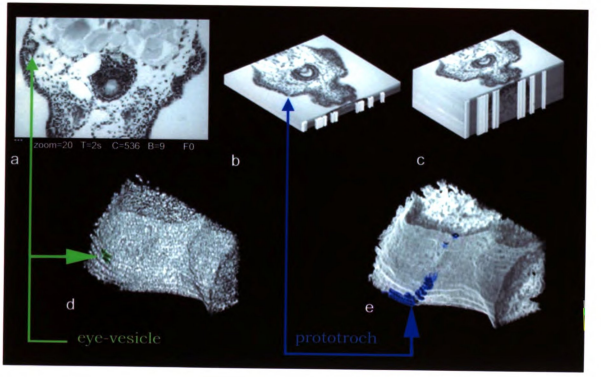
zoom=20 T=2s C=536 B=9 F0
a
b
c
d
e
eye-vesicle
prototroch

Figure 21 Digital dissection: processing of images

The images a-c show the steps used in "dissection" or segmentation of the nervous system "by hand" (prior to 3D reconstruction) using Photoshop 3.0.

The step of converting the non-nervous tissue to black (pixel value "0") does not affect the registration of the resulting images of the nervous system. The final set of images is saved as a separate data set and can be visualize separately by 3D reconstruction or visualized "merged" together with the whole embryo.

This is the original image of section 8.

It has been converted to a TIF file format and the rectangular shaped pixels have been converted to square pixels. Thus the original 512 x 512 pixels are now 512 x 341.


HSA94e8 section #8


This is the same image with the gray scale inverted and the info bar cropped out. 512x300


In this picture all but the nervous system has been removed by hand using Photoshop. The registration of the NS is left unchanged.

Figure 22 Shifting the range of voxel-values:
Original image and histogram

Image a) is an image of the "digitally" dissected nervous system (as shown in Figure 21 c).

Image b) shows the histogram and voxel value statistics (lower right hand box in blue).

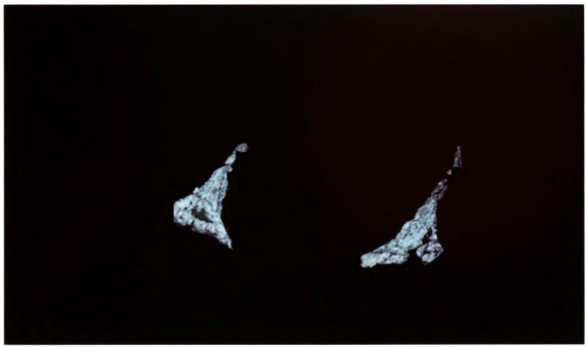

a Original image with unaltered histogram


b Histogram of unaltered image above (a)

Figure 23 Shifting the range of voxel-values:
Image and histogram after multiplying the values by 63

Image a) shows what the image looks like after multiplying each voxel value by 63. Only 256 values are shown at a time for 8bit data.

Image b) is the corresponding histogram for the image above. Notice in the statistics, the computer keeps tracks of all the voxel values, although only 256 values appear in the image and histogram windows.

a Image after multiplying by 63 (only first 256 values are shown)

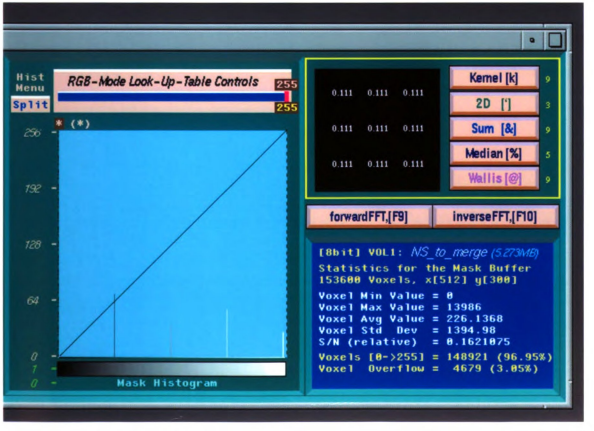


b Histogram of above image

Figure 24 Shifting the range of voxel-values:
Image and histogram after multiplying the values by 63 and dividing by 256

Image a) shows the image of the nervous system after being multiplied by 63 and divided by 256.

The histogram in image b) shows the voxel-value range of the above image "squeezed" into one quarter of its original range.

a Image after x63 and divided by 256

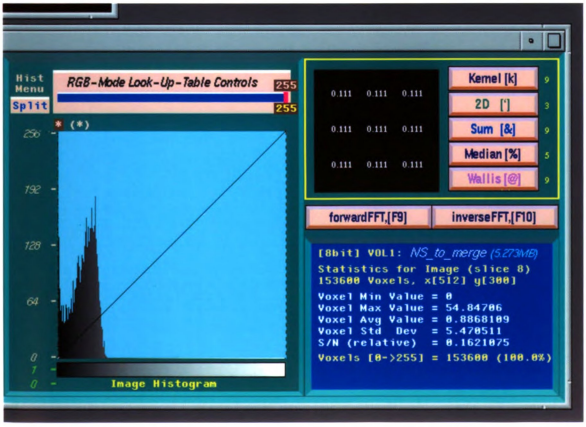


b Histogram after x63 and divided by 256

Figure 25 Shifting the range of voxel-values: Image and histogram after multiplying the values by 63 and dividing by 256 and shifting all non-zero voxel values by 64 ("bias=64")

The last mathematical manipulation of the nervous system data set, adding 64 to all non-zero value voxels, has the effect of shifting the range of voxel values for the data set from 0-63 to 64-127. By using the "bias" function the background of the image stays at voxel value "0" (in this case the color lookup table in use has "0" equals black as seen in image a). Thus, the program can maintain the distinction between the "object" (nervous system volume) and the "background".

The range of voxel values has been "squeezed" into one quarter of its original range, thus reducing the volumes visual resolution to ¼ its original. This has no effect though on the spatial resolution.

a Image after x 63 divided by 256 and "bias" 64

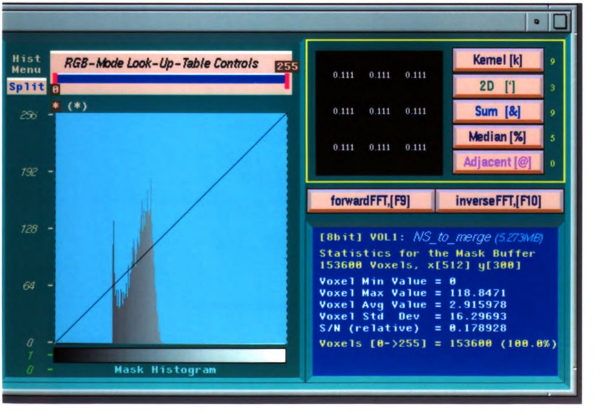


b Histogram after x 63 divided by 256 and "bias" 64

Figure 26 Image "stack" order

A) Images stacked in the proper order to maintain the correct left-right axes. Image number "1" is on the bottom, with images 2, 3, and 4 stacked on top.

B) Images are in an improper stack order.

Redrawn from Czymmek et al., Exp. Mycol. 18:275-293, 1994.

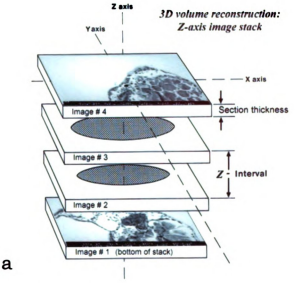


a

Correct image stack order

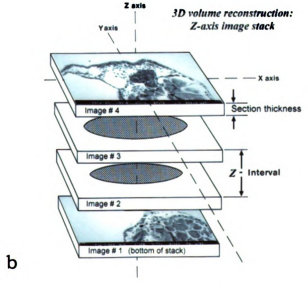


b

Incorrect image stack order

(Modified drawing from Czymmek, et al., 1994)

Figure 27 Comparison of SEM of whole embryo with partial 3D reconstruction: Effects of correct and incorrect image stack order

The SEM Images a) & b) show a snail embryo and the region reconstructed in images c) & d), which is the left cephalic plate and left side of the foot.

Image c) is a 3D reconstruction with the proper order of images, thus the resulting reconstruction appears correctly as the left side of the embryo.

Image d) is a mirror image of image c) and shows what the reconstruction would look like if done with the reverse order of images. Thus, image d) appears to be the right side of the embryo.

As can be seen by the above images, whether the reconstruction looks like it is of the left or right side of the embryo depends on the stack order of the images.

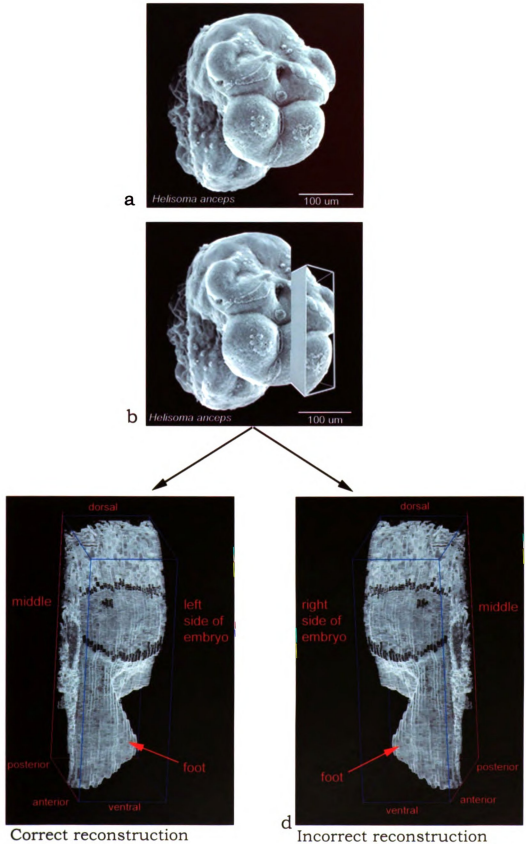
a
Helisoma anceps
100 um
b
Helisoma anceps
100 um
dorsal
middle
left
side of
embryo
posterior
foot
anterior
ventral
c
Correct reconstruction
dorsal
right
side of
embryo
middle
foot
posterior
anterior
ventral
d
Incorrect reconstruction

Figure 28 Order of sections on the microscope slide vs. the order of digital images needed to reconstruct correctly in 3D

As can be seen in this figure, the order of the images collected from a microscope slide must be reversed (i.e., the sequence of images reversed) to maintain the correct left-right axis.

***Correction for image "stack" order needed for 3D reconstruction***

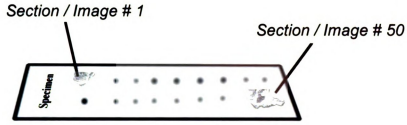


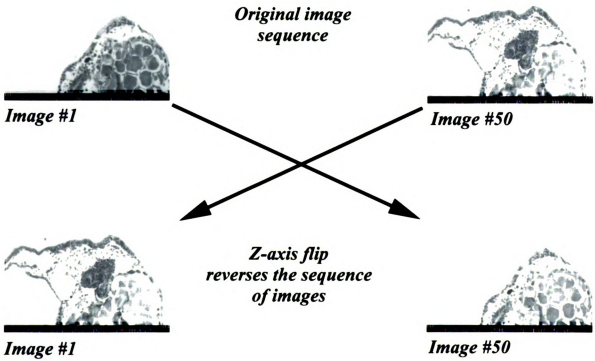

Figure 29 Digital realignment of sections of section images using "negative" interpolations

The use of "negative" interpolations to spread out sections with empty space between them (white area between sections), and changing the view to the X-Z axes plane, allows one to see very clearly just how many voxels a given slice maybe out of alignment with the other slices. This technique also makes it possible to count the exact number of voxels any slice is out of alignment, and thus know by how much and in which axis to make any needed adjustments.

X-Z view of "negative" interpolations

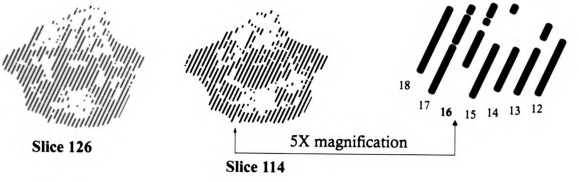


**HSA94e10**

Figure 30 Computer generation of 3D voxels from 2D pixels

The volume rendering program used in this study (VoxelView/E by Vital Images, Inc.) uses the 2D (x, y-axes) pixel dimensions to calculate a virtual 3D (x, y, z-axes) voxel. To render an image, the program stacks the voxels of each image from back to front (towards the screen).

(Redrawn from Vital Images, Inc. Fairfield, IA.)

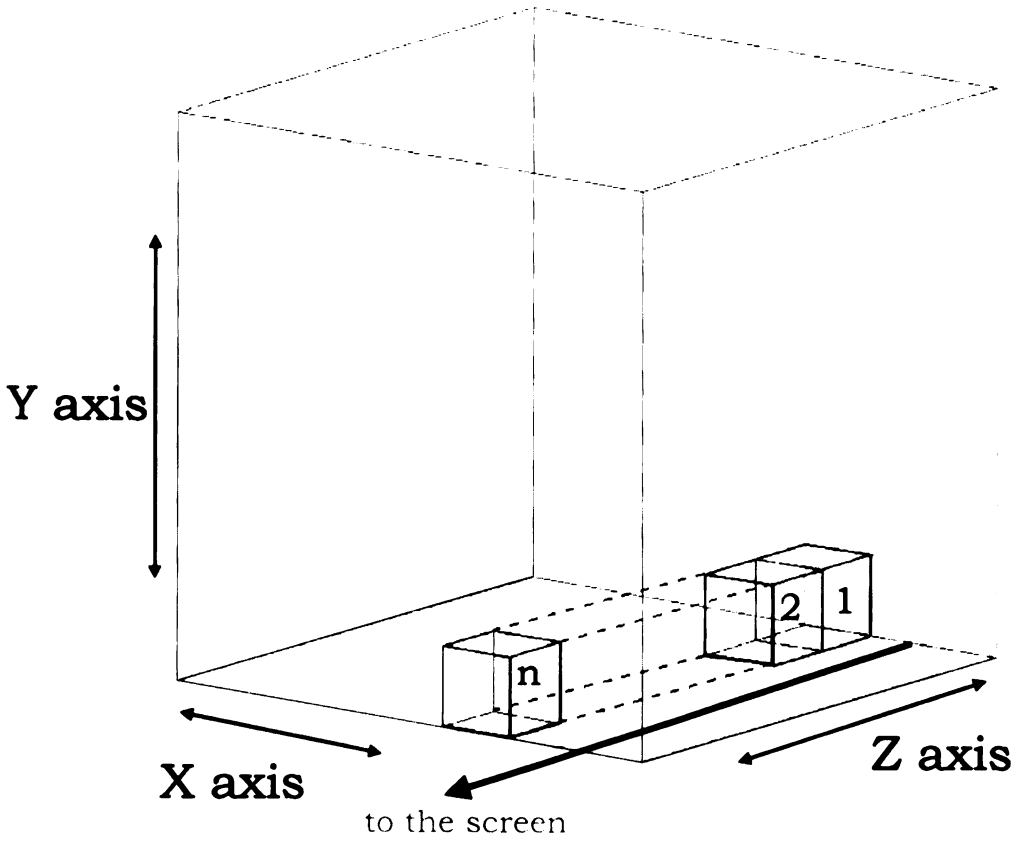


From 2D pixels
to 3D voxels

Figure 31 Maintaining the correct image aspect ratio: rectangular to square pixels

Images created on the LSM are collected and displayed with rectangular pixels having a 3:2 aspect ratio. The images are collected with 512x 512 pixels (x,y). When one of these images is displayed on a computer using 1:1 aspect ratio (square) pixels, the image appears stretched in the y-axis as shown in image a).

Image b) show correction for this by resampling along the y-axis, converting from 512x 512 pixels to 512x 341 (x,y) thus, returning the image to its correct aspect ratio.

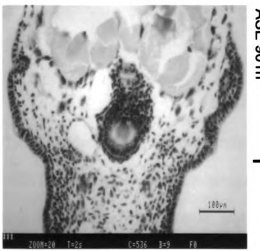


a) 512 x 512 pixels

b) 512 x 341 pixels

*Chapter 5*

# DISCUSSION

*"A scientist is not one who can answer questions, but one who can question answers."*

*Theodore Schick Jr., Skeptical Enquirer, 21-2:39*

## TECHNIQUE ISSUES

The approach developed for this study, while replete with powerful new tools for embryological investigations, is only as effective as the techniques are free of error, and as the approach offers advantages over, not just equal to, other approaches. At all stages in the creation of knowledge errors can occur. One criterion of the competence of an approach to the acquisition or creation of new knowledge is in its robustness against the creation of artifacts, and its ability to help detect or correct for self-generated error. The approach developed in this study meets this challenge.

## Repeatability & Reliability

The more traditional methods of embedding, sectioning, and staining embryos for light microscopy were employed for creating the serial sectioned embryos (as described in Chapter 3: Materials & Methods), and thus are susceptible to most of the same criticisms. Issues such as quality of fixation, mechanical disruption (and thus displacement of structures), shrinkage of tissues, and uncertainty of staining properties are always present with these techniques.

The physical sections on glass slides will deteriorate from within minutes to years, whereas digital data can (theoretically) be maintained at extremely high coherence indefinitely. Several copies were made of all digital images, and stored on separate data medium: hard-drive of computer, 100 MB Zip disks, QIC tape, and CD.

When working on digital data, unlike "the real thing", it is possible to make multiple "exact" copies at each stage of data analysis. Thus, manipulations to the data are functionally non-destructive, reversible and repeatable. This allows multiple different analyses to be performed on identical copies of data, reducing the wide variance of results caused by unknown individual variation (when numerous different original samples are used for each analysis). Since the copies are identical, all individual variation originating from the specimen itself (as well as those artifacts and changes created by physical processing) are identical.

The original set of images, as well as intermediate sets, are always available. This creates the ability go back a step or more and change processing of the images from that point forward, without having to start the whole process over from the beginning with a new sample. Thus, the same sample can be analyzed and manipulated repeatedly, as new algorithms become available. Working with true copies reduces the number of specimens required and makes combining of multiple analyses more accurate. It also means one can compare results of different processing steps with their exact counterparts.

## New Capabilities

Another criterion for critiquing an approach is how well it compares in capabilities to other similar techniques.

### *"Re-sectioning" of embryos*

The technique of "re-sectioning" the same specimen in different planes is a powerful technique. The benefits of being able to look at images of structures cut through different planes have been utilized by people using confocal microscopy to study small semi-transparent specimens, as well as by people using imaging techniques such as CAT scans and MRI for relatively large specimens (Baba, 1991).

Although digital re-sectioning provides additional spatial information, there is a loss in spatial resolution. As with the other imaging technologies (such as confocal microscopy, CAT scans, and

MRI), resolution in the z-axis, the long axis perpendicular to the plane of scanning (x, y-axes) is the limiting factor (Pawley, 1990; Radermacher, 1991). When re-sectioning the embryos in planes other than parallel to the "real" section plane, the resolution is not as good along the z-axis (compare Figure 12 with Figure 20 a).

Being able to put the slices "back-together" and to see the whole specimen at once greatly aids in the interpretation and thus acquisition of information from the 2D images. For example, if the specimen to be examined is not able to be precisely oriented when either mechanically sectioned or "optically" sectioned, the resulting 2D images can be difficult to interpret.

In the present study, by being able to look at slices of the specimen, and tell where in the whole specimen they are from, allowed for the discovery and exact placement of the small ingression of cells in the stylommatophoran snail *Anguispira alternata*, and the determination that they were not the earliest indication of the point of invagination of the eye-vesicle. From the 2D section images of the embryo, while showing an ingression of cells from the ectoderm, it was not possible to definitively determine that they were not the beginning of the development of an eye. By being able to precisely determine their exact location within the cephalic plate, and compare the reconstruction with later reconstructions showing the precise location of the invagination of the eye-vesicles, it becomes evident that this

small ingression of cells could not be the anlage of the developing eye (Figures 8 & 10).

In addition, while the 2D sections were needed to help identify the several small groups of cells close to the above-mentioned ingression of cells as cells resembling ( in staining characteristics and morphology) the cells forming ganglia, it was not evident that these ganglion-like cells formed a branch from the developing cerebral ganglion until they were able to be viewed as a whole within the 3D reconstructed embryo (Figures 8 & 9).

What the cells from this small point of ingression within the cephalic plate become was not determined in this study. It is possible that this small dorso-medial ingression corresponds to one of the "cephalic tubes" referred to by Henchman (1890) and Raven (1966). Henchman's descriptions and drawings based on 2D sections of a large invagination leading to the formation of a tube, as well as her description of the position and types of cells involved correspond to the large ventro-lateral invaginations found in the present study (Figures 8, 10, 11). Reports of a second invagination or cephalic tube occurring in some gastropods (Henchman, 1890; Raven, 1966; Moffett, pers. comm.) do not state from where within the cephalic plates they arise, or give a detailed enough description to determine if the small dorso-medial ingression of cells discovered in the present study corresponds to them.

Satisfactory identification of these cells requires a finer grained (more embryos of intermediate stages) analysis than provided here.

### *Digital "dissection" of embryos*

The snail embryos studied in this investigation are far too small to be dissected by hand in any useful manner. The ability to dissect digitally the virtual embryos proved to be a beneficial method for determining the shape, position and trajectory of branches (including the connectives and commissure) of the cerebral ganglion. Moreover, unlike dissection of the real specimen, digital dissection (since working on an exact copy) does not destroy the rest of the embryo. The structures dissected "out" can be compared directly to the rest of the unaltered embryo as well as to the same structures from younger and older stage embryos [Figures 6 & 13].

In the present study, there were two ways the structures of interest were differentiated from the non-nervous tissues of the rest of the virtual embryo depending on whether or not the result was to be a single volume with all structures, or several separate volumes each containing a different "dissected" structure. (See Material & Methods chapter for discussion of differences of working with single versus multiple volumes.)

A) Independent volumes of digitally "dissected" structures

In the first method, the resulting images of the "dissected" structures were saved as a new set of images (Figure 21). The registration or

alignment relative to the rest of the embryo of the digitally separated structures was not affected.

This method maintains the full visual resolution of the structures of interest (as well as the spatial resolution), and thus functions, such as Fourier Transformations or other filtering functions, are able to analyze finer details in the reconstructed volumes. Digitally dissected structures, which were made into separate volumes in this manner, were visualized within the unaltered original data set (in this case, the whole embryo) using the function "Multi-channel View" in VoxelView. This function allowed the simultaneous viewing of several volumes "merged" together in the same 3D space (Figure 9), with the ability to assign different ranges of colors and opacity to each volume.

B) Voxel-value partitioning

The second method was performed after the images of the sectioned embryo were reconstructed. If done prior to interpolation, the color ranges get partially mixed together during that process. If there are relatively few images (and few interpolations), and one does not want to sub-divide the volume into several separate volumes (e.g., so as to use functions such as VoxelSlicer, etc.) the nervous system, eyes, etc., can be assigned to a given sub-range of voxel values. Since the workstation used in this study had only 64 megabytes of RAM memory available, the original eight data bits per pixel were sub-divided. With

more memory, the volumes could be converted to 9-16 data bits per pixels thereby maintaining full visual resolution.

Once the structures of interest were assigned a unique range (or single) voxel-value, the software could then be used to differentiate the structures by assigning a different "color lookup table" (LUT) to that range of voxel-values (i.e., staining "digitally" the different structures, see below) or by making the other structures more transparent (lower opacity) allowing for the visualization of the internal developing nervous system (Figures 7, 8, 11, 13, 14, 17). In this same manner, the rest of the embryo could have its full range of voxel values made completely transparent or "turned off" (i.e., not rendered) (Figure 6). Neither of these techniques had any effect on the spatial alignment or registration of the voxels being manipulated.

Each separate volume, along with the combined one, can be viewed at the same time. Thus the cerebral ganglia were able to be viewed independently from multiple angles, while simultaneously viewing them in relation to other structures within the whole embryo (Figures 9 & 11). The trajectory of the two branches (besides the connectives and commissure) of the cerebral ganglia of *A. alternata* were able to be determined and verified independently of the structures to which they were directed.

3) Digital "staining" of structures

If the physical staining of the specimen differentiates even the slightest amount, (or if there are differences in the thickness and optical opacity in the sections when imaged and digitized), the computer can enhance that difference and make it more visible and quantifiable (see Figure 14). The intestine from the stomach to the anus on the right side of the image is visible due solely to the developing gut being composed of a denser concentration of cells.

For structures that were previously dissected digitally and made into separate data sets or volumes, the application of separate LUTs can be used to add color to increase contrast, thus making the different structures recognizable when all the structures are visualized together. The application of different colors can be applied to structures within a single volume using the same "Grease Pencil" functions as described above. This was used to make readily distinguishable developing nervous system, prototroch, and eye-vesicles within the whole embryo.

*Accuracy of visualizations*

As stated above, the changing of voxel values for structures of interest only affects visual resolution, not spatial resolution. Whether changing the histogram of the structures of interest after separating them from the rest of the embryo, or while still "inside", the effect on their histogram and visualization can be seen in Figures 22-25 which

show the assignment of the developing ganglia to the histogram range 64-127.

Volume rendering allows one to work with "fuzzy" uncertain boundaries among developing structures, in contrast to surface rendering techniques, which require *a priori* determination of distinct hard edges of structures before any visualization of structures in 3D. Enhancing the visualization of structures can be done using the Grease Pencil function of *VoxelMath 2.1* to shift the range of voxel values while maintaining full visual and spatial resolution. By "selective application" of mathematical functions using Grease Pencil, the area of interest can be shifted to its own range of voxel values (e.g., 256-512 for 9-16 bit images) maintaining its full visual and spatial resolution. The application of pseudo-color (via the use of LUTs) can then be applied to highlight the area of interest visualized in 3D within the whole specimen. This does not create hard boundaries of the structures of interest, but allows one to selectively add color or contrast to a limited region within the specimen and visualize in 3D within the whole specimen helping to visually differentiate structures. Other functions such as digital filtering of data in 3D, can also be selectively applied using Grease Pencil, as well as applied to the whole volume to help differentiate structures using information from all three dimensions.

The accuracy of digital dissections or digital staining is based on the ability to distinguish the structures to be manipulated. Unlike

surface rendered reconstructions (which are only of the outlines of structures), more of the data is represented in the volume rendered reconstruction. Adjustments can be made after all the separate volumes are "merged" back together if it is determined after further study that the digitally dissected structures are not what they were believed to be.

### *Quantitative Measurements*

It is important to be able to measure structures and be able to follow quantitatively their development or changes over time. Quantitative measurements are needed to compare and determine individual differences within and between species, thus allowing for the creation of accurate "normal" tables of development. The determination of intra-specific as well as inter-specific differences will help determine changes in developmental processes of evolutionary significance.

The ability to easily and accurately perform quantitative measurements of microscopy data is an important capability. Recent discussions on the Confocal Listserv (CONFOCAL@LISTSERV.ACSU.BUFFALO.EDU, 1999) attest to the amount of interest (and confusion) on this subject. The problem is in trying to make accurate measurements of distances among structures or to determine their size (volume) from two-dimensional images of structures that are three-dimensional. The use of three-dimensional reconstruction by volume-rendering techniques allows for making easy, accurate, and repeatable quantitative measurements.

Measuring structures from their images (image analysis) requires distinguishing the objects to be measured from their background and other structures. Algorithms for "mathematical morphology" (Gauthier, et al., 1992) techniques including functions such as "dilation," "erosion," etc. are all available within *VoxelMath 2.1* with the added feature that unlike image analysis of single 2D images, volume rendering can apply these algorithms to the whole volume, utilizing the 3D information as well. And unlike techniques, such as Stereology (Weibel, 1979) which are labor intensive, and more probabilistic than voxel counting (Rigaut, et. al., 1992), morphometrics has become "point and click."

A) Measuring distances between structures: the TRACE function

Accurate measurement of distance cannot be made from a single two-dimensional image ("x-y axes") (e.g., the computer screen or print) of structures that are also separated by some distance in the third dimension ("z-axis"). Modern confocal microscopes are able to produce sets of 2D images at progressively deeper planes along the z-axis (z-series) and computers can display these sets of images as if "stacked" on top of each other. The opacity levels can be varied so as to render an image very accurately as to the true structure. This gives very useful "qualitative" data regarding the relative position of structures in the 3D. The standard micron bar applied to the image is only useful for structures that reside exactly in the same plane as that to which the

line of measurement is applied. By converting 2D pixels into 3D voxels (Figure 30), the computer converts information of spatial position into a format that is now quantifiable. Since the voxels have a positional value assigned along a z-axis as well as the x and y-axes, each voxel is locatable within a 3D Cartesian coordinate system. The change from 2D to 3D increases the size of the data set. Massive increase in modern computer power (memory, storage, and processor speed) allows manipulation of this increase in size of the 3D data set.

To explore this capability, the lateral distance between the developing cerebral ganglion and the buccal mass was measured. Since the shape or surface of these developing structures were not smooth, it was necessary to be able to take multiple measurements between them from different regions and compare the results. The "Trace" function allowed the five separate measurements to be made, and calculated the results statistically (Figure 16). Thus allowing for a more confident assessment of the "real world" distance between the structures.

B) Measuring the volume of structures: the SEED function

Measurements of volumes of 3D structures from 2D images is a complex task. The accuracy of the 2D images, the number of interpolations (if used), and the ability to distinguish structures from one another and their background all can affect the accuracy of the resulting values. One of the great advantages of using volume rendering methods instead of methods such as Stereology (Weibel, 1979) is the

fact that volume rendering does not require the use of hard boundaries (edges) to be pre-determined by the researcher.

The "SEED" function of *VoxelView/E* allows the researcher to select the range of voxel values, gradient values (or even hexadecimal values) combined with different levels of sensitivity to their "physical" connection to the structure to be measured, as criteria. The program will then display the selected voxels measured within the whole volume thus making it possible see where the boundaries were determined and if they agree with other evidence (i.e., by looking at the volume in 2D sections or resections, and comparisons to other staining techniques and specimens).

The program *VoxelMath 2.1* can be used to make direct quantitative (by values and position) comparisons of multiple "seeded" volumes. Thus the effect of changes in criteria on volume measurements can be directly compared and contrasted. To explore this capability, the volume of the developing nervous system was measured for one of the *Helisoma anceps* embryo (Figure 17; Table 4). The measurement of the developing ganglia included the developing ganglia besides the cerebral ganglion on the right side (Figure 17a), thus accounting for the much larger volume of 144305.00 $\mu m^3$ measurement (Table 4). The values for the right and left eye-vesicles are much closer in value (14154.00 $\mu m^3$, and 14342.00 $\mu m^3$, respectively). All these volume measures correspond well with estimates bases on the total size

of the embryo studied, and measurements correspond to what would be expected from looking at the 3D reconstructions and 2D section images.

For measurements of both distance and volume, the program automates the calculations, and allows multiple measurements to be taken, performs the statistical analysis "on the fly" and produces the calculations in several formats and tables. These calculations can be imported into statistical analysis programs or spread sheets. Multiple measurements can thus quickly, reliably, and repeatedly be determined.

## Accuracy of reconstructions

The following is a discussion of several issues regarding spatial resolution and accuracy, both quantitatively as well as qualitatively, of 3D reconstruction.

### *Left-right axis in reconstruction*

In reconstructing snail embryos, maintaining the correct left-right axis in the 3D reconstructions is important because of the following: First, though basically bilateral, snails are asymmetrical in their left-right axis. Second, the species in this study differ in the directions their bodies coil; *A. alternata* is "**dextral**" (coils to the right), and *H. anceps* is "**sinistral**" (coils to the left). Dextral snails have the opening to their respiratory, reproductive, and excretory systems on the right side of their bodies, while sinistral snails have these structures and openings

on the left side of their bodies. Thus, the left-right axes are reversed between dextral and sinistral snails. Third, there are also asymmetrical differences in the timing of development of both left/right paired structures such as the nervous system, and unpaired organs such as the reproductive organs. Finally, some snails go through "torsion" during development, (a process in which their bodies twist 180 degrees along their dorso-ventral axis. In the current study torsion was not an issue because all the structures of interest are located in the anterior/dorsal part of the embryo unaffected by the twisting of the more ventral/posterior part of the embryo.)

Maintaining the Correct Left-Right Axis:

Because of the way the *VoxelView/E* program reconstructs the volume, there is potential for reversal of the z-axis of the volume that would reverse whichever axis of the embryo is represented along this dimension. *VoxelView/E* uses the "compositing method" (or object order) of volume reconstruction. The program reconstructs (or builds) the volume from back-to-front by laying down whichever image has the file name "1" (or "0") then stacking the file named "2" on top of it, and so on, stacking the highest numbered (named) file on top (Figure 26 A). If this is not the correct order for the images to be stacked, the resulting embryo will have its left-right axis reversed. For example, the resulting reconstruction will appear to be of the right side of the embryo (Figure

27 d), as opposed to being reconstructed as the correct left side of the embryo (Figure 27 c).

Correction is accomplished by renaming the files in reverse order, i.e., if there are fifty images in the set, image number "1" becomes image number "50", and image number "50" becomes image number 1, etc., as shown in Figure 28 c. Renaming of files was carried out with the program *VoxelMath* 2.1 by "flipping" the images along their z-axis ("Flip-Z"), thus functionally reversing the order of the images. This was done just before the volume interpolation ("Resample Z") step to decrease processing time. Contrary to what is stated in the manual of *VoxelView/E* for the "Position Volume" function, the "Flip Z-axis" function in *VoxelMath* actually does reset the "origin" for the volume, (i.e., the reference point 0,0,0 (x, y, z)), and thus changes the view of the specimen in relation to the axes lines displayed when using the "Annotations" option in *VoxelView/E* (Figures 6, 7, 8).

### *Alignment of images*

Since one of the objectives of this study was to determine the precise, three-dimensional location of the developing cerebral ganglia in relation to where the eyes develop, it was important that structures other than these be used to create or check the alignment of sections. Points of reference in the images used for alignment were structures other than the developing nervous system, e.g., the buccal mass, radular sac, esophagus, shell field, foot anlage etc. This decreases the

effects of expectations about the relative positions of the structures of study (in this case the nervous system) on the alignment process. Since the embryos were mechanically sectioned, alignment is still relative, not absolute.

Digital Alignment & Registration of the Image

The small size of the embryos studied not only limited the ability to orient the embryos very accurately in paraffin (as mentioned previously), it also interfered with embedding markers of some sort to act as fiduciary marks (points visible in all sections that when aligned correctly form a line(s) perpendicular to the plane of sectioning, and allow accurate and objective alignment of the sections). Therefore, the sections were aligned by hand on the LSM (as described in the Materials and Methods chapter). Although there are commercial software programs for alignment of images, these were unavailable for this study.

During the course of this study, it was discovered that two features within the software programs used for the volume reconstructions could be combined to create very precise, and more accurate digital re-alignment of the images of sections. If the interpolation value for a given volume is set to a negative integer in the "_dimensions" file, *VoxelView/E* and *VoxelMath* will display the volume with empty space between the slice images (Figure 29). Using this feature coupled with *VoxelMath's* ability to view 2D slices of the volume in the XZ and YZ views as well as the XY view, allows for the

determination of which slice is out of alignment with others, and by how many voxels ( Figure 29). *VoxelMath 2.1* can then be used to shift or rotate the problem slice(s) the exact number of voxels needed to improve its alignment with other sections, as compared with whole mounts, video images, or SEM images of other embryos at the same stage of development.

**Pixels to Voxels**

The computer program creates in essence, a three-dimensional "voxel" from the two-dimensional pixels, and stacks them one on top of each other to form a three-dimensional virtual model of the specimen, called a "volume." The voxels created are iso-dimensional in appearance, that is the program uses the x and y pixel dimensions as the z-axis dimension for calculation of the voxels, creating a three-dimensional volume (Figure 30).

Two issues affecting the accuracy of the reconstructions are specific to the creation of 3D voxels from 2D pixels: 1) changes in aspect ratio of pixels; and 2) interpolation of voxels along the z-axis.

1) Changes in aspect ratio of pixels

The first issue arises from the fact that the digital images were created on an LSM that creates rectangular pixels. The resulting pixels need to be converted to square pixels for the 3D reconstruction software to create proportionally correct 3D renderings. The LSM creates images

with 512x512 (x, y) pixels. The rectangular pixels can be converted to square pixels maintaining the correct proportions of the specimen by resampling the images either along the y-axis (512x341) or the x-axis (768x512). While it can be argued it is better to resample along the x-axis (thus not reducing the resolution of the image in either axis), doing so requires much more computer resources and disk storage space. Since the LSM scans the images along the x-axis, it can be argued that the resolution in the y-axis is not as accurate and so the y-axis should be the axis resampled. (See Pawley, 1990 and Häder, 1991, for discussions of digital imaging in biology.) Resampling along the y-axis creates images of 512x341. This is the default sampling method of programs such as *VoxelScanZeiss*, and was used for the present study.

2) Interpolation of voxels along the z-axis

In this study, the embryos were mechanically sectioned at five or ten microns. Since all sections were digitized in sequence, the "section thickness" of five or ten microns is also the "Z-Interval" (Figure 26). This is the "real world" z-axis dimension/resolution. Since the x and y-axes dimensions are smaller than the z-axis dimension (Table 1) and the program computes the z-axis dimension of each voxel equal to the x and y-axes, when the program stacks the images (a single layer of voxels), the resulting volume will look distorted ("squashed") in the z dimension (Figure 20 b) .

To correct for this squashing effect, images created by mathematical interpolation are placed in between the original or "real" images. The insertion of interpolated images between the real images expands the volume in the z-axis dimension creating a more accurate appearance of the specimen (Figure 20c). The computer program uses linear interpolation of the real "slice" (2D) images to determine the voxel values for the slice images to be inserted between them.

For example, some of the embryos used in this study were imaged with a 20x objective with a "zoom" (or magnification by the LSM) of 20 (for a total on-screen magnification of 400). This creates a field of view (in x-axis) of 709.7μm, scanned with 512 pixels making each pixel represent 1.386μm in the x-axis dimension (see Table 2). Since the sections were mechanically cut at 10μm thick, (10μm divided by 1.386μm=) 7.215 voxels would be needed to fill (expand) the distance from one image to the next. Without interpolations, the computer "squeezes" all the information in the 10 μm thick section into 1.386μm and displays the volume as flattened (Figure 20 b). Flattening of the volume only occurs visually, since the computer will still measure the distance as 10μm if that value was entered in the "dimensions file".

If the number of voxels needed to fill in the "z-interval" is a whole number (e.g., "three"), that number minus one (since the original image thickness is included in the distance between the top of one image and the top of the next), can be entered into the "interpolations" field of the

"_dimensions" file for the volume. In this example the value "2" would be entered (three voxels to fill the space, minus one voxel of the original image equals two interpolated voxels needed).

In the previous example which requires 7.215 voxels (of 1.386 μm) the program *VoxelMath* 2.1 is used to create interpolations using non-integer resample values ( Scalar value of 7.215) using the "Resample Z" function in the Merge Window. Since it is impossible to have a partial voxel (or pixel), the program calculates the number needed and resets the distance value of each voxel so the distance is displayed as well as measured with a "whole number" of voxels. If the "dimensions file" (or image header) has the correct resolution values for the volume as created, the function "Resample XYZ" will make all axis resolutions equal.

*Reduction of interpolations: Sub-sectioning the sections*

Interpolation of voxels, while improving the visualization of the samples, does not add any real data, thus it is better to keep the number of interpolations needed as low as possible to get more accurate quantitative (and qualitative) information. If the z-axis or distance between images is larger than the x-y axis resolution, then interpolated voxels need to be created. Since mechanically sectioned embryos stained with non-fluorescent dyes were used in the present study, the use of higher magnification objectives, could only increase the pixel resolution (i.e., the smaller the area represented by a single pixel) in the

x and y-axes; the resolution in the z-axis of the created voxel stays the same and thus more interpolations would be needed.

The 20X and 25X objects were used to create higher magnification and resolution images of the developing eye-tentacle region of the embryos. As shown in Table 2, the images created require approximately 7-9 interpolations. This many interpolations create volumes that have large "steps" between sections, degrading the quality of the reconstructions. Both the 20X and 25X objectives have "depth of focus" that are smaller (see Table 1) than the thickness of each section. Two images of each section were created: one at the top of the section, and one focused 5 microns down or into the sample. This was possible due to the LSM having a mechanized scanning stage (i.e., a computer controlled stage that can be moved in the z-axis in nano meter range step-sizes). The level of accuracy, precision, and consistency of optically sub-sectioning the mechanically sectioned images would not have been possible using a standard microscope and digital camera.

Optically sub-sectioning created two images slightly different from each other due to the fact that most of the cells of the sample are less than 5 microns in diameter, so some cells appear in one of the images in focus, and in the other image many are not visible at all. The cells within the 10μm thick sections were spread back out more accurately. This allowed for a reduction by half the number of interpolated images per "real" image (although the total per section was the same) required

(see Table 2) thus creating a little more accurate reconstructions. With the use of fluorescent staining, it should be possible to use confocal microscopy to "optically" resection the sections and if the z-axis step size and optical depth can be made to match the x, y-axes resolution, then no interpolations would be necessary.

## BIOLOGICAL ISSUES

### Determination and delimitation of cells and tissue types

Only a few species of pulmonate gastropods have ever been studied with respect to development of their cerebral ganglia. Of stylommatophorans, one of the most, if not the most, detailed study was done on the slug *Limax maximus* by Henchman (1890). She determined that the cerebral ganglia developed from ectodermal thickenings of the cephalic plates, with a single large invagination forming the "cephalic tubes." Whether there is one large invagination for the cerebral tubes per side or two has been reported differently, depending on which species were studied (See Henchman, 1890, and Raven 1966, for reviews). Reports of differences (and disagreements) in development demonstrates the problem with assigning "model" status to a species to represent a large (and largely unstudied) group of organisms.

Independent of their number, the cerebral tubes being such obvious structures helped to determine which groups of cells were

forming the cerebral ganglia. Large proliferation of cells, which occurs at the innermost ends of the cerebral tubes, end up next to (in contact with) the groups of cells forming the cerebral ganglia.

The developing nervous system in these snail embryos is composed of only a few cells at the time of eye development. The cells that give rise to the eye-vesicles in the species studied do not show cyto-differentiation until after they have separated from the overlying ectoderm and formed a true vesicle.

The cells forming the ganglia did show some cellular differences at this early stage of development using standard hematoxylin stains. When stained with Heidenhain's hematoxylin the cells forming the cerebral ganglia showed nuclei that were larger, more transparent, and rounder than the surrounding ectodermal cells or mesodermal cells (Figure 19). The position of the cells forming the cerebral ganglia, (relative to other developing structures such as the buccal mass, stomodeum, cephalic plates) was also used in their identification.

By looking at a series of embryos selected at different stages of development, it is possible to extrapolate over time what a given group of cells will become. The ability to determine the precise location in all three-dimensions for a given group of cells frozen in time and to make direct side by side comparisons with cells in the same location in other embryos at later or earlier stages of development greatly facilitates the determination and discovery of which cells develop into what

structures. The ability to study the developing embryo in all three dimensions simultaneously, with the accuracy and precision that volume rendering creates, is a great advancement for embryological research.

## Gastropod phylogeny

If we knew the relationship(s) of the Basommatophora to the Stylommatophora, what the differences in development of the eye-tentacle complex means in regards to the evolution of these two groups would be more apparent. Pulmonates are considered a grade of structure, with its three orders (discussed below) reaching it independently (Solem, 1985). Data from comparative morphology, biochemistry, genetic structure, and biogeographic studies have not been able to determine with any level of confidence the relationships among pulmonate orders (Solem, 1985).

## Structure of the eye-tentacle complex in gastropods

Gastropod snails and slugs have a wide range of patterns of their eye-tentacle complex. Prosobranch gastropods have a single pair of cephalic tentacles, with eyes located on short eye-stalks situated at the base of the cephalic tentacles. Alternatively, the eyes are located in small bulges in the base of the tentacles, or embedded in the skin around the base of the tentacles[5].

Opisthobranch gastropods are the most diverse of all groups, a fact that is also reflected in their sensory systems. Many opisthobranchs have large cephalic sensory structures called "rhinophores" which vary in structure from folded to linear, sheathed or unsheathed in gross structure (Schmekel, 1985). Some opisthobranchs also have cephalic tentacles, which are more or less outgrowths of the labial palps or lips.

Pulmonates are the most successful in freshwater and terrestrial habitats. This subclass in composed of three orders all named by the structure of their eye-tentacle complex; the Basommatophora, Stylommatophora, and the very peculiar slug group Systellommatophora. Aquatic snails of the order Basommatophora have a single pair of cephalic tentacles, with eyes located at the base of the tentacles. The eyes are either fused to the base (as in the basommatophoran snails *Helisoma*), or embedded in the epithelium between the tentacles as in *Lymnaea*.

The largest, and most successful group of terrestrial gastropods, the Stylommatophora, have two pairs of cephalic tentacles, with eyes located at the summit of the larger and posterior set. The tentacles of stylommatophoran gastropods are completely retractable by invagination, and can be manipulated with very precise control through a large range of movement.

The last group, the Systellommatophora, is a small group of terrestrial slugs that have, like the Stylommatophora, two sets of tentacles with their eyes located at the tip of the larger and more posterior set of tentacles. Where these two groups differ is in the fact that the tentacles of the Systellommatophora are only contractible, not retractable by invagination. They also have a uniform cerebral ganglion structure, different enough for van Mol (1967) to keep them in their own group (Solem, 1985).

## Sensory functions of gastropod tentacles

While aquatic snails do appear to have chemo-sensory and tactile functions of their tentacles (Boudko, et al., 1999; Chase and Tolloczko, 1985; Chia and Koss, 1982, 1984; Audesirk and Emery, 1978; Audesirk, 1975) most still have an organ for chemo-reception called an "osphradium" associated with the ctenidium or gills contained in the mantle cavity. Terrestrial snails and slugs have lost this structure, and their tentacles (and lips) have taken over as the main site for chemo-reception (Bullock and Horridge, 1965;Haszprunar, 1988).

At the tip of each tentacle of stylommatophoran gastropods is a highly innervated chemo-sensory pad, supported by a complex and large tentacular ganglion. The tentacular ganglia have been estimated to contain 100,000 neurons each in the terrestrial snail *Achatina fulica* (Chase and Tolloczko, 1993). This ganglion has a connection to the

cerebral ganglion that is independent of the innervation of the eye; the optic nerve runs directly to the cephalic ganglion.

It is not known what, if any, the adaptive significance of these two very different patterns of the main sensory structures associated with life in different environments may be. How this restructuring of such important organ systems occurred evolutionarily is not known. The adaptive value of some of the structural changes of the tentacles in terrestrial gastropods are more easily explainable, given the lack of surrounding water to help support the tentacles, as well as the osphradium not being functional in a terrestrial environment. (Although loss of the osphradium has also occurred in several orders of opisthobranchs, such as the Nudibranchia, Pleurobranchomorpha, and some of the Saccoglossa (Schmekel, 1985)). The evolution of a second pair of cephalic tentacles, a large complex tentacular ganglia, and the change in eye position are modifications which are harder to explain.

## Homology of sensory structures

What, if any, are the homologous relationships between these sensory systems? Are the cephalic tentacles of aquatic snails homologous with the anterior or posterior pair of tentacles of terrestrial snails? Or are the posterior (optic) tentacles of terrestrial snails homologous with the "eye-stalks" of some prosobranch groups? Is the

anterior pair of tentacles of terrestrial snails derived from the labial palps found on some aquatic snails?

While the question of homology of gastropod sensory systems, such as the rhinophores, tentacles, and labial palps or lips, seems straightforward, and has been treated as such in the literature, when the actual structures and functions are compared among the great diversity of gastropod groups, it becomes clear it is not such a simple question.

The epithelium of gastropods is only one cell layer think, and there are several cell types which require access to the surface, such as the epidermal, ciliated, glandular, and neural sensory cells (Boudko, et al., 1999; Hyman, 1967; Simkiss, 1985). There are two ways gastropods have overcome this space limitation; one, create a second population of sensory nerve cells with their cell bodies located below the basal lamina of the epidermis with dendrites extended to the surface in-between the other cells (Boudko, et al., 1999); and two, increase the surface area that is innervated by growing out the epidermis into tentacles and rhinophores.

The rhinophores are believed by some authors to have evolved from a sensory organ called "Hancock's Organ" and the dorsal lateral edge of the cephalic shield of an Cephalaspidean opisthobranch. The rhinophores of opisthobranchs and the cephalic tentacles of prosobranchs (and thus also pulmonates) cannot be, therefore,

homologous (Schmekel, 1985). The Cephalaspidea do not have any other cephalic tentacles, suggesting the tentacles of other opisthobranchs may not be homologous with those of prosobranchs or pulmonates either. This is quite interesting since the opisthobranchs are believed to have arisen from prosobranchs with tentacles. The diversity of pattern of the eye-tentacle complex attests to the evolutionarily flexible gastropod body plan, (another reason for the great confusion of phylogenetic relationships).

More representative studies of species within the numerous diverse orders and families of gastropods in regards to the development of their sensory systems, including shared gene-complexes and gene expression patterns, as well as more phylogenetic studies to determine the relationships and thus direction of morphological changes are needed. Until then, the questions as to which sensory structures are really homologous and how they are modified developmentally and evolutionarily can not be answered.

## Development

The present study set out to determine: the precise location within the cephalic plates of eye-vesicle formation; and if the cerebral ganglia move into a position to be able to interact with the overlying ectoderm in the exact area required for their induction; and to determine if there is a difference in the position of the cerebral ganglia

relative to the overlying ectoderm that may account for the changes in the position of the eyes relative to the tentacles between these two groups.

In both species studied in this investigation the eyes were found to develop by invagination of the ectoderm in the dorso-lateral region of the cephalic plates; posterior and slightly dorsal to the tentacle anlagen. The eye vesicles do not develop on the tentacle anlagen and thus the location of the eyes at the tip of the tentacles cannot be explained by the eye-vesicle anlage being on the tentacle anlage and thus being carried up as the tentacle elongates.

The above finding suggests that in at least in this stylommatophoran snail the change in development accounting for the change in position of the eyes relative to the tentacle anlagen occurs for some other reason later in development. Since the tentacles of stylommatophoran gastropods are hollow, as opposed to the solid tentacles of basommatophoran snails, the eye vesicles, once they separated from the overlying ectoderm, may just move ("migrate"?) in to the "open space" created by the elongation of the developing tentacles. In addition, the present study did not find any connection of the eye vesicles with the cerebral ganglia during the stages of development studied. Thus, unlike the basommatophoran snail, which was found to have nearly continuous connection between the eye vesicles and cerebral ganglia, the eye vesicles of the stylommatophoran snail are

"free" to move in to, and along with, the developing tentacles. How this movement occurs, whether pushed by the development of the optic nerve, or possibly pulled by a subsequent connection with the epithelium of the developing tentacle, will not be known until further study.

As mentioned previously, a large indentation of the cephalic plate, ventro-lateral (under) to the developing tentacles, was seen in young veliger stage (stage B) embryos of both snail species studied. These indentations, which appear as "tube-like" structures in older embryos, correspond with what has been reported in the literature as the "cerebral tubes." Although only one large indentation/tube was found in the present study, the literature reports two cerebral tubes for some basommatophorans. A possible second tube was not readily obvious in *Helisoma anceps*, but was not specifically looked for either. In the stylommatophoran snail *Anguispira alternata*, the present study did find a small ingression of cells, dorso-medially within the cephalic plate. Descriptions in the literature are insufficient to determine if this small ingression of cells corresponds with what has been reported as a second cephalic tube in some other species.

While this study did find that in the basommatophoran snail *H. anceps* the cerebral ganglia were in the required spatial-temporal position to be able to induce the overlying ectoderm to form the eyes, we must not assume a causal connection (*post hoc ergo propter hoc*)[6] i.e.,

that induction does therefore occur during normal development in *H. anceps*. To definitively determine if induction by the cephalic ganglia does occur, contact with the cephalic plate by a cerebral ganglion must be experimentally blocked to see if eyes still form. However, we cannot rule out induction, either, from this study's findings.

On the other hand, since in the stylommatophoran snail *Anguispira alternata* the cerebral ganglia were not found anywhere near the point of invagination of the eye-vesicles in the cephalic plates, either before or during invagination of the eye-vesicles, induction can be considered unlikely. There is the possibility that the cerebral ganglia either did have contact with the cephalic plates earlier in development and then moved away, or that they had contact, but for such a short time that they were missed in this study. Both of these alternatives are of course possibilities that this approach can easily examine by looking at earlier stages and specimens collected closer together in a developmental time sequence.

### *Experimental evidence of possible inductive interactions between the cerebral ganglia and overlying ectoderm of the cephalic plates*

Two other lines of research support or suggest that the cerebral ganglia may have inductive interactions with the overlying ectoderm to form the eyes.

1) The first line of research includes studies on prosobranchs and basommatophorans and include deletion of macromere and micromere

cells studies and experimental disruption of development by treatments such as a) exposure to ions such as lithium, b) heat-shock, and c) centrifugation. All these methods cause very characteristic malformations of the developing embryos (Verdonk, 1965; Cather, et al., 1976; Morrill, 1982). (See Raven, 1966, for review.)

What is so intriguing about these studies in regards to the question of the possible role of induction by the cerebral ganglia in the formation of the eyes, is that is all these studies report the same order of disruption of development -- "eyes>tentacles>cerebral ganglia" (Raven, 1966). Most of these studies looked at whole embryos, and thus could not report on the presence of cerebral ganglia, and the eyes were only reported if they had reached the point of pigmentation (Verdonk, 1965). The studies that did look at sectioned material, such as in studies on *Limnaea stagnalis*, in the sections one clearly sees a cerebral ganglion in contact with the eye (Raven, 1966). Even more telling is that where there are "supernumerary" eyes there are also supernumerary cerebral ganglia connected (Raven and Beenakkers, 1955). Where the eyes develop close together, there the cerebral ganglia also are closer together (shortened commissure) (Raven and Bennakkers, 1955; Raven, 1966). All these findings are in accord with the idea that the cerebral ganglia may in fact perform an inductive role in development. Although no comparable studies have been carried out on stylommatophoran gastropods.

2) The second line of research involves studies of transplantation of cerebral ganglia from one host to another in Pulmonate snails. The most interesting studies are those of Moffett and Austin (1981). They found that after transplantation of a cerebral ganglion into an adult host of the basommatophoran snail *Melampus bidentatus* (Say) "supernumerary" eyes and tentacles developed. One eye develops on the transplanted ganglion itself, and one at the base of the new extra tentacle, located just above the implanted cerebral ganglion. Thus, clearly in at least this species and in the adult, the cerebral ganglia are capable of inducing (either directly or indirectly) the formation of eyes and tentacles.

While there have been transplantation studies of the cerebral ganglia in the stylommatophoran snail *Helix aspersa* (Gomot, et al., 1990) and the stylommatophoran slug *Limax maximus* (Sokolove, et al., 1983) neither reported any development of supernumerary eyes or tentacles. Both studies were looking to determine if the cerebral ganglia could survive over time, with the study on *H. aspersa* lasting up to a year post implantation. The study on *Limax maximus* had the cerebral ganglion transplanted in the foot region, and even the basommatophoran snail *Melampus bidentatus* does not develop eyes or tentacles when the cerebral ganglia are transplanted there (Moffett, pers. comm.) )

These transplantation studies reflect what was found in the present investigation -- that the cerebral ganglia may in fact play a role by inducing the eyes and tentacles in the basommatophorans and that this inductive role may have changed in stylommatophoran snails.

## Evolutionary modifications are modifications of development

Developmental biologists have known for a long time that the same mechanisms of development operate in all groups of animals. More recently, biologists studying the molecular basis of development have discovered the same developmental/genetic control mechanisms underlying some of these developmental mechanisms, for example, homeobox genes, HOX, PAC6, etc. (Raff and Popodi, 1996). The fact that developmental/genetic control mechanisms are so highly conserved across all groups of animals (and some plants) may explain long-term evolutionary trends, as well as the specific types of morphological changes that have occurred (Raff, et al. 1990).

During the last couple of decades, biologists have begun re-evaluating the role of development in evolutionary change (Atkinson, 1992). They have come to realize that not only does morphological evolution require changes in the underlying developmental program, but the mechanisms for evolutionary innovation are developmental and genetic control mechanisms (Maderson, 1975; Raff and Kauffman,

1983; Buss, 1987; Raff, et al. 1990,Gilbert, et al., 1996; Sommer and Sternberg, 1996). Developmental mechanisms are beginning to be thought of as not just "passive reflections" of changes in the underlying genes. (See Gerd Müller's *Developmental Mechanisms at the Origin of Morphological Novelty: A Side-Effect Hypothesis* ( 1990), for a discussion of non-genetic control mechanisms of development.) But, seen as an active participant not only in determining which types of morphological changes can occur, but also as the source of evolutionary novelty -- creation of new body plans and new structures.

This view is a departure from previous thoughts on the relationship of development to evolution, i.e., that only phyletic information resides in the ontogeny of individuals (Gould, 1977). The view that development plays an active role in evolution redefines evolutionary changes in terms of how they occur, rules that govern them, evidence of their occurrence, and changes the "level of study" of them (Raff, et al. 1990). In recent books, such as "Embryos, Genes, and Evolution" (Raff & Kaufman, 1983), "The Evolution of Individuality" (Leo Buss, 1987), "Evolutionary Innovations" (ed. Matthew Nitecki, 1990), Raff's most recent book, "The Shape of Life" (1996), and "The Origin and Evolution of Larval Forms" (Eds. Brian K. Hall and Marvalee H. Wake, 1999), the authors all argue for an integrated approach in the study of development and evolution. A more robust evolutionary and developmental synthesis, superseding the "Modern Synthesis" of the

1950's, is developing. Consequently, evolutionary questions are starting to be studied in terms of the "active" role development plays in specifying evolutionary modification, as well as the evolution of novel structures.

There have been two main lines of approach for studies seeking to understand the role of development in shaping evolutionary change. The first approach (based on theoretical considerations) presupposes that changes in morphology in response to selection are not truly random, but limited or channeled (directed?) by the nature of the complex interaction of underlying genetic and developmental systems (Raff, et al. 1990). This is referred to as "developmental constraint" (Waddington, 1941) on evolution and may account for some long-term evolutionary trends (Raff, et al. 1990). The idea is that underlying developmental processes and patterns of gene expression may set directional rules governing evolution.

In this approach, one looks for developmental/genetic control mechanisms that may be able to act as buffers to selection and in which systems these act. C. H. Waddington came up with the concept of "canalization" of developmental pathways. He showed that developing systems "...show a certain degree of stability, in the sense that it is quite difficult to persuade the developing system *not* to finish up by producing its normal end result." (Waddington, 1966). Recent work on the heat-shock protein (Hsp90) (Rutherford and Lindquist, 1998) may

have discovered the first molecular mechanism for buffering of development.

The second approach is a more general one looking to discover changes in the developmental programs of the organisms being compared. In this approach one compares differences in underlying developmental programs of two or more groups of animals, and tries to determine which developmental/genetic control mechanism can help explain the specific type/direction of change that occurred. This approach is based on the concept of "dissociability" of developmental processes (Raff, et al. 1990), and was described by Needham, (1933) as:

*Developmental processes which happen together or sequentially in time are not necessarily tightly coupled mechanistically and may be shifted relative to each other in evolution without disrupting development.*

There have been two main processes suggested which are of evolutionary significance: heterochrony and induction. The first process, heterochrony, is relative changes in timing of developmental process, usually in reference to somatic versus gonadal or reproductive structures. In the book *Embryos and Ancestors* (1958) de Beer "generalized" the term "to mean a change in developmental timing of a feature relative to the equivalent feature in its ancestor" (Raff, 1996). Heterochrony has been generally regarded as one of, if not the most, universal and important modes of how development evolves (de Beer, 1958; Gould, 1977; Buss, 1987). Recently though, researchers argue it is heterochronic pattern that is common and not heterochronic

processes leading to evolutionary changes. "There has been surprisingly little (essentially none!) in the way of critical tests of the basic assumption that observed heterochronies are dissociations of processes in time." (Raff, 1996). After setting out to write a "review of cases in which heterochronic processes had an important role in larval evolution..." Hart and Wray,(1999) had came to this conclusion: "Heterochrony has been a potent general organizing principle in the history of evolutionary biology...However, it seems to us that heterochrony as a process has been relatively unimportant in both the evolution of larval forms and the revival of interest in them...."

The second process, induction, has been studied since the 1920s for its important role in organizing the differentiation of different regions of the embryo (Raff, 1996). Has Spemann and Hilde Mangold were the first to study the "organizer" in amphibian embryos, and determined "that activation of the genetic material resulted from the epigenetic interactions among inducing and induced tissues" (Raff, 1996). Induction may thus act as a constraint to changes in developmental patterns or process. Changes in inductive interaction, such as dissociation of previously required inductive events, may allow for specific evolutionary modification (Raff and Kaufman, 1983).

Whether the dissociation of a previously required inductive interaction has allowed for the major restructuring of the stylommatophoran eye-tentacle complex will only be known after more

species from each of these pulmonate groups are studied as well as the other species of prosobranch and opisthobranch gastropods. How representative the species looked at in this investigation are for their respective groups is not known, and will not be known till more comparative studies, on a more representative survey of members of each group, are performed. In the course of the investigation a powerful approach has been developed for making the kinds of comparisons, qualitative and quantitative, that are needed to answer these types of developmental and evolutionary questions.

## CONCLUSION

In the stylommatophoran snail *Anguispira alternata*, this study did not find the cerebral ganglia in close proximity to the cephalic plates in the precise location of the eye vesicles either before or during invagination.

In the basommatophoran snail *Helisoma anceps*, this study did find the cerebral ganglia to be in contact with the cephalic plates from the very beginning of eye-vesicle invagination, and to maintain connection even after the eye vesicles had separated from the overlying ectoderm.

As for the question of whether there is a difference in the location of the point of invagination of the eyes that could account for the difference in the pattern of the eye-tentacle complex in the adults, the answer is no. The point of invagination of the eye vesicles was in the same dorso-lateral position of the cephalic plates for both species.

The use of laser scanning microscopy combined with three-dimensional reconstruction using volume rendering techniques was found be a powerful tool for this type of embryological study. It was effective and efficient for determination of the precise position of the cerebral ganglia and the trajectory of its "branches" within the embryo, before, during, and after eye-vesicle formation. The techniques and functions available by this approach also allowed the precise

measurement of distance between the developing cerebral ganglion and buccal mass to be determined, and to compare the volumes of the developing eye-vesicles, as well as the cerebral ganglia. The ability to analyze the same embryo from multiple angles, re-section the same embryo in different planes, and "dissect out" digitally the structures of interest, meant this study needed far fewer real embryos at each stage of development.

The ability to rotate the whole reconstructed embryo, or "sub-volumes" of it, and to enhance visualization by such techniques as digital "dissection," digital "staining" , etc., allowed the unequivocal determination that none of the "branches" of the developing cerebral ganglia in the stylommatophoran *A. alternata* connect with or even point to the place in the overlying cephalic plates where the eye-vesicles form (Figure 8 & 9).

The evolution of scientific beliefs, practices and approaches is as interesting a subject matter as that to which the philosophical approach of the "scientific method" has been, and continues to be, applied. It can be argued that the part of the scientific enterprise that has developed the fastest, and brought with it a far more sophisticated understanding of the world within and around us, is that of scientific instrumentation.

In 1890, Annie P. Henchman made the argument for the use of the *modern* technique of serial sectioning to study the development of gastropod embryos in her paper on "The Origin and development of the

Central Nervous System in *Limax maximus*." Referring to the confusion and contradiction in the findings of other researchers studying the development of the nervous systems in gastropods, she writes:

> *Since the observations of the earlier writers, down to about 1874, were carried on without the aid of sections, their conclusions do not merit that degree of confidence which is to be accorded those who have availed themselves of this means of study.*

In 1992, Louse Page, in trying to make sense of the conflicting and confusing results of studies on the development of the nervous system in opisthobranch gastropods, takes this one step further making the argument that serial *thin* sections are needed to study the developing nervous system in gastropods.

> *All previous accounts of sequential neurodevelopment in nudibranchs have been histological, yet this method cannot reveal with certainty all neuronal ingression sites from ectodermal proliferation placodes or trajectories of early connectives and axon tracts.*

In 1999, the present investigation, while utilizing just a few of the abundant number of sophisticated tools that are made available only by the technique of three-dimensional reconstruction by "volume rendering," has demonstrated the power and richness of this approach to overcome problems in the study of embryogenesis. A hundred years

from now, what will researchers say about what we consider "cutting edge" and "sophisticated" research methods? It will be exciting for future generations to see what new technologies were created. Even more exciting will be what has been learned about the many varied and wonderful organisms on this planet and how they develop.

# APPENDICES

# APPENDIX A

## ASSORTED COMPUTER SYSTEM COMMANDS

File manipulation commands for the SGI (Unix) workstation

Case Sensitivity

The UNIX operating system is "case sensitive" which means the system recognizes uppercase (or capital) characters and their lowercase version as different characters. For example, the letters "a" and "A" are treated as different characters. The DOS operating system is not case sensitive, so the letters "a" and "A" are treated as the same character.

TAR (Tape Archive) commands

1) To copy files to the 150-megabyte QIC tape drive in the SGI:

IRIS 1% tar cv {full or relative file or directory path name}

E.g., to copy the directory "embryo_volume_1" in the user directory "murphy" the command would look like:

"IRIS 1% tar cv /usr/people/murphy/embryo_volume_1"

2) To retrieve files from the 150-megabyte QIC tape drive in the SGI:

IRIS 2% tar xv {full file or directory path name}

E.g., to retrieve the single file "image_file_1.tif" the command would look like:

"IRIS 1% tar cv

usr/people/murphy/embryo_volume_1/image_file_1.tif"

3) To print out a list in the console window the complete contents of a tape in the drive:

"IRIS 3% tar t"

4) To store all the files in a directory in a single TAR file located on the harddrive:

IRIS tar cf {name of tar file to store all files in} {path name of directory to store in tar file}

"IRIS 1% tar cf /usr/people/murphy/embryo_1.tar usr/people/murphy/embryo_ 1"

The resulting file (icon looks like a "safe") can be transferred to the DELL PC via FTP. If the .tar file is smaller than 100MB it can be stored on a ZIP™ Disk.

5) To retrieve individual files or directories from the tar archive file:

IRIS tar cf {name of tar file} {path name of directory or file retrieve}

"IRIS 22% tar xfv /usr/people/murphy/embryo_1.tar usr/people/murphy/embryo_1/image_1.tif"

# APPENDIX B

## VOXELMATH AND VOXELVIEW INFO

### 1) VoxelMath Memory display

```
IRIS 22%
~
**********************

Welcome to VoxelMath:

**********************

/usr/people/murphy/Committee_Meeting_Stuff/all


Physical memory Status:

  Free ........  37.89 Mbytes

  Available ...  67.54 Mbytes
  Total .......  72.00 Mbytes

Volume 1 dimensions: x[512] y[300] z[36] (8-bit) Voxels

Memory requested for THIS volume:     5.27 Mbytes
Memory requested for ALL volumes:     5.27 Mbytes
Memory needed, including buffers:    16.77 Mbytes
Memory needed, including program:    23.93 Mbytes
Maximum physical memory available:   65.79 Mbytes
Maximum virtual memory available:    77.80 Mbytes
```

## 2) Reading a Tiff image file "header"

```
[This volume had the "color" button on the LSM on when the
images were collected. Thus the LSM_PC program saved the
color information in RGB/colormap in the image file.
(tiff version on our SGI IRIX 4.0.5C is something like
2.4. VoxelView and VoxelMath need version 6.0 of tiff to
read.)]

IRIS 6% VoxelLoader -h ./ANG96/ASE901-F/ase901-F
"
"
/usr/people/murphy/disk2/ANG96/ASE901-F/ase901-F

    000.tif                 001.tif                 002.tif
    003.tif                 004.tif                 005.tif
    006.tif                 007.tif                 008.tif
    009.tif                 010.tif                 011.tif
    012.tif                 013.tif                 014.tif
    015.tif                 016.tif                 017.tif
    018.tif                 019.tif                 020.tif
    021.tif                 022.tif                 023.tif
    024.tif                 025.tif                 026.tif
    027.tif                 028.tif                 029.tif
    030.tif                 031.tif                 032.tif
    033.tif                 034.tif                 035.tif
    036.tif                 037.tif                 038.tif
    039.tif                 040.tif                 041.tif
    042.tif                 043.tif                 044.tif
    045.tif                 046.tif                 047.tif
    048.tif                 049.tif

TIFF Directory at offset 0x8
"
  Subfile Type: (0 = 0x0)

  Image Width: 512 Image Length: 512

  Bits/Sample: 8
"
  Compression Scheme: none

  Photometric Interpretation: palette color (RGB from
colormap)
  Software: "ZIF 1.81 MAR-93"
```

```
  Make: "Carl Zeiss, Oberkochen, Germany"
  Model: "Laser Scan Microscope"
  Samples/Pixel: 1
  Planar Configuration: single image plane
  Color Map: (present)

Volume header:
    magic=              43970
    volume_form=        1
    size=               38797312
    pathname=
/usr/people/murphy/disk2/ANG96/ASE901-F/ase901-F
    data bits=          8
    normal bits=        0
    gradient bits=      0
    bits/voxel=         8
    orig. xsize=        512
    orig. ysize=        512
    orig. zsize=        50
    xsize=              512
    ysize=              512
    zsize=              148
    interpolations=     2
    xoffset=            0.00
    yoffset=            0.00
    zoffset=            0.00
    voffset=            0.00
    xscale=             1.3860
    yscale=             0.9240
    zscale=             5.0000
    vscale=             1.0000
    xunits=
    yunits=
    zunits=
    vunits=
    xlabel=             X
    ylabel=             Y
    zlabel=             Z
    vlabel=       Voxel_Value
```

3) TIFF Header Comparison TIFF

A) Saved in Photoshop 3.0-5.5, converted to MODE grayscale.

This method keeps the barscale from the LSM.

/usr/people/murphy/disk2/ANG96/0H02/Right_eye_tentacle/36/g1.tif: Warning, unknown field with tag 34377 (0x8649) ignored.

```
/usr/people/murphy/disk2/ANG96/0H02/Right_eye_tentacle/
36g1.tif
/usr/people/murphy/disk2/ANG96/0H02/Right_eye_tentacle/36/
g1.tif: Warning, unknown field with tag 34377 (0x8649)
ignored.
TIFF Directory at offset 0x8
  Subfile Type: (0 = 0x0)

  Image Width: 512 Image Length: 512

  Resolution: 72, 72 pixels/inch
  Bits/Sample: 8
  Compression Scheme: none
  Photometric Interpretation: min-is-black
  Samples/Pixel: 1
  Rows/Strip: 512
  Planar Configuration: single image plane

Volume header:
    magic=              43970
    volume_form=        1
    size=               262144
    pathname=
/usr/people/murphy/disk2/ANG96/0H02/Right_eye_tentacle/36
    data bits=          8
    normal bits=        0
    gradient bits=      0
    bits/voxel=         8
```

B) TIFF converted and saved in LSM_PC: MODE RGB (Index color in Photoshop 3.0-5.5?)

This method loses the barscale from LSM.

```
IRIS 6% VoxelLoader -h
/usr/people/murphy/disk2/ANG96/0H02/Right_eye_tentacle/36
"
"
/usr/people/murphy/disk2/ANG96/0H02/Right_eye_tentacle/36
"
    036.tif
"
TIFF Directory at offset 0x8
  Subfile Type: (0 = 0x0)

  Image Width: 512 Image Length: 512

  Bits/Sample: 8
  Compression Scheme: none
  Photometric Interpretation: palette color (RGB from
colormap)
  Software: "ZIF 1.81 MAR-93"
  Make: "Carl Zeiss, Oberkochen, Germany"
  Model: "Laser Scan Microscope"
  Samples/Pixel: 1
  Planar Configuration: single image plane
  Color Map: (present)

Volume header:
    magic=              43970
    volume_form=        1
    size=               262144
    pathname=
/usr/people/murphy/disk2/ANG96/0H02/Right_eye_tentacle/36
    data bits=          8
    normal bits=        0
    gradient bits=      0
    bits/voxel=         8
```

# APPENDIX C

## DIMENSIONS FILE FOR VOLUMETRIC DATA SET: VOXELVIEW'S "_DIMENSIONS" FILE

*VoxelView Data Set Descriptor File (field format shown):

**********

| | | | | |
|---|---|---|---|---|
| * [zsize] | [xsize] | [ysize] | [interps] | [bits/voxel] * |
| * [zoffset] | [xoffset] | [yoffset] | [voffset] | * |
| * [zscale] | [xscale] | [yscale] | [vscale] | * |
| * [zunits] | [xunits] | [yunits] | [vunits] | * |
| * [zlabel] | [xlabel] | [ylabel] | [vlabel] | * |

*This header must also remain in the file VERBATIM!! **********

| | | | | |
|---|---|---|---|---|
| 37 | 412 | 300 | 0 | 8 |
| 0.000000 | 499.042969 | 499.042969 | 0.000000 | 0 |
| 10.00000 | 1.380000 | 1.380000 | 1.000000 | |
| microns | microns | microns | greyscale | |
| z_axis | x_axis | y_axis | voxelvalue | |

# APPENDIX D

## IMAGE ROTATION STEPS

The correction can be done in a couple of ways: a) the digital image on the computer can be "flipped" horizontally (left to right) and then flipped vertically (top to bottom); or b) the image can be "rotated" 180 degrees. The program *VoxelMath* allows one to rotate or flip all the images that comprise a sample in a single step.

A) 1. Flip all images in x-axis: In the Merge Volume window, under section "Unary (V1) Operations" selection "Flip X-Axis": This reverses the voxel order along the x-axis, thus functionally "flipping" the volume left-to-right. This creates a second volume data set in memory (only). 2. Repeat procedure on newly created volume data set and select option "Flip-Y Axis" to reverse the voxel order along the y-axis, thus functionally flipping the volume top-to-bottom.

B) Rotate the volume: function "Twist" in the "Operations Window: Ops Panel: Math Buttons." "Argument value" set to 180. This rotates (twists) the image 180 degrees. "Do Opts on Vol" will rotate the whole stack of images 180 degrees. New volume saved. (The original non-rotated volume is left intact.)

# APPENDIX E

## MATERIALS & SUPPLIES

Chemicals

Mayer Albumen Adhesive (042611 Carolina Biological Supply Company)

Alpha brand white chalk No. 314005 by Weber Costello, or Hygieia brand by Dixon

Video Equipment

Mitsubishi SVHS video recorder (HS-U62) and a Quasar VHS video recorder (VH200)

Video images were captured on either Maxell XL-HIFI T-120 or Polaroid Supercolor Plus T-120 VHS tape media

Computer Equipment

Dell Dimensions P90 Computer with Six gigabyte hard drive and sixty-four megabytes of RAM

Silicon Graphics, Inc. Personal Iris running IRIX 4..0.5.C with 72 Megs RAM, 780 internal Hard Drive and 2 GB external SCSI Hard Drive with 500MB swap file.

# APPENDIX F

## ASSORTED BIBLIOGRAPHIC REFERENCES

**Page , L. R. citations**

Page, Dr. Louise R. Bickell; Teaching: Developmental Biology; Reasearch: Developmental Biology: My research investigates how evolutionary innovations and patterns of phylogeny might be understood in terms of changes to developmental programmes. I am currently studying comparative patterns of development in gastropods to test long-standing hypotheses about the early evolution and phylogeny of this group. These studies focus on morphogenesis of the nervous system, shell musculature, and shell form and employ electron microscopical and immuno-cytochemical methods. Molluscs are useful models for this research because hypotheses about historical changes in shell form and shell muscles can be tested against the fossil record; Dept. Biology, Univ. Victoria, Victoria, B.C., V8W Canada **(http://www.oz.net/cgi-bin/hgs/search.pl/nervous/&/system/)**

Bickell Page, L.R. 1989. Autotomy of cerata by the nudibranch mollusc Melibe leonina: a morphological and neurophysiological inquiry. American Zoologist 28(4):68A.[N]

Bickell Page, L.R. 1989a. Autotomy of cerata by the nudibranch Melibe leonina (Mollusca): ultrastructure of the autotomy plane and neural correlate of the behaviour. Philosoph. Trans. Roy. Soc. London, series B, Biological Sciences 324(1222):149-172.[N]

Bickell Page, L.R. 1991. Repugnatorial glands with associated striated muscle and sensory cells in Melibe leonina (Mollusca, Nudibranchia). Zoomorphology 110(5):281-291.[N]

Bickell Page, L.R., see also: Page, L.R.

Page, L.R. 1992. New interpretation of a nudibranch central nervous system based on ultrastructural analysis of neurodevelopment in Melibe leonina. I. Cerebral and visceral loop ganglia. Biol Bull 182:348-365

Page, L.R. 1992. New interpretation of a nudibranch central nervous system based on ultrastructural analysis of neurodevelopment in Melibe leonina. II. Pedal, pleural, and labial ganglia. Biol Bull 182:366-381

Page, L.R. 1992. Thoughts on the Developing Opisthobranch Nervous System Comparisons to Monoplacophorans. American Zoologist 32(5):118A.

Page, L.R. 1992. New interpretation of a nudibranch central nervous system based on ultrastructural analysis of neurodevelopment in Melibe leonina. I. Cerebral and visceral loop ganglia. Biol. Bull. 182(3):348-365.[N]

Page, L.R. 1992a. New interpretation of a nudibranch central nervous system based on ultrastructural analysis of neurodevelopment in Melibe leonina. II. Pedal, pleural, and labial ganglia. Biol. Bull. 182(3):366-381.[N]

Page, L.R. 1993. Development of behavior in juveniles of Melibe leonina (Gastropoda; Nudibranchia). Mar Behav Physiol 22:141-161

Page, L.R. 1993. Developmental analysis reveals labila and subradular ganglia and the primary framework of the nervous system in nudibranch gastropods. J Neurobiol 24(11):1443-1459

Page, L.R. 1993. Developmental analysis reveals labial and subradular ganglia and the primary framework of the nervous system in nudibranch gastropods. J. Neurobiol. 24(11):1443- 1459.[N]

Page, L.R. 1993a. Development of behaviour in juveniles of Melibe leonina (Gastropoda, Nudibranchia). Marine Behaviour & Physiology 22(3):141-161.[N]

Page, L.R. 1994. The ancestral gastropod larval form is best approximated by hatching-stage opisthobranch larvae: evidence from comparative development studies, pp. 206-223. In: W. H. Wilson, S. A. Stricker, & G. L. Shinn. (Eds.). Reproduction and development of marine invertebrates; symposium, Friday Harbor, Washington, USA, June 9-11, 1992. ix+325 pp. Johns Hopkins University Press.[N]

Page, L.R. 1995. Similarities in Form and Developmental Sequence for Three Larval Shell Muscles in Nudibranch Gastropods. Acta Zool. 76(3):177-191.

Page, L.R., see also: Bickell-Page, L. R.[N]

## Gastropod Phylogeny: Other References

Bandel, K. (1993) Caenogastropoda during Mesozoic times. **Scripta Geologia, Special Issue 2: 7-56.**

Adamkewicz, S.L., Harasewych, M.G. (1994) Use of random amplified polymorphic DNA (RAPD) markers to assess relationships among beach clams of the genus Donax. **The Nautilus, Supplement 2: 51-60.**

Bandel, K., Riedel, F. (1994) Classification of fossil and Recent Calyptraeoidea (Caenogastropoda) with a discussion on neomesogastropod phylogeny. **Berl. Geowis. Abh. (E) 13: 329-367.**

Bieler, R. (1992) Gastropod phylogeny and systematics. **Annual Review of Ecological Systems, 23: 311-338.**

van den Biggelaar, J.A.M. (1993) Cleavage pattern in embryos of Haliotis tuberculata (Archaeogastropoda) and gastropod phylogeny. **Journal of Morphology, 216: 121-139.**

van den Biggelaar, J.A.M. (1996) The significance of the early cleavage pattern for the reconstruction of gastropod phylogeny. In **Origin and Evolutionary Radiation of the Mollusca,** Taylor, J.D. (ed), Oxford University Press, Oxford. Pp. 155-160.

Freeman, G., Lundelius, J.W. (1992) Evolutionary implications of the mode of D quadrant specification in coelomates with spiral cleavage. **Journal of Evolutionary Biology, 5: 205-248.**

Fretter, V., Graham, A. (1962) **British Prosobranch Molluscs**, Ray Society, London.

Golikov, A.N., Starobogatov, Y.I. (1975) Systematics of prosobranch gastropods. **Malacologia, 15: 185-232.**

Haszprunar, G. (1985a) The fine morphology of the osphradial sense organs of the Mollusca. Part 1: Gastropoda-Prosobranchia. **Philosophical Transactions of the Royal Society of London, B 307: 457-496.**

Haszprunar, G. (1985b) The Heterobranchia- a new concept of the phylogeny and evolution of the higher Gastropoda. Zeit. Zool. System.Evol.-forsch. 23: 15-37.

Haszprunar, G. (1988) On the orgin and evolution of major gastropod groups, with special reference to the Streptoneura (Mollusca). **Journal of Molluscan Studies, 54: 367-441.**

Haszprunar, G. (1993) Sententia. The Archaeogastropoda: a clade, a grade or what else? **American Malacological Union Bulletin, 10: 165-177.**

Healy, J.M. (1988) Sperm morphology and its systematic importance in the Gastropoda. In: **Prosobranch Phylogeny, Malacological Review Supplement 4: 251-266.** Ponder, W.F. (ed).

Healy, J.M. (1996) Molluscan sperm ultrastructure: correlation with taxonomic units within the Gastropoda, Cephalopoda and Bivalvia. In: **Origin and Evolutionary Radiation of the Mollusca.** Taylor, J.D. (ed), Oxford University Press, Oxford. Pp. 99-113.

Kantor, Y.I. (1996) Phylogeny and relationships of Neogastropoda. In: **Origin and Evolutionary Radiation of the Mollusca.** Taylor, J.D. (ed), Oxford University Press, Oxford. Pp. 221-230.

Lindberg, D.R. (1988) The Patellogastropoda. **Malacology Review, Supplement 4: 35-63.**

Lindberg, D.R., Ponder, W.F. (1991) A phylogenetic analysis of the Gastropoda. **Geological Society of America. Abstracts, 1991 annual meeting, 23 (5): A160-A161.**

Lindberg, D.R., Ponder, W.F. (1992) Discovering key innovations in the phylogeny of gastropod molluscs. **Program Abstracts, XI Hennig Society Meeting, 1992: 48.**

Lindberg, D.R., Ponder, W.F. (1996) An evolutionary tree for the Mollusca: Branches or roots? In: **Origin and Evolutionary Radiation of the Mollusca,** , Taylor, J.D. (ed), p. 67-75.

Ponder, W.F. (l970) Some aspects of the morphology of four species of the neogastropod family Marginellidae with a discussion on the evolution of the toxoglossan poison gland. **Journal of the Malacological Society of Australia, 2(l): 55-8l.**

Ponder, W.F. (l973) The origin and evolution of the Neogastropoda. **Malacologia, l2(2): 295-338.** Ponder, W.F. (ed) (1988) Prosobranch phylogeny. **Malacological Review, Supplement 4, 346 pp.**

Ponder, W.F. (1991) Marine valvatoidean gastropods - implications for early heterobranch phylogeny. **Journal of Molluscan Studies, 57: 21-32.**

Ponder, W.F., Lindberg, D.R. (1996a) Gastropod phylogeny - challenges for the '90s. In: **Origin and Evolutionary Radiation of the Mollusca**, Taylor, J.D. (ed), p. 135-154.

Ponder, W.F., Lindberg, D.R. (1996b) (In press). Towards a phylogeny of gastropod molluscs - a preliminary analysis using morphological characters. **Zoological Journal of the Linnean Society.**

Ponder, W.F., Warèn, A. (1988) Classification of the Caenogastropoda and Heterostropha - a list of the family-group and higher category names. In: **Prosobranch Phylogeny. Malacology Review, Supplement 4: 288-326.**, Ponder, W.F. (ed).

Reid, D.G. (1989) The comparative morphology, phylogeny and evolution of the gastropod family Littorinidae. **Philosophical Transactions of the Royal Society of London, Series B, 324: 1-110.**

Riedel, F. (1995) An outline of cassoidean phylogeny (Mollusca, Gastropoda). **Contr. Tertiary and Quaternary Geology, 32: 97-132.**

Rosenberg, G., Kuncio, G.S., Davis, G.M., Harasewych, M.G. (1994) Preliminary ribosomal RNA phylogeny of gastropod and unionoidean bivalve mollusks. **Nautilus, Supplement 2: 111-121.**

Salvini-Plawen, L.V., Haszprunar, G. (1987) The Vetigastropoda and the systematics of streptoneurous Gastropoda (Mollusca. **Journal of Zoology, London. 211: 747-770.**

Taylor, J.D. (1996) (ed.). **Origin and evolutionary radiation of the Mollusca.** Oxford University Press, Oxford.

Taylor, J.D., Kantor, Y.I., Sysoev, A.V. (1993) Foregut anatomy, feeding mechanisms, relationships and classification of the Conoidea (=Toxoglossa) (Gastropoda). **Bulletin of the Natural History Museum of London. (Zoology) 59:125-170.**

Taylor, J.D., Morris, N.J. (1988) Relationships of neogastropods. **Malacology Review, Supplement 4: 167-179.**

Taylor, J.D., Morris, N.J., Taylor, C.N. (1980) Food specialization and the evolution of predatory prosobranch gastropods. **Palaenotology, 23: 375-409.**

Thiele, J. (1929-31) **Handbuch der Systematischen Weichtierkunde. Vol. 1. Jena.**

Tillier, S., Masselot, M., Hervé, P., Tillier, A. (1992) Phylogénie moléculaire des Gastropoda (Mollusca) fondée sur le séquençage partiel de l'ARN ribosomique 28 S. **Comp. Rend. Acad. Sci. (Paris) 134 (ser. 3): 79-85.**

Tillier, S., Masselot, M., Guerdoux, J., Tillier, A. (1994) Monophyly of major gastropod taxa tested from partial 28S rRNA sequences, with emphasis on Euthyneura and hot-vent limpets Peltospiroidea. **Nautilus, Supplement 2: 122-140.**

Tillier, S., Masselot, M., Tillier, A. (1996) Phylogenetic relationships of the pulmonate gastropods from rRNA seqences, and tempo and age of the stylommatophoran radiation. In: **Origin and Evolutionary Radiation of the Mollusca.** Taylor, J.D. (ed), Oxford University Press, Oxford. Pp. 267-284.

Wenz, W. (1938-1944) Gastropoda, Teil 1: Allgemeiner Teil und Prosobranchia. In: **Handbuch der Pälaozoologie, 6.** Schindewolf, O.H. (ed), Berlin. vi+1639 pp.

**Snail image citation: http://www.nearctica.com/nathist/mollusks/gastrop.htm**

# BIBLIOGRAPHY

# LITERATURE CITED

*"Originality is the art of concealing your sources."*

*- Unknown*


Andrews, E. B. (1965). The functional anatomy of the mantle cavity, kidney and blood system of some pilid gastropods (Prosobranchia). *J. Zool.* **146**: 70-94.

Andrews, E. B., and Little, C. (1972). Structure and function in the excretory system of some prosobranch snails (Cyclophoridae). *J. Zool.* **168**: 395-422.

Atkinson, J. W. (1992). Conceptual issues in the reunion of development and evolution. *Synthese.* **91**: 93-110.

Audesirk, T. E. (1975). Chemoreception in *Aplysia californica*. I. Behavioral localization of distance chemoreception used in food-finding. *Behav. Biol.* **15**: 45-55.

Audesirk, T. E., and Emery, D. G. (1978). Sensory cells in *Aplysia*. *J. Neurobio.* Vol. **9**. No. 2, pp. 173-179.

Baba, N. (1991). Computer-aided three-dimensional reconstruction from serial section images. In "Image Analysis in Biology," ( Donat-P. Häder, Ed.) pp. 251-270. CRC Press, Boca Raton.

Barker, G. M. (1999). Naturalised terrestrial Stylommatophora (Mollusca: Gastropoda). Fauna of New Zealand 38, 253 pages.

Blochmann, F. (1882). Ueber die Entwicklung der *Neritina fluviatilis* Müll. *Z. wiss. Zool.* **36**: 125.

Boettger, C. R. (1954). Die Systematik der euthyneuren Schnecken. *Zool. Anz., Suppl.* **17**: 253-279.

Boudko, D. Y., Switzer-Dunlap, M., Hadfield, M. G. (1999). Cellular and Subcellular Structure of Anterior Sensory Pathways in *Phestilla sibogae* (Gastropoda, Nudibranchia). *J. Comp. Neurol.* **403**: 39-52.

Bullock, T. H., and Horridge, G. A. (1965). *Structure and Function in the Nervous Systems of Invertebrates.* Vol. **2.** W. H. Freeman and Company, San Francisco.

Burch, J.B. 1982. Freshwater snails (Mollusca: Gastropoda) of North America. *Bull. Environ. Protec. Agency*, EPA-600/3-82-026: i-vi, 1-294.

Camey, T., and Verdonk, N. H. (1970). The early development of the snail *Biomphalaria glabrata* (Say) and the origin of the head organs. *Neth. J. Zool.* **20:** 93-121.

Carazzi, D. (1905-6). L'embriologia dell' *Aplysia* e i problemi fondamentali dell' embriologia compara. *Arch. Ital. Anat. Embriol.* **4**: 231, 459; **5**: 667.

Casteel, D. B. (1904). The cell-lineage and early larval development of *Fiona marina*, a nudibranch mollusc. *Proc. Acad. Nat. Sci. Philadelphia* **56**: 325.

Chase, R., and Tolloczko, B. (1985). Secretory glands of the snail tentacle and their relation to the olfactory organ (Mollusca, Gastropoda). *Zoomorphology* **105**: 60-67.

Chase, R., and Tolloczko, B. (1993). Tracing neural pathways in snail olfaction: From the tip of the tentacles to the brain and beyond. *Microsc Res Tech* **24**: 214-230.

Chia, F.-S., and Koss, R. (1982) Fine structure of the larval rhinophores of the nudibranch, *Rostanga pulchra,* with emphasis on the sensory receptor cells. *Cell and Tissue Research.* **225**: 235-248.

Chia, F.-S., and Koss, R. (1984) Fine structure of the cephalic sensory organ in the larva of the nudibranch *Rostanga pulchra* (Mollusca, Opisthobranchia, Nudibranchia). *Zoomorphology.* **104**: 131-139.

Conklin, E. G. (1897). The embryology of *Crepidula. J. Morph.* **13**: 1.

-------- (1907). The embryology of *Fulgur.* A study of the influence of yolk on development. *Proc. Acad. Nat. Sci. Philadelphia* **1907**: 320.

Creek, G. A. (1951). The reproductive system and embryology of the snail Pomatias elegans (Müller). *Proc. Zool. Soc. London* **122**: 599-640.

Crofts, D. R. (1937). The development of *Haliotis tuberculata*, with special reference to the organogenesis during torsion. *Phil. Trans. R. Soc. Lond.* **B228**: 219-268.

Delsman, H. C. (1912). Ontwikkelingsgeschiedenis van *Littorina obtusata*. Diss. Amsterdam 1912. ---Cf. Entwicklungsgeschichte von *Littorina obtusata*. *Tijdschr. Ned. Dierk. Ver.* (2) **13**: 170 (1914).

Eakin, R. M., and Brandenburger, J. L. (1967): Differentiation in the eye of a pulmonate snail *Helix aspersa*. *J. Ultrastruc. Res.* **18**: 391-421.

Fretter, V., and Graham, A. (1962). *British Prosobranch Molluscs.* Ray Soc., London.

Gilbert, S. F., Opitz, J. M., Raff, R.A. (1986). Resynthesizing Evolutionary and Developmental Biology. *Developmental Biology.* **173**: 357-372.

Gomot, P., Gomot, L., Marchand, C. –R., and Colard, C. (1990). Extirpation and transplantation of the brain of the snail Helix aspersa: a study of the survival of the animal and the implant. *Can. J. Zool.* **68**: 1505-1512.

Graham, A. (1985). Evolution within the Gastropoda: Prosobranchia. In "The Mollusca," (E. R. Trueman and M. R. Clarke, eds.), Vol.**10**, pp. 151-186. Academic Press, Inc., New York.

Hart, M. W., and Wray, G. A. (1999). Heterochrony. In "The Origin and Evolution of Larval Forms," (B. K. Hall and M. H. Wake, eds.). Pp. 159-165. Academic Press, Inc. San Diego.

Haszprunar, G. (1988). On the origin and evolution of major gastropod groups, with special reference to the streptoneura. *J. Moll. Stud.* **54**: 367-441.

Henchman, A. (1890). The origin and development of the central nervous system in *Limax maximus*. *Bull. Mus. Comp. Zool. Harvard College.* Vol. 20. No. 7.

Heymons, R. (1893). Zur Entwicklungsgeschichte von *Umbrella mediterranea* Lam. *Z. wiss. Zool.* **56**: 245.

Holmes, S. J. (1900). The early development of *Planorbis*. *J. Morph.* **16**: 369.

Hyman, L. H. (1967). *The Invertebrates. Volume VI. Mollusca I.* McGraw-Hill Book Company. New York.

Jacob, M. H. (1984). Neurogenesis in *Aplysia californica* resembles nervous system formation in vertebrates. *J Neurosci.* Vol. **4**, No. 5: 1225-1239.

Kofoid, C. A. (1895). On the early development of *Limax. Bull. Mus. Comp. Zool. Harvard Coll.* **27**:35.

Maderson, P. F. A. (1975). Embryonic tissue interactions as the basis for morphological change in evolution. *Amer. Zool.* **15**: 315-327.

Meisenheimer, J. (1896). Entwicklungsgeschichte von *Limax maximus* L. I. Furchung und Keimblätterbildung. *Z. wiss. Zool.* **62**: 415.

Milne-Edwards, H. (1846). Sur la classification naturelle des mollusques gastéropodes. Institut 14(1), 295-296. As stated in: Schmekel, L. (1985). Aspects of Evolution within the Opisthobranchs. In "The Mollusca," (E. R. Trueman and M. R. Clarke, eds.), Vol.10, Evolution, pp. 221-267. Academic Press, Inc., New York.

Moffett, S. and Austin, D. R. (1981). Implanted cerebral ganglia produce supernumerary eyes and tentacles in host snails. *J. Exp. Zool.* **216**: 321-325.

Moor, B. (1983). Organogenesis. In "The Mollusca," (K. M. Wilbur, ed.), Vol. **3**: *Development*, N. H. Verdonk, J. A. van den Biggelaar, and A. S. Tompa, eds. Academic Press, Inc., New York.

Moritz, C. E. (1939). Organogenesis in the gastropod *Crepidula adunca* Sowerby. *Univ. Calif. Berkeley Publ. Zool.* **43**: 217-248.

Morrill, J. B. (1982). Development of the Pulmonate Gastropod, *Lymnaea*. In "Developmental Biology of Freshwater Invertebrates." Pp. 399-483. Alan R. Liss, Inc. New York.

Müller, G. B. (1990). Developmental Mechanisms at the Origin of Morphological Novelty: A Side-Effect Hypothesis. In "Evolutionary Innovations." (Ed. Matthew H. Nitecki).pp. 99-130. University of Chicago Press. Chicago.

Page, L. (1992): New interpretation of a nudibranch central nervous system based on ultrastructural analysis of neurodevelopment in *Melibe leonina*. I. cerebral and visceral loop ganglia. *Biol. Bull.* **182**: 348-365.

Pawley, J. B. (Ed.)(1990). *Handbook of Biological Confocal Microscopy.* Plenum Press. New York.

Raff, R. A. (1996). *The Shape of Life: Genes, Development, and the Evolution of Animal Form.* The University of Chicago press. Chicago.

Raff, R. A., and Popodi (1996). Evolutionary Approaches to Analyzing Development. In "Molecular Zoology: Advances, Strategies, and Protocols." (Eds. J. D. Ferraris and S. R. Palumbi). Pp. 245-265. Wiley-Liss, Inc. New York.

Raven, C. P. (1966). *Morphogenesis: the Analysis of Molluscan Development.* Pergamon Press, Oxford.

Raven, C. P., and Beenakkers, A. M. Th., (1955) On the nature of head malformations obtained by centrifuging the eggs of *Limnaea stagnalis. J. Embr. Exp.* Morph. **3**, 286.

Rigaut, J. P., Carvajal-Gonzalez, S., Vassy, J. Confocal image cytometry - Quantitative analysis of three-dimensional images obtained by confocal scanning microscopy. In "Image Analysis in Biology," (Donat-P. Häder, Ed.) pp. 109-133. CRC Press. Boca Raton.

Robert, A. (1902). Recherches sur le développement des Troques. *Arch. Zool. Exp. Gén.* (3) **10**: 269.

Rutherford, S. L., and Lindquist, S. (1998). Hsp90 as a capacitor for morphological evolution. *Nature* **396**: 336-342.

Schmekel, L. (1985). Aspects of Evolution within the Opisthobranchs. In "The Mollusca," (E. R. Trueman and M. R. Clarke, eds.), Vol.**10**, Evolution, pp. 221-267. Academic Press, Inc., New York.

Simkiss, K. (1985). Molluscan Skin (excluding Cephalopods). In "The Mollusca," (E. R. Trueman and M. R. Clarke, eds.), Vol.**11**, pp. 11-36. Academic Press, Inc., New York.

Sokolove, P. G., Melrose, G. R., Gordon, T. M., O'Neill, M. C. (1983). Stimulation of Spermatogonial DNA Synthesis in Slug Gonad by a Factor Released from Cerebral Ganglia under the Influence of Long Days. *General and Comparative Endocrinology.* **50**: 95-104.

Solem, A. (1974). *The Shell Makers: Introducing Mollusks.* Wiley, New York.

Solem, A. (1985). Origin and Diversification of Pulmonate Land Snails. In "The Mollusca," (E. R. Trueman and M. R. Clarke, eds.), Vol.**10**, Evolution, pp. 269-293. Academic Press, Inc., New York.

Thompson, T. E. (1976). "Biology of Opisthobranch Molluscs." Ray Soc., London. As stated in: Schmekel, L. (1985). Aspects of Evolution within the Opisthobranchs. In "The Mollusca," (E. R. Trueman and M. R. Clarke, eds.), Vol.**10**, Evolution, pp. 221-267. Academic Press, Inc., New York.

van Mol, J. (1967). Étude morphologique et phylogénétique du ganglion cérébroïdes des Gastréropodes Pulmonés (Mollusques). *Mem. Cl. Sci., Acad. R. Belg. Collect.* 80 **37**: 1-168.

Verdonk, N. H. (1965). "Morphogenesis of the Head Region in *Limnaea stagnalis* L." Thesis. Utrecht.

Verdonk, N. H., and van den Biggelaar, J. A. M. (1983). Early Development and the Formation of the Germ Layers. In "The Mollusca," (Verdonk, N. H., and van den Biggelaar, J. A. M., eds.), Vol. **3**, Development, pp. 91-122. Academic Press, Inc., New York.

Waddington, C. H. (1941). Evolution of developmental systems. *Nature* **147**:108-110.

----------(1957). *The Strategy of the Genes.* Allen & Unwin. London.

---------- (1962). *New Patterns in Genetics and Development.* Columbia Univeristy Press. New York.

---------- (1966). *Principles of Development and Differentiation.* The Macmillan Company. New york.

Walter, U. (1999). When fuzzy thinking is a good thing. [Online] HMS Beagle. Issue **60**. Available August 06, 1999. http://biomednet.com/hmsbeagle/60/viewpts/op_ed.

Weibel, E. R. (1979) *Stereological Methods.* Academic Press, London.

Wierzejski, A. (1905). Embryologie von *Physa fontinalis* L. *Z. wiss. Zool.* **83**: 502.

Wilson, E. B. (1892). The cell lineage of *Nereis. J. Morphol.* **6**: 361-481.

Wolpert, L. (1998). *Principles of Development.* Oxford University Press, New York.

Zilch, A. (1959). Gastropoda. Teil 2. Euthyneura. In "Handbuch der Paläozoologie" (W. Wenz, ed.), Vol. **6**, pp. 1-200. Gebr. Borntraeger, Berlin.

## ENDNOTES

[1] for arguments against this division see Boettger, 1954; Zilch, 1959.

[2] Although, contrary to what Verdonk and van den Biggelaar (1983) wrote, it is the *third* cleavage and not the second cleavage that determines the "cleavage pattern" for the embryo, and thus the handedness, "dextral" or right-handed coiling, or "sinistral" or left-handed coiling, of the shell. See Raven, 1966, for examples showing this to be true.

[3] While all *published* work agrees on the pretrochal origin of the cerebral ganglia, Louise Page (pers. comm.) believes she has discovered migrating *posttrochal* cells contributing to the formation of the cerebral ganglia in the opisthobranch *Melibe leonina.*

[4] Whether one or two occur on each side is uncertain. See Henchman (1890) and Raven (1966) for review.

[5] One of the most striking exceptions are the Strombidae which have what appears to be exceedingly long eye-stalks, with just a small distal branch of tentacle (Hyman, 1967).

6 Assumed Causal Connection

In its classical form, this fallacy is called the post hoc ergo propter hoc, which is Latin for "After this, therefore as a result of this." Known also as "false cause," this fallacy involves a confusion of the time of an event or action and the results of that event or action. Simply because something happens at a particular time, and something else happens after it, the two need not be related in any way but temporally. (http://www.rhetor.com/compete/fallacies.htm, 1999)